2017

Deep Groundwater Evolution at Outokumpu, Eastern Finland: From Meteoric Water to Saline Gas–Rich Fluid

Riikka Kietäväinen

Academic Dissertation

GTK

gtk.fi

Deep Groundwater Evolution at Outokumpu, Eastern Finland: From Meteoric Water to Saline Gas-Rich Fluid

by

Riikka Kietäväinen
Geological Survey of Finland
P.O. Box 96
FI-02151 Espoo, Finland

ACADEMIC DISSERTATION

Department of Geosciences and Geography, University of Helsinki

To be presented, with the permission of the Faculty of Science of the University of Helsinki, for public examination in auditorium D101, Physicum, Kumpula Campus, on March 31st 2017, at 12 o'clock noon.

Unless otherwise indicated, the figures have been prepared by the author of the publication.

Supervisors
Professor Juha Karhu
Department of Geosciences and Geography
University of Helsinki, Finland

Professor Ilmo Kukkonen
Department of Physics
University of Helsinki, Finland

Docent, Senior Scientist Lasse Ahonen
Geological Survey of Finland
Espoo, Finland

Pre-examiners
PhD habil., Head of Laboratory Wolfram Kloppmann
French Geological Survey (BRGM)
Orléans, France

Assistant Professor Randy L. Stotler
University of Kansas, USA

Opponent
PhD habil., Senior Researcher, Laboratory Head Niklaus Waber
University of Bern, Switzerland

Front cover: Tube sampling at the Outokumpu Deep Drill Hole.
                   Photo: Riikka Kietäväinen, GTK.

ABSTRACT

Within Precambrian continental shields, saline, gas-rich groundwaters are found in all over the world from bedrock fractures and pore spaces in the upper crust. Several processes, from seawater evaporation or freezing followed by infiltration to water-rock interaction, have been suggested to be responsible for the characteristic features of these waters. In addition to reactions between water and the bedrock, active microbial communities inhabiting these waters, i.e. the deep biosphere, may play a significant role in shaping their surroundings by biogeochemical reactions, especially by contributing to the deep carbon cycle.

The origin and evolution of deep groundwater in the 2.5 km deep Outokumpu Deep Drill Hole in eastern Finland was investigated using geochemical and isotopic methods. The sample material included water and gas derived from the drill hole by tube sampling, pumping and pressurised methods, as well as fracture minerals. Similar results were obtained for water samples using different sampling techniques. However, as uncontrolled degassing took place during tube sampling and pumping, it is suggested that pressurised methods should be used for gas sampling.

Five water types were discerned along the drill hole, which reflect changes in lithology and indicate isolation from the surface and from each other within the Outokumpu bedrock. An evolutionary model was proposed that includes precipitation and infiltration of meteoric water at warmer than present climatic conditions, a shift in the stable isotopic composition of water and an increase in salinity through water-rock interaction between virtually stagnant groundwater and the bedrock, and both the abiotic and biotic formation of hydrocarbons. Two independent lines of evidence from water stable isotopes and the accumulation of radiogenic and nucleogenic noble gases indicated isolation of the Outokumpu Deep Drill Hole groundwaters from the meteoric water cycle from the Eocene-Miocene epochs, placing the evolutionary model in the time frame of millions to tens of millions of years.

The results shed light on how deep groundwaters have evolved in geochemical and microbiological processes through time and space. Furthermore, they emphasise the complexity of these environments, as they are being increasingly utilised for underground construction, and provide background information for assessment of the long-term safety of nuclear waste disposal.

Keywords: groundwater, geochemistry, isotopes, water-rock interaction, residence time, deep drilling, biosphere, noble gases, carbon, Outokumpu, Fennoscandian Shield

Riikka Kietäväinen
Geological Survey of Finland
P.O. Box 96
FI–02151 Espoo, Finland

E-mail: riikka.kietavainen@gtk.fi.

CONTENTS

ACKNOWLEDGEMENTS

ABBREVIATIONS

bsl	below surface level
CRDS	cavity ring down spectrometer
DIC	dissolved inorganic carbon
DOC	dissolved organic carbon
EC	electrical conductivity
FTT	Fischer-Tropsch type
GC	gas chromatography
GMWL	global meteoric water line
ICP-MS	inductively coupled plasma mass spectrometer
ICP-OES	inductively coupled plasma optical emission spectrometer
IRMS	isotope ratio mass spectrometer
LMWL	local meteoric water line
PDS	positive displacement sampler
QMS	quadrupole mass spectrometer
SEM	scanning electron microscopy
STP	standard temperature and pressure
TIMS	thermal ionisation mass spectrometer
TOC	total organic carbon
VPDB	Vienna PeeDee Belemnite
VSMOW	Vienna Standard Mean Ocean Water

LIST OF ORIGINAL PUBLICATIONS

This thesis is comprised of three original publications and one review paper, which are referred to in the text by their Roman numerals (Papers I–IV).

I Kietäväinen, R., Ahonen, L., Kukkonen, I. T., Hendriksson, N., Nyyssönen, M. & Itävaara, M. 2013. Characterisation and isotopic evolution of saline waters of the Outokumpu Deep Drill Hole, Finland – Implications for water origin and deep terrestrial biosphere. Applied Geochemistry 32, 37–51.

II Kietäväinen, R., Ahonen, L., Kukkonen, I. T., Niedermann, S. & Wiersberg, T. 2014. Noble gas residence times of saline waters within crystalline bedrock, Outokumpu Deep Drill Hole, Finland. Geochimica et Cosmochimica Acta 145, 159–174.

III Kietäväinen, R. & Purkamo, L. 2015. The origin, source and cycling of methane in deep crystalline rock biosphere. Frontiers in Microbiology 6, 725. (Review)

IV Kietäväinen, R., Ahonen, L., Niinikoski, P., Nykänen, H. & Kukkonen, I. T. 2017. Abiotic and biotic controls on methane formation down to 2.5 km depth within the Precambrian Fennoscandian Shield. Geochimica et Cosmochimica Acta (in press).

AUTHOR'S CONTRIBUTIONS

I Riikka Kietäväinen took part in the planning of the study, collected the samples, interpreted the geochemical and isotope results, prepared the figures and tables and wrote the paper.

II Riikka Kietäväinen took part in the planning of the study, collecting the samples, and analysing the isotopic composition of noble gases, calculated the residence times, interpreted the results, prepared the figures and tables and wrote the paper.

III Riikka Kietäväinen was responsible for the geological and geochemical part of this review article, including the compilation of background data and writing of the sections on geological methane and geochemical methods, and she also contributed to the writing of the other sections.

IV Riikka Kietäväinen was responsible for planning the study and taking the samples. She selected, described and analysed the calcites, performed the calculations, interpreted the geochemical and isotope results, prepared the figures and tables and wrote the paper.

1 INTRODUCTION

The Earth is a wet planet, not only from the surface but also beneath the ground. Free (gravitational) water occupies fractures and pores of the upper crust at least down to 11 km depth (Kremenetsky & Ovchinnikov 1986, Stober & Bucher 2004). Deep groundwaters can be defined as virtually stagnant groundwaters characteristically enriched in dissolved solids, which typically occur at depths of several hundreds of metres within the bedrock (Frape et al. 2004, Gascoyne 2004). To emphasise the abundant dissolved gas component frequently found in deep groundwaters, the term fluid is also often used instead.

The history of deep continental drilling began in central China, where deep groundwaters had been used for salt and gas production for centuries, and in 1835, a depth of more than 1000 m was reached, a first in the world (Kuhn 2004). While the Chinese took advantage of fluids deep within sedimentary rocks, salty waters were also accidentally encountered in underground mines in continental shields, for example in Canada, where they were recognised to cause corrosion and to yield harmful, sometimes even explosive, gases in the mine air (Fritz & Frape 1982, Frape et al. 2004). From the late 1970s onwards, deep saline groundwaters within continents have aroused considerably more interest because of projects aiming at the deep geological disposal of nuclear waste (e.g. Tsang et al. 2015).

The occurrence and evolution of deep groundwaters within continental shields is therefore not only a matter of basic research and curiosity, but has several important implications. Information on deep groundwaters within the bedrock is needed in assessing corrosion and scaling risks at underground construction sites such as mines, tunnels and geothermal heat plants, to prevent the migration of unwanted compounds from mine environments, waste dumps, CO_2 storage sites and unconventional gas production fields, and in securing drinking water quality. In Finland, the long-term safety of geological disposal is a particularly timely issue, as the final disposal of nuclear wastes into the ONKALO repository in Olkiluoto, SW Finland, is scheduled to start in the 2020s[1].

As a part of this research continuum, this thesis study aimed to examine the origin and evolution of deep saline and gas-rich groundwaters. The water, gas and mineral samples for this study were taken from the 2.5 km deep Outokumpu Deep Drill Hole in eastern Finland and analysed using geochemical and isotopic methods. The study was designed to assess the groundwater residence time and water-rock-microbe interaction, and to provide insights into deep groundwater evolution at Outokumpu, as well as provide a reference for similar studies around the world.

1.1 Deep groundwaters within Precambrian continental shields

At present, dozens of sites within Precambrian shields in Fennoscandia, Ukraine, Canada and South Africa are known to host deep groundwaters with total dissolved solid (TDS) contents of up to 400 g L⁻¹ (e.g. Vovk 1987, Nurmi et al. 1988, Blomqvist 1999, Frape et al. 2004, Onstott et al. 2006, Katz et al. 2011, Stotler et al. 2012) (Fig. 1). Some key characteristics of deep groundwaters in Finland within the Fennoscandian Shield are listed in more detail in Table 1. The geochemistry of deep saline groundwaters is typically dominated by Ca^{2+}, Na^+ and Cl^- ions (e.g. Nurmi

---

[1] http://www.posiva.fi/en/final_disposal/general_time_schedule_for_final_disposal#.V6wfO_l97AU (visited 11.8.2016)
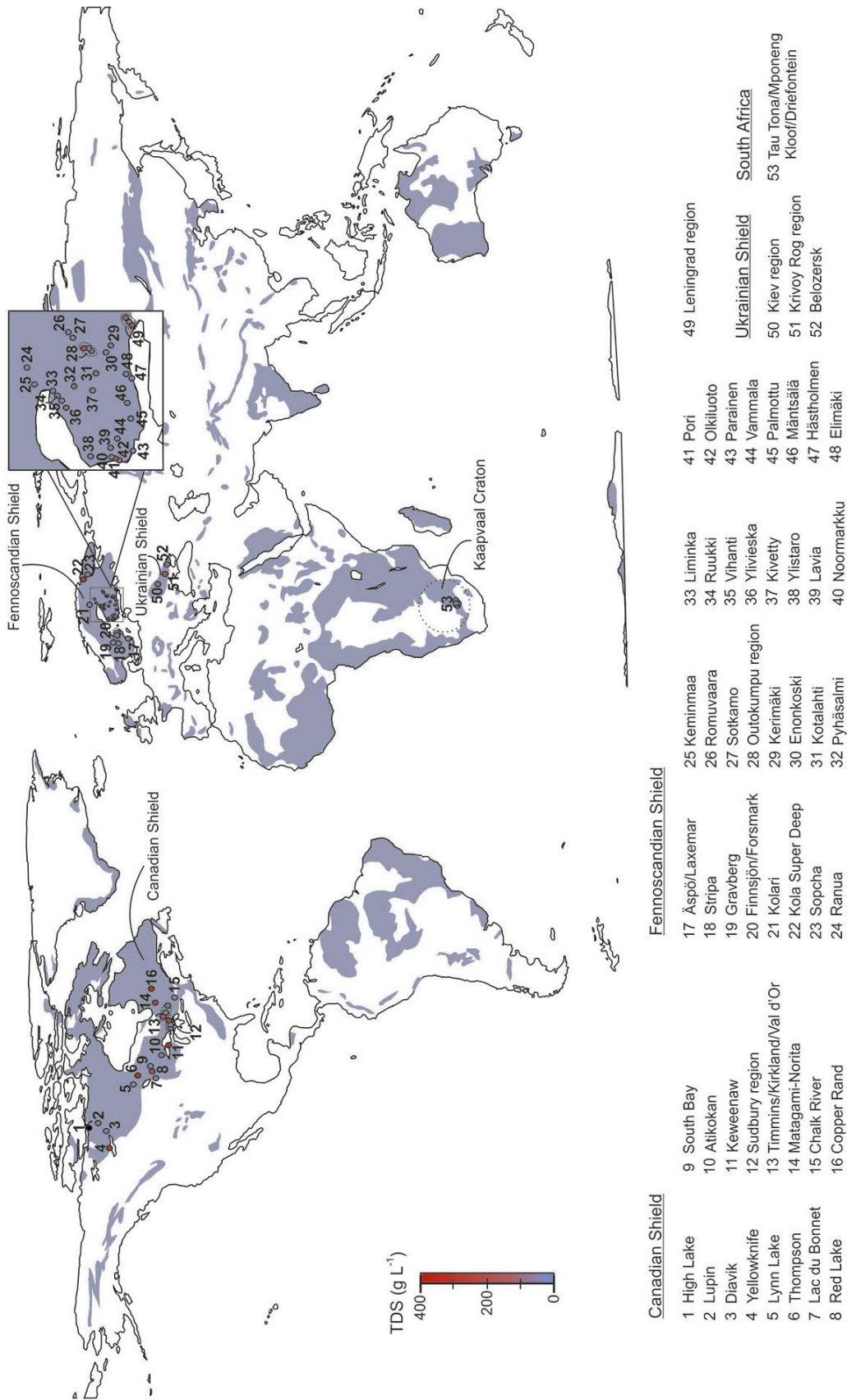
Fig. 1. Deep (>300 m) groundwater study sites within Precambrian shields around the world. Exposed Precambrian (>545 Ma) crust is showed in grey. The circles are colour coded according to the maximum values for total dissolved solids (TDS) observed in each site (no data from site 1). TDS values are from Stotler et al. (2012) (sites 1−16), Frape et al. (2004) (18), Szewzyk et al. (1994) (19), Smellie and Wikberg (1991) (20), Mathurin et al. (2014) (17, 20), Krementsky and Ovchinnikov (1986) (22), Vovk (1987) (23, 49, 50−52), and Onstott et al. (2006) and Katz et al. (2011) (53). See Table 1 for the references for the sites 21 and 24−48. Map modified after Chorlton (2007) and Sherwood Lollar et al. (2014).

Table 1. Characteristics of deep (>300 m) groundwaters within the Fennoscandian Shield in Finland. Maximum values are given for the sampling depth and total dissolved solids (TDS).

Site	Main rock types	Sampling depth (m)	TDS (g L^{-1})	pH	Water types	Main gases	References
Kolari	Monzonite, diorite, skarn	648	2.65	6.8-8.6	Ca-SO$_4$		Halonen et al. (1990), Frape et al. (2004)
Ranua	Gabbro, ultramafite, quartzdiorite	680	0.51	7.1-9.7	Na-Ca-Cl		Lamminen (1995), Ruskeeniemi et al. (1996)
Keminmaa	Gabbro, norite	340	0.45	6.8-7.0	Ca-HCO$_3$		Blomqvist et al. (1986), Ruskeeniemi et al. (1996)
Romuvaara	Tonalite gneiss	566	0.17	8.4	Na-HCO$_3$	N$_2$	Haveman et al. (1999), Pitkänen et al. (1996)
Sotkamo	Mafic-ultramafic volcanite, quartz-sericiteschist	541	12.5	7.3-10.2	Ca-Na-Cl		Halonen et al. (1990), Frape et al. (2004)
Juuka, Miihkali	Serpentinite, mica gneiss, black schist	1020	168	9.4-10.2	Ca-Na-Cl/ Na-Ca-Cl	CH$_4$	Sherwood Lollar et al. (1993b), Ruskeeniemi et al. (1996), Blomqvist (1999)
Outokumpu Deep Drill Hole	Mica schist, granodiorite, black schist, serpentinite	2480	68.9	6.5-10.1	Na-Ca-Cl/ Ca-Na-Cl	CH$_4$-N$_2$-H$_2$	Paper I (this study)
Sukkulansalo (Outokumpu)	Mica schist, black schist, serpentinite	1060	28.1	7.7-8.7	Ca-Na-Cl	CH$_4$-N$_2$	Nurmi et al. (1988), Sherwood Lollar et al. (1993b), Frape et al. (2004), Ivanovich et al. (1992)
Kerimäki	Mica gneiss, black schist, gabbro	700	5.3	8.7-9.5	Na-Ca-Cl	N$_2$-CH$_4$	Nurmi et al. (1988)
Enonkoski	Mica gneiss, black schist, serpentinite	492	27.6	6.9-7.4	Na-Ca-Cl	CH$_4$-N$_2$	Sherwood Lollar et al. (1993a), Ruskeeniemi et al. (1996), Frape et al. (2004)
Kotalahti	Mica gneiss, amphibolite, black schist, skarn	900	55	9.3-9.8	Ca-Na-Cl	CH$_4$	Blomqvist et al. (1986)
Pyhäsalmi	Metavolcanics, VMS-type Cu-Zn ore	2400	76.2	7.0-8.9	Ca-Na-Cl	N$_2$-He	Miettinen et al. (2015)
Liminka	Shale	780	41	6.5-7.2	Na-Cl-SO$_4$	CH$_4$-N$_2$	Nurmi et al. (1988)
Ruukki	Mica gneiss, mica schist	315	1.5		Na-Ca-Cl		Lamminen (1995), Frape et al. (2004)
Vihanti	Mica gneiss, granite, skarn	763	9.5	8.6-9.4	Na-Cl/ Ca-Na-Cl		Halonen et al. (1990)
Ylivieska	Serpentinite, gabbro	545	82.8	7.0-8.6	Na-Ca-Mg-Cl	CH$_4$-N$_2$	Sherwood Lollar et al. (1993a), Ruskeeniemi et al. (1996)
Kivetty	Granite, granodiorite	855	0.2	7.8 - 9.0	Na-Ca-HCO$_3$	N	Anttila et al. (1999), Haveman et al. (1999), Pitkänen et al. (1998)
Lavia	Granite, quartz diorite	1001	0.05	8.9	Na-HCO$_3$	N$_2$	Lahermo and Lampén (1987), Mitrega and Lahermo (1991)
Ylistaro	Biotite gneiss, mica schist	407	19.8	6.6-8.0	Na-Ca-Cl/ Ca-Na-Cl	CH$_4$-N$_2$	Blomqvist et al. (1986), Sherwood Lollar et al. (1993a)
Noormarkku	Mica gneiss, gabbro	575	46.7	7.8-10.7	Ca-Na-Cl		Lamminen (1995), Ruskeeniemi et al. (1996), Frape et al. (2004)
Pori	Sandstone	613	119	6.7-7.9	Na-Ca-Cl/ Ca-Cl	N$_2$-H$_2$	Blomqvist et al. (1986), Sherwood Lollar et al. (1993a, 1993b)
Olkiluoto	Migmatitic gneiss, mica gneiss, granite	960	84	7.8 -8.3	Na-Ca-Cl/ Ca-Na-Cl	CH$_4$-N$_2$	Haveman et al. (1999), Pitkänen and Partamies (2007)
Parainen	Amphibolite, mica gneiss, skarn	500	6.5	7.1-8.5	Na-Ca-Cl	N$_2$-O$_2$	Nurmi et al. (1988)
Vammala	Mica gneiss, black schist, serpentinite	678	2.8	7.5	Na-Ca-Cl	N$_2$-CH$_4$	Blomqvist et al. (1986), Sherwood Lollar et al. (1993a), Ruskeeniemi et al. (1996)
Palmottu	Garnet-cordierite gneiss, granite	417	1.6	6.2 -9.4	Na-SO$_4$/ Na-Cl	N$_2$-H$_2$	Ahonen et al. (2004), Kaija et al. (1998), Frape et al. (2004)
Mäntsälä	Gabbro, diorite	855	50.3	8.0-9.9	Ca-HCO$_3$/ Na-Ca-Cl/ Ca-Na-Cl		Ruskeeniemi et al. (1996), Frape et al. (2004)
Hästholmen	Rapakivi granite	985	31.8	6.8 - 8.5	Na-Cl	N$_2$-He	Haveman et al. (1999), Luukkonen et al. (1999)
Elimäki	Rapakivi granite	403	2.46	6.5-6.9	Na-Ca-Cl		Blomqvist et al. (1986), Lamminen (1995)

et al. 1988, Frape et al. 2004, Bucher & Stober 2010). Other features shared by the deep saline groundwaters include a distinctive water stable isotope composition, which deviates from all other water bodies such as rain water, shallow fresh groundwater and surface water, sea water and magmatic and metamorphic fluids (Fig. 2), as well as high amounts of non−atmospheric gases, including methane (CH_4), hydrogen (H_2) and helium (He) (Sherwood et al. 1988, Sherwood Lollar et al. 1993a,b, 2014, Ward et al. 2004, Stotler et al. 2010a) (Table 1).

With such peculiar characteristics and a location within the bedrock devoid of salt deposits, and in most cases far away from modern oceans (Fig. 1), studies of deep saline groundwaters in continental shields have yielded several hypothesis of how they were formed. The increase in salinity with depth together with the linear trend of water stable isotopes between fresh and saline groundwaters often observed in deep con−

tinental groundwater studies (Fig. 2) has led to a hypothesis that the characteristics of deep saline groundwaters result from mixing between a highly concentrated shield brine and more recent surface−sourced fresh and/or brackish water (Fritz & Frape 1982, Frape & Fritz 1987, Pearson 1987, Nurmi et al. 1988, Laaksoharju et al. 2008, Mathurin et al. 2014).

The increased salinity of the brine has been related to the weathering (hydrolysis) of silicates (Edmunds et al. 1987, Grimaud et al. 1990), formation of zeolites (Stober & Bucher 2004, Bucher & Stober 2010), radiolytic decomposition of water (Vovk 1987), dissolution and leakage of fluid inclusions (Nordstrom et al. 1989) and concentration of seawater by evaporation (Bottomley et al. 1994, Gascoyne 2004, Greene et al. 2008) or freezing (Herut et al. 1990, Bein & Arad 1992, Starinsky & Katz 2003, Katz et al. 2011). The isotopic shift above the meteoric water line has, in addition to the processes mentioned above,
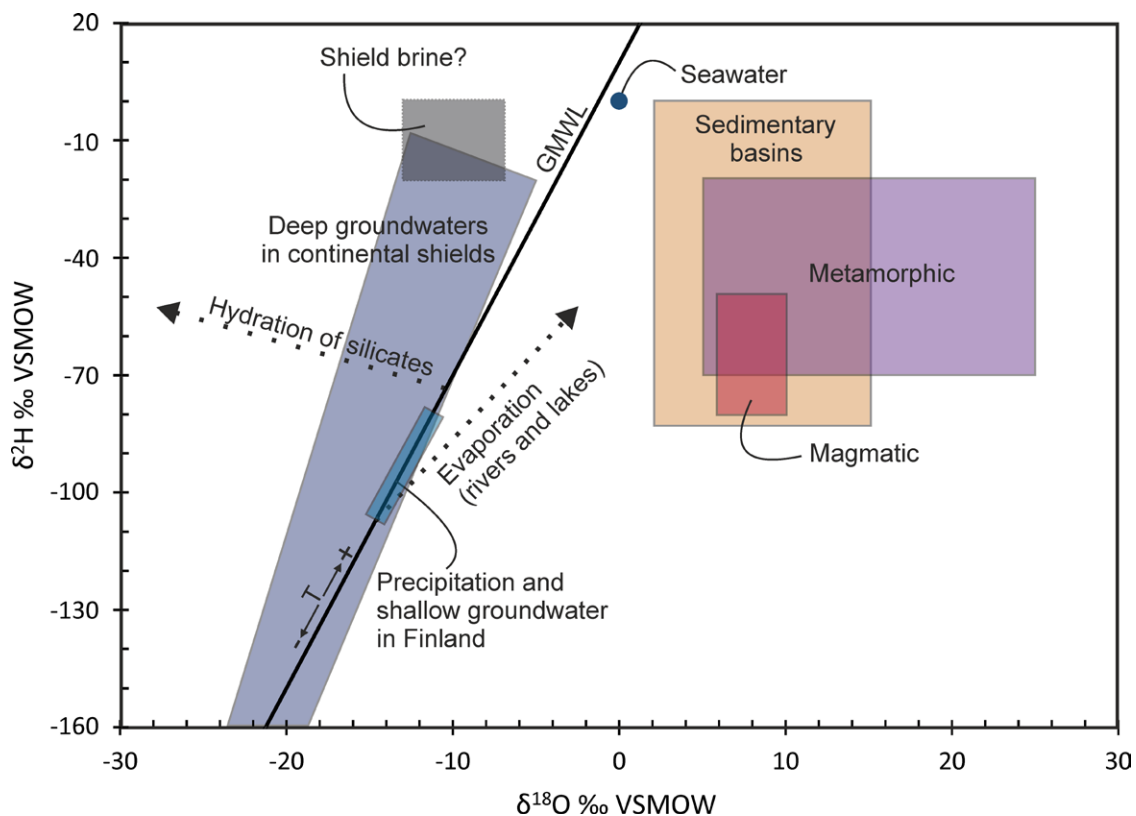
Fig. 2. Typical ranges of water stable isotopes in various geological environments combined after Clark and Fritz (1997), Kloppmann et al. (2002) and Hoefs (2004) and references therein. GMWL = Global Meteoric Water Line (Craig 1961). Isotopic composition of mean annual precipitation and shallow groundwater in Finland is from Kortelainen (2007). The slope of the evaporation line increases from 3.9 to 6.8 with increasing humidity (Gonfiantini 1986), the one shown here is based on 50 % humidity. Starting points of both hydration and evaporation lines were arbitrary selected.

been linked to fractionation between water and hydrogen containing volatiles, namely CH_4, H_2 and H_2S (Clark & Fritz 1997), the dissolution-precipitation of calcite and precipitation of goethite (Kloppmann et al. 2002).

To summarise, the three most widely held models for deep saline groundwater evolution are 1) water–rock interaction within the bedrock (e.g. Fritz & Frape 1982, Frape & Fritz 1987, Nurmi et al. 1988), 2) an external origin in temperate conditions (evaporation-infiltration) (Bottomley et al. 1994, Gascoyne 2004, Greene et al. 2008), and 3) an external origin in cold conditions (freezing-infiltration) (Herut et al. 1990, Bein & Arad 1992, Starinsky & Katz 2003, Katz et al. 2011). Consequently, the estimates of the time available or needed to produce the observed geochemical and isotopic features (i.e. groundwater residence time) vary from tens of thousands of years in the freezing-infiltration model (Bein &

Arad 1992) to a much greater time span necessitated by the low temperature water–rock interaction model (Clark & Fritz 1997, Gascoyne 2004), or even longer if they would be remnants of metamorphic fluids (Kremenetsky & Ovchinnikov 1986).

Considering the origin of gases, possible CH_4 and H_2 formation pathways are summarised in Figure 3. In deep saline groundwaters, microbial, abiotic and thermogenic origins of CH_4 have been suggested (Sherwood et al. 1988, Sherwood Lollar et al. 1993a,b, 2006, Ward et al. 2004, Stotler et al. 2010a, Simkus et al. 2016). Microbiological studies from deep groundwaters in Finland, Sweden and South Africa have confirmed the potential for microbial methanogenesis in these environments (Paper III and references therein). At the same time, there is increasing experimental and field evidence that the abiotic synthesis of CH_4 is a relevant mechanism in
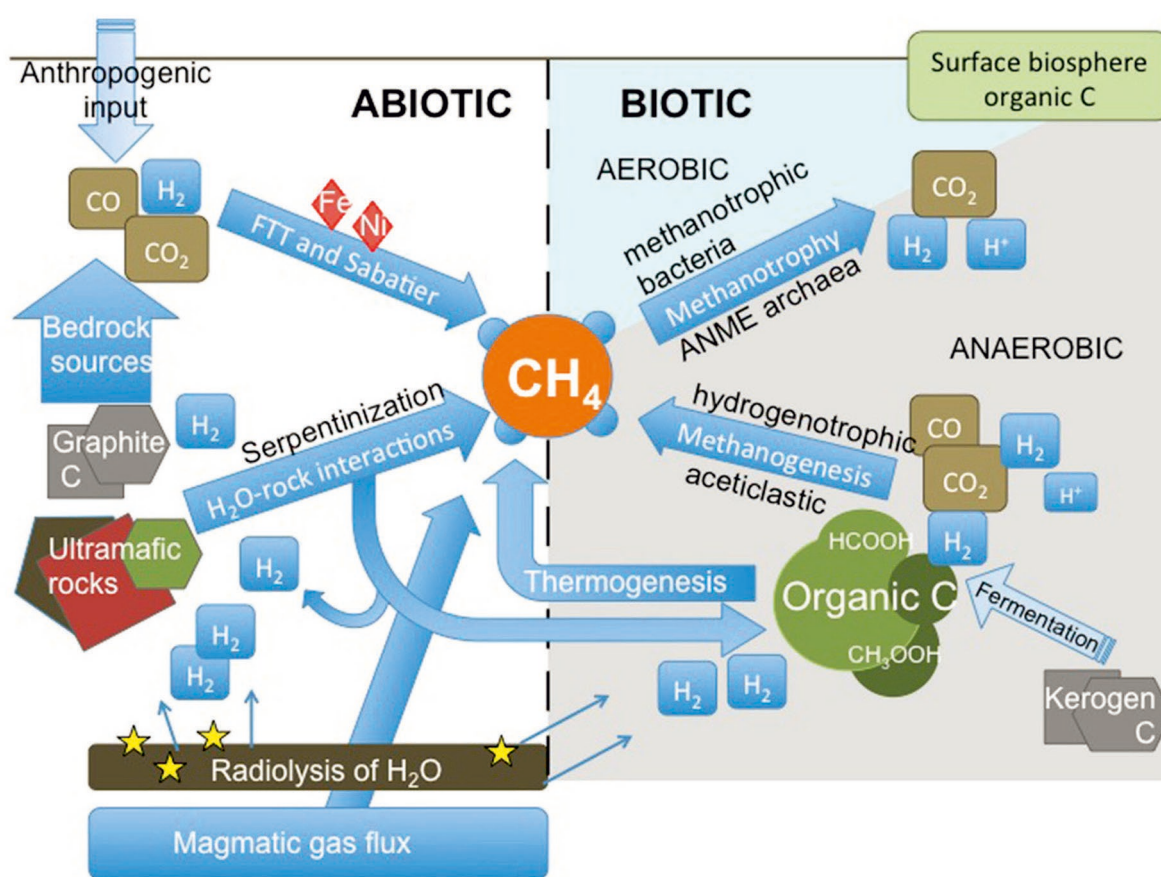
Fig. 3. Schematic showing the potential sources of CH_4 and H_2 in continental bedrock. Abiotic CH_4 production mechanisms include metal catalysed Fischer-Tropsch type (FTT) synthesis ($CO + 3H_2 \rightarrow CH_4 + H_2O$) and Sabatier reaction ($CO_2 + 4H_2 \rightarrow CH_4 + 2H_2O$) and formation from graphitic C in the presence of H_2. Inorganic substrates are also used by hydrogenotrophic microbes, but thermogenic CH_4 and aceticlastic (heterotrophic) methanogenesis require an organic carbon source. H_2 needed in CH_4 formation may originate from radiolysis, serpentinisation ($6Mg_{1.8}Fe_{0.2}SiO_4 + 8.2H_2O \rightarrow 1.8Mg(OH)_2 + 3Mg_3Si_2O_5(OH)_4 + 0.4Fe_3O_4 + 0.4H_2$) and other water-rock reactions or microbial processes. Figure adopted from Paper III.

low-temperature (>30 °C) upper crustal conditions (Neubeck et al. 2011, Szponar et al. 2013, Etiope & Ionescu 2014). Hydrogen, which fuels both abiotic and microbial CH_4 production, may originate from the radiolysis of water (Vovk 1987, Lin et al. 2005, Dzaugis et al. 2016), water–rock reactions (Neal & Stanger 1983, Devirts et al. 1993, McCollom & Bach 2009, Mayhew et al. 2013) or microbial processes (e.g. Nandi & Sengupta 1998).

1.2 Deep continental biosphere

Within the continental bedrock, life has been encountered at least down to 3.5 km below the surface level (bsl) (Szewzyk et al. 1994, Borgonie et al. 2011). Deep subsurface life is mainly limited to single-celled microorganisms, including bacteria, archaea and fungi (e.g. Pedersen 2014). In addition, viruses have been found in the deep continental biosphere (Kyle et al. 2008, Nyyssönen et al. 2014), and even multicellular organisms (nematodes) have been observed deep inside the bedrock fractures (Borgonie et al. 2011). In total, it has been estimated that the deep continental biosphere may cover up to 20% of the Earth's biomass (McMahon & Parnell 2014).

Thus, it is perhaps surprising to notice that the deep biosphere in continental shields was not recognised before the late 1980s (Pedersen & Ekendahl 1990, Pedersen 1993). However, considering the overall low number of deep groundwater studies prior to the 1980s, challenges related to sampling deep drill holes and mines, and generally low cell numbers of between 10^6 to 10^3 cells mL^{-1} of groundwater (McMahon & Parnell 2014), the lack of data is not so unexpected. Furthermore, many of the microbes found in these environments remain uncultured because of their extreme living conditions and slow cell turn-over times of up to thousands of years (Hoehler & Jørgensen 2013), and molecular biological methods capable of investigating the uncultured microbes have only recently been developed (see also Paper III).

The general requirements for life, including water, space, a suitable temperature and pressure and sources of energy, carbon and nutrients for biosynthesis, also apply at great depths. Probably the first of life's requirements to become limiting is temperature, as the known limit for life is 122 °C (Takai et al. 2008). In Finland, where the geothermal gradient is 15 °C km^{-1} on average (Kukkonen 1989), this temperature is met at more than 8 km bsl. High pressure is hardly a limiting factor, as some microorganisms have been observed to grow at pressures exceeding 100 MPa (Pikuta et al. 2007), which is equal to a hydrostatic pressure caused by a 10 km water pillar.

Devoid of direct energy from sunlight, the deep dark biosphere has taken geochemical energy into use. Chemotrophic organisms respire various chemical compounds available in groundwater and the bedrock from O_2 (aerobic reactions) to anaerobic electron acceptors such as Fe^{3+} and nitrate (NO_3^-) (e.g. Canfield et al. 2005, Konhauser 2007). The dependence on geochemical energy means that the deep biosphere is in constant interaction with the geosphere. For example, deep dwelling microorganisms can convert sulphate to sulphide (SO_4 reduction), produce CH_4 (methanogenesis) or oxidise it (methanotrophy), thereby affecting the dispersal or retention of various chemical compounds (e.g. Pedersen 2014).

Most of the studies on the deep continental biosphere have considered autotrophic organisms to dominate in these environments, as they could use inorganic carbon (CO_2/DIC) as the sole source of carbon (Paper III). Their energy metabolism is also independent of organic carbon compounds, and chemolithoautotrophs instead gain energy by oxidising reduced inorganic compounds such as nitrite (NO_2^-), Fe^{2+}, sulphide, CH_4 and H_2 (e.g. Canfield et al. 2005, Konhauser 2007). However, there is increasing evidence that heterotrophs, which use organic compounds as a source of carbon and/or energy, also play an important role in deep microbial communities (Purkamo et al. 2015, 2016, Wu et al. 2016).

1.3 Isotopes in deep groundwater studies

Isotopes, i.e. atoms that have the same number of protons but a different number of neutrons, are broadly studied in different scientific disciplines, including the hydrogeochemistry of deep groundwaters. Isotopes are usually measured as isotope ratios by mass spectrometric methods and the stable isotope ratios (R) such as $^{18}O/^{16}O$, $^2H/^1H$ and $^{13}C/^{12}C$, reported using δ-notation per mill (‰) relative to international standards:

$$\delta(‰) = \left(\frac{R_{sample}}{R_{standard}} - 1\right) * 1000 \qquad (1)$$

The standards used for the isotope systems considered in this thesis include Vienna Standard Mean Ocean Water (VSMOW) for H and O (in water) and Vienna PeeDee Belemnite (VPDB) for C and O (in calcite). Following a common practice, the results for radiogenic isotopes such as noble gases and strontium are given as isotope ratios without normalisation to a standard.

Isotope methods are based on comparisons of the isotopic compositions of different phases rather than the absolute values. Several notations are used for this purpose. Isotopic separation (Δ) observed between phases x and y is simply the difference in their δ-values in ‰ (Eq. 1):

$$\Delta_{x-y} = \delta_x - \delta_y \qquad (2)$$

while the isotope fractionation (α) between phases x and y is:

$$\alpha_{x-y} = \frac{1000 + \delta x}{1000 + \delta y} \qquad (3)$$

which is correlated with temperature (T, in Kelvin) as follows:

$$_y = aT^{-2} + bT^{-1} + c \qquad (4)$$

Experimentally determined and calculated fractionation factors for different phase pairs and temperature ranges have been compiled, for example, by Clark and Fritz (1997) and Chacko et al. (2001).

In contrast to the mainly temperature-controlled equilibrium fractionation, kinetic fractionation arises from incomplete or unidirectional reactions, which are typical features of microbial processes and diffusion (e.g. Hoefs 2004). Kinetic fractionation can lead to ex-

tremely large differences between the isotopic composition of the reactant and the product, as observed in experimental conditions (e.g. Clark & Fritz 1997, Canfield et al. 2005). However, in natural environments, the interpretation of isotopic results is challenged by several fractionating processes occurring in parallel and due to incomplete background information on initial isotopic compositions. The openness of the system, i.e. the possibility of starting materials being replaced and products being deposited or escaping, also plays a key role in isotopic evolution (e.g. Clark & Fritz 1997).

In cases where the partitioning of isotopes takes place between two reservoirs, one of which is diminishing, the isotopic composition of the residual changes exponentially according to a law called Rayleigh distillation (e.g. Clark & Fritz 1997). The general expression of the Rayleigh law is:

$$R = R_o * f^{(\alpha-1)} \qquad (5)$$

where R is the isotopic ratio of the reactant, R_o is the initial ratio and f is the remaining fraction of the initial reservoir. Many reactions relevant for deep groundwater evolution from the hydration of silicates (e.g. Kloppmann et al. 2002) to partial degassing of noble gases (Ballentine et al. 2002, Matsumoto et al. 2004) have been shown to follow Rayleigh fractionation.

Origin and evolution of deep saline groundwaters

The most famous example of the Rayleigh distillation in hydrogeology is the fractionation of water stable isotopes in precipitation, which leads to ^{18}O and ^2H depletion in the cold regions and forms the basis for interpreting the global hydrological cycle (Clark & Fritz 1997). The correlation between $\delta^{18}O$ and δ^2H of precipitation is defined as the Global Meteoric Water Line (GMWL; Craig 1961):

$$\delta^2H = 8\delta^{18}O + 10 ‰ \qquad (6)$$

Fine-tuned by observations at the regional scale, local meteoric water lines (LMWLs) have also been derived, for example, for Finland (Kortelainen 2007). The isotopic composition of hydro-

gen and oxygen in precipitation is also reflected in shallow fresh groundwaters (Fig. 2).

The deviation of isotopic composition of water from the GMWL is commonly described as the deuterium excess (d) (Dansgaard 1964):

$$d = \delta^2 H - 8\delta^{18}O \tag{7}$$

Similarly, oxygen depletion can be calculated to gain a numerical value for the deviation of the oxygen isotopic composition from the GMWL (or LMWL). Although used more rarely, oxygen depletion in combination with deuterium excess may be a good measure of isotopic evolution in cases where the driving force for the shift is other than evaporation, such as in deep saline groundwaters (Kloppmann et al. 2002).

In the study of deep groundwaters, stable isotopes of water are a self-evident starting point, which display characteristic compositions of hydrogen and oxygen (Fig. 2), and are a powerful tool to investigate mixing relations between contrasting water bodies and water–rock interaction (e.g. Frape et al. 1984, Kloppmann et al. 2002). Usually, one or more other isotopes from dissolved phases (e.g. Cl, Br, B) are used to support these studies, as well as to investigate the origin of salinity (e.g. Bottomley et al. 1999, Stotler et al. 2010b). Some of the most frequently used are strontium isotopes, of which [87]Sr is radiogenic (from [87]Rb), and therefore potentially reflects the changes in water–rock interaction with time and lithology, in addition to being a suitable tracer to study mixing (Smalley et al. 1988, McNutt et al. 1990, Négrel & Casanova 2005, Négrel et al. 2003, 2005, Wallin & Peterman 2015).

Groundwater residence time

Radioactive isotopes decay at constant rates and thus can be used for age dating of geological materials. As the only way to measure the residence time of water molecules is by using tritium (^{3}H), with a half-life of only 12.43 years, most residence time calculations of deep saline groundwaters rely on indirect methods based on either the accumulation or decay of the dissolved components. Previous studies on deep saline groundwaters have indicated that the residence times often exceed the range for ^{14}C and even [36]Cl dating, i.e. are more than 50 ka and 1.5 Ma, respectively (Louvat et al. 1999, Lippmann et al.

2003, Gascoyne 2004). The ^{14}C results in carbon-poor groundwaters are especially challenging to interpret because of the potential for dissolution of modern carbon from the atmosphere and the precipitation-dissolution of calcite (e.g. Ivanovich et al. 1992). Therefore, the accumulation of chemically inert radiogenic and nucleogenic noble gases ([4]He, [21]Ne and [40]Ar), which accumulate with time as products of the radioactive decay of U, Th, K in the bedrock, can be better used for dating purposes in cases where extremely long residence times are expected (e.g. Torgersen 1980, Lippmann et al. 2003, Trinchero et al. 2014). Necessary background informaton includes the concentrations of radioactive elements in and physical properties of the bedrock (e.g. Torgersen 1980, Ballentine et al. 2002).

Tracing the deep carbon cycle

Hydrocarbons occur in abundance in deep saline groundwaters (Table 1), and the cycle of carbon between the geosphere and the biosphere is of great importance in understanding water–rock–microbe interactions. Geochemical methods in the study of the origin, source and cycling of carbon in the deep continental biosphere are reviewed in Paper III. In brief, isotopic fractionation may be used for separating between abiotic and microbial processes, as well as between different metabolic strategies, such as microbial methanogenesis by autotrophic and heterotrophic pathways (e.g. Schoell 1980, Sherwood Lollar et al. 1993a,b, 2006, 2008, Whiticar 1999, Canfield et al. 2005, Valentine et al. 2004). The separation of different hydrocarbon-generating mechanisms (Fig. 3) is mainly based on the isotopic composition of CH_4, as microbes are known to prefer lighter isotopes due to their lower bond strength (Schoell 1980, Whiticar 1999), while the most ^{13}C-rich CH_4 is commonly related to abiotic processes (Etiope & Sherwood Lollar 2013). However, significant overlap between the different pathways may occur, especially in carbon-limited environments (Bradley et al. 2009, Tazaz et al. 2013). Consequently, compositional evidence of gases, together with the isotopic composition of longer chained hydrocarbons and other hydrogen- and carbon-bearing phases (i.e. H_2, H_2O, $CaCO_3$, CO_2), is needed to gain a more complete picture of carbon cycling (e.g. Bernard et al. 1976, Stotler et al. 2010a, Potter et al. 2013, Paper III).

1.4 Outokumpu Deep Drill Hole

This thesis study was based on geochemical samples collected between the years 2010 and 2012 in the Outokumpu Deep Drill Hole, eastern Finland (62°43'02.63''N, 29°03'55.01''E), and its drill core. The Outokumpu Deep Drill Hole is a scientific geolaboratory that was drilled in 2004–2005 by the Russian drilling company NEDRA on assignment from the Geological Survey of Finland (GTK). The nearly vertical (maximum deviation 9°) drill hole has an inner diameter of 22 cm and reaches the depth of 2516 m below the surface (Kukkonen 2011). Rotary drilling was carried out with steel-tooth drilling bits, and the drilling and flushing fluid was retrieved from the municipal water supply. The continuous coring and the lack of casing below 39 m depth mean that both the rock material and groundwater are directly accessible. The only additives used during drilling were concrete, which was used to stabilise the drill hole walls mainly in the uppermost 300 m, bentonite and peat for maintaining the proper viscosity of the drilling fluid and to stabilise the walls between 400 to 950 m depth, and sodium fluorescein (uranine) dye, which was added to the drilling water whenever water was fed in the flush water circuit in order to monitor mixing with the formation fluids (Ahonen et al. 2011).

The lithology along the Outokumpu Deep Drill Hole is presented in Figure 4. The drill hole mainly dissects metasedimentary rocks, i.e. mica schist and biotite gneiss (Västi 2011). These were formed ca. 1.9 Ga from turbiditic greywacke by metamorphism at amphibolite facies (550–675 °C at 3–5 kbar) (Kontinen & Sorjonen-Ward 1991, Säntti et al. 2006, Lahtinen et al. 2010). Between 1300 and 1600 m depth, an ophiolitic rock assemblage (Outokumpu assemblage) of approximately the same age consisting of serpentinite, black schist, skarn and quartz rock was found, which is known to host the Outokumpu Cu-Co-Zn sulphide deposits (Loukola-Ruskeeniemi 1999, Kontinen et al. 2006), although indications of economic concentrations of metals were not encountered in the drill hole. Thin layers of black schist and disseminated graphite are also found in association with mica schist throughout the drill hole (Fig. 4). Below 2 km depth, the main rock types are pegmatitic tonalite and granodiorite (Västi 2011). These granitic rocks dissect the mica schist and are presumably related to the nearby Maarianvaara granites, which date back to 1.86 Ga (Huhma 1986). Quaternary silt and sand layer of over 30 m thick covers the bedrock, which was eroded to its present level at the latest by 600 Ma (Kohonen & Rämö 2005).

Water occupies the pores and fractures of the Outokumpu bedrock, which has an average porosity of 0.5% (Airo et al. 2011). Hydraulic tests were conducted at 500 m intervals during the drilling, and revealed a rapid decrease in hydraulic conductivity with depth from 7.5×10^{-6} m s^{-1} (0.45 mm min^{-1}) at 500 m to 5.3×10^{-7} m s^{-1} (0.0032 mm min^{-1}) at 1000 m depth, while the deeper sections were defined as impermeable (Ahonen et al. 2011). The testing system was also equipped with a pressurised sampler, from which samples were separated at the surface for the geochemical analysis of water and gas. While the 500 m and 2500 m samples contained almost no intrinsic fluid based on the sodium fluorescein concentrations, almost pure formation fluid was captured from 1000 m depth which also contained abundant gases, mainly CH_4 and N_2 (Ahonen et al. 2011).

Increased salinity of the water was already detected during drilling. The subsequent measurements of electrical conductivity (EC) directly after drilling in February 2005, in April and September 2006, September 2008 and August 2011, confirmed the influx of saline water from fracture zones into the drill hole at rates from 90 mL min^{-1} at 790 and 990 m depths to 10 mL min^{-1} at 2390 m depth (Sharma et al. 2016) (Fig. 4). Due to an order of magnitude decrease in hydraulic conductivity, salinity kept increasing from 2006 to 2011 below 1000 m depth, while in the upper part, EC stabilised more readily (Fig. 4). In 2007 and after, samples of water no longer contained sodium fluorescein or tritium, and the stable isotopic composition of water clearly deviated from the meteoric water line (Ahonen et al. 2011).

The drill hole bottom temperature at 2516 m reaches only a moderate 40 °C (Kukkonen et al. 2011), and the conditions have been proved to be suitable for microbial life. The microbial cell densities decrease with depth from 10^5 to 10^3 cells mL^{-1}, and a slight decrease in cell density has typically also been observed during pumping (Itävaara et al. 2011a, 2011b, Purkamo et al.
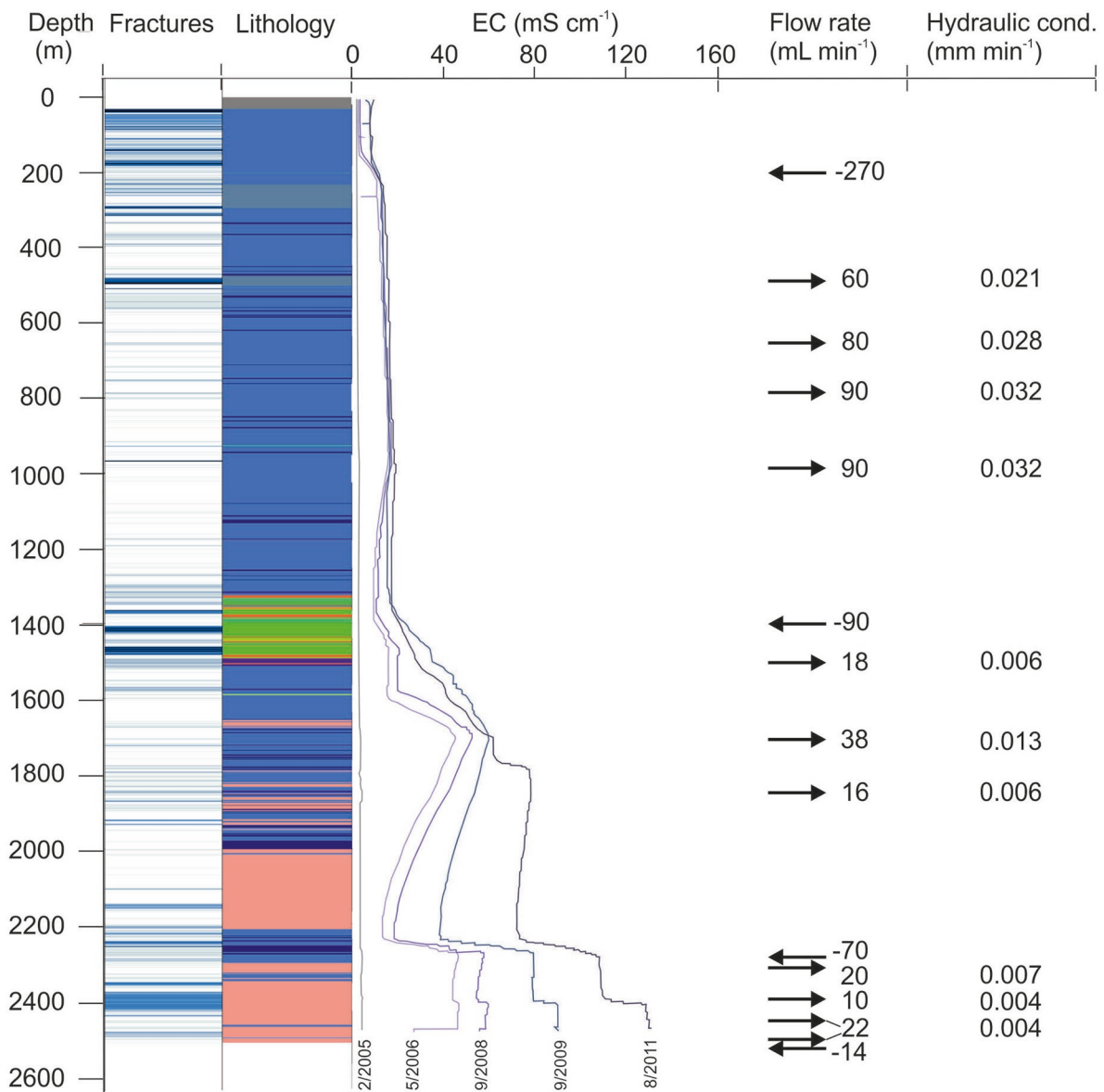
Fig. 4. Fractures, lithology, electrical conductivity (EC) logs, flow rates and hydraulic conductivities along the Outokumpu Deep Drill Hole. Lithologies are: blue = mica schist, dark blue = biotite gneiss, purple = black schist, green = serpentinite, red = skarn, yellow = quartz rock and pink = pegmatitic granite (Västi 2011). Negative flow rates indicate flow from the drill hole into the fractures (arrows pointing left). Modified after Ahonen et al. (2011), Kukkonen et al. (2011) and Sharma et al. (2016).

2013, 2016). Bacteria, archaea and viruses were all detected (Nyyssönen et al. 2014). Furthermore, molecular biological methods have been used to characterise the microbial communities and their metabolic potential. Despite the decline in biomass with depth, diversity remains high, including microbial groups with the potential for sulphate and nitrate reduction, hydrogenotrophic and versatile types of hetero-trophic methanogenesis and acetogenesis, as well as methanotrophy (Itävaara et al. 2011a,b, Nyyssönen et al. 2014, Purkamo et al. 2013, 2015, 2016). In addition, so-called microbial dark matter, i.e. microbes without known cultured relatives and metabolic features, are common, especially in the deepest parts of the Outokumpu Deep Drill Hole (Purkamo et al. 2016).

2 AIMS OF THIS THESIS

Even though the presence of saline groundwaters deep within continental shields has been known for more than a century, understanding of the origin of salinity and abundant dissolved gases, in addition to their unique isotope composition, is still debated. The presence of microorganisms has added an important, yet poorly understood, third player in the game, commonly thought to be an interplay between water and the bedrock. Access to these environments only through deep mines and drill holes means that technical challenges are also frequently faced in these studies.

At the same time, there is an increased need to better characterise deep groundwaters and to know how they have evolved because of the increased use of bedrock in the construction of underground facilities and exploitation of deep ores and geothermal energy. This is also the case in Finland, where nuclear wastes have been decided to be deposited deep within the bedrock.

The objective of this thesis study was to examine groundwater and dissolved gases in the Outokumpu Deep Drill Hole, as an example, in order to understand how the groundwater has evolved via geochemical and microbiological processes through time and space. More specifically, the aims were to:

- Test and develop sampling methods to obtain representative water and gas samples down to 2.5 km depth (Papers I, II and IV). Hypothesis: Different sampling techniques are better for vertical profiling than obtaining well-focused samples from fracture zones or studying dissolved gases.
- Characterise the salinity, water stable isotope composition and dissolved gases in the Outokumpu Deep Drill Hole groundwater (Paper I). Hypothesis: Salinity, a shift in the isotopic composition above the meteoric water line and the abundance of gases increase with depth due to the mixing of fresh groundwater with concentrated shield brine.
- Determine the origin of deep groundwater at Outokumpu (Paper I). Hypothesis: Deep saline groundwaters originate from meteoric water by water–rock interaction.
- Determine the time scale of deep groundwater evolution (Papers I and II). Hypothesis: Millions of years are needed to produce the high salinity and water stable isotope composition typical of deep saline groundwaters within continental shields.
- Determine the origin of methane (Papers III and IV). Hypothesis: Methane is produced *in situ* from CO_2 and H_2 by methanogenic microorganisms and in abiotic reactions.

3 MATERIAL AND METHODS

Samples for this thesis study were collected from the 2516 m deep Outokumpu Deep Drill Hole, located in eastern Finland, between the years 2010 and 2012. In addition, samples for the fracture mineral study were taken from the Outokumpu drill core at depths between 100.90 and 2240.70 m.

The different fluid sampling techniques used were pumping with and without expandable packers (Ahonen et al. 2011, Purkamo 2015), tube sampling (Nurmi & Kukkonen 1986) and pressurised sampling using both Leutert positive displacement sampler (PDS) (Regenspurg et al. 2010) and PAVE pressurised sampling device (Haveman et al. 1999, Ahonen et al. 2011). A summary of the sampling campaigns is provided in Table 2.

Pumping times varied from 16 to 117 days (Table 2). To monitor possible changes in the fluid with time during pumping, the temperature, dissolved O_2 concentration, redox potential, electrical conductivity (EC) and pH were measured on-line using sensors (WTW and Hamilton) attached to a flow-through cell (Fig. 5). Field measurements also included the determination of alkalinity by titration to pH 4.5 and analysis of the gas composition using a quadrupole mass spectrometer (QMS) from the PDS samples. Atmospheric volume fractions of gases were also measured on site in Outokumpu with a QMS, and the results were used to correct the gas composition for air contamination (Paper II).

Table 2. Fluid sampling campaigns in the Outokumpu Deep Drill Hole in 2010 –2012.

Time	Sampling method	Depth	Total water volume retrieved
		m	m³
27.5.-20.9. 2010	Pumping, packer at 1190 m depth	2260	6.9
21.9.-9.11. 2010	Pumping between packers	500	9.8
15.-19.5. 2011	Tube	0-2450	0.154
8.-17.6. & 14.7.-2.8. 2011	Pumping	2300	3.2
3.-18.8. 2011	Pumping	1820	1.0
24.-29.8. 2011	Positive displacement sampler	500, 970, 1470, 1820, 2350, 2480	0.005
5.9.-6.10. 2011	Pumping	970	3.8
10.-13.10. 2011	Tube	0-1050	0.066
5.5.-18.6. 2012	Pumping between packers, PAVE	180	22.5

Fig. 5. On-line fluid monitoring during pumping. Attached to the flow through cell are (from left to right) a combined electrical conductivity (EC), O_2 and temperature sensor and sensors for measuring the redox potential and pH. The pumped fluid enters the cell from the bottom left end and comes out through the tube on the upper right end. Photo: Ilmo Kukkonen, University of Helsinki.

Details of the sampling and the geochemical and isotopic analysis of water and gas are provided in Papers I, II and IV. In brief, the samples taken for the determination of cations and isotopic composition of dissolved inorganic carbon (DIC) were filtered and treated with ultra-pure 65% HNO_3 and 85% H_3PO_4, respectively. Sulphide samples were fixed with 1 M NaOH and 1 M zinc acetate and sulphate samples were filtered (<0.45μm). Unfiltered and untreated samples were used for other anion analyses and the determination of total organic carbon (TOC) and alkalinity. Samples for dissolved organic carbon (DOC) determination, as well as the isotopic analysis of water and strontium, were filtered (<0.45 μm) but not chemically treated. Gas samples from the tube sampler and pumped fluid were taken into head space bottles sealed with rubber septa and flushed with argon or N_2 and sample water prior to gas collection or into inverted glass bottles (Schott) in a bucket filled with sample water. Noble gas samples were collected into copper tubes and gas sampling bulbs made of glass in an evacuated sampling line and into copper tubes directly attached to the tube sampler.

Thin sections and carbon tape-mounted preparations were prepared for optical and scanning electron microscopic (SEM) investigations of the mineralogy of fracture fillings and veins. Cal-

cites were separated for isotope analysis under a microscope by using a steel blade (Paper IV).

Analyses of cations and anions (Article I), gas composition (Papers I, II and IV) and the isotopic composition of hydrocarbons and H_2 (Paper IV) were conducted at commercial laboratories according to standard protocols. Ion-coupled plasma mass spectrometric and optical emission spectrometric (ICP-MS and ICP-OES) methods were used for the determination of cations at Labtium Oy. Anions were determined by ion chromatography at Labtium Oy (Br, Cl) and TVO Nuclear Services (SO_4) and by spectrophotometry at Ramboll Analytics (sulphide). TOC and DOC were analysed with a TOC analyser at Labtium Oy. Gas compositions were analysed by gas chromatography (GC) at Ramboll Analytics. Isotopic compositions of gases were determined using an isotope ratio mass spectrometer (IRMS) at the University of Waterloo Environmental Isotopes Laboratory (uwEILAB) and Hydroisotop GmbH. Measurement uncertainties (at the 95% confidence level) were ≤10% for Ba, Br, Mg and Si, 10–20% for Ca, Na and I, 20–25% for Cl and Sr, 30–35% for B, K and Li, 11% for SO_4 and 11–40% for sulphide. High salinity challenged the analysis and the high uncertainties are due to the dilution of the samples. The relative uncertainties of gas composition determinations were <8% for hydrocarbons, <3% for H_2, <4% for O_2 and N_2, <6% for CO_2 and <10% for He and Ar. Analytical errors related to the isotope determination of gases were ±0.5‰ for $\delta^{13}C$ and ±7‰ for δ^2H of hydrocarbons, and ±10‰ for δ^2H of H_2.

The isotopic composition of water was determined by both IRMS and cavity ring down spectrometric (CRDS) methods at the Geological Survey of Finland (GTK) (Paper I). Even though the former method is based on a separate analysis of O from CO_2 gas equilibrated with water and H from H_2 produced by high temperature reduction of water with zinc, while the CRDS optically determines the absolute abundances of isotopologues of water molecules, a good correlation was found between the results of these fundamentally different methods when applied to the same samples. Analytical errors were <0.1‰ for $\delta^{18}O$ and ≤1.0‰ or <0.5‰ for δ^2H in the IRMS and CRDS methods, respectively.

The isotopic composition of strontium ($^{87}Sr/^{86}Sr$) was determined at GTK (Paper I). Strontium was purified from evaporated samples using EICHROM Sr-specific resin (50–100 µm), the isotopic ratio was determined with a thermal ionisation mass spectrometer (TIMS) in a dynamic mode and the $^{87}Sr/^{86}Sr$ ratios were normalised to a $^{87}Sr/^{86}Sr$ ratio of 0.1194. The precision of the analysis was approximately 0.002% at the 2σ level.

The relative abundance and isotopic composition of noble gases were determined at GFZ Potsdam using an IRMS specifically designed for the analysis of noble gases (Paper II). After gas purification in a line consisting of a cold trap, two Ti-sponge getters and two Zr-Al getters, noble gases were cryostatically absorbed at 50 K (Ar, Kr and Xe) and at 11 K (He and Ne) and released into analysis one noble gas at a time by sequentially heating the cold heads to 70, 100 and 150 K to release Ar, Kr and Xe, and to 35 and 120 K to release He and Ne, respectively. The reproducibility of the analysis was tested by analysing an artificial gas mixture of known composition and isotope ratios. In addition to the analytical uncertainty of the isotope ratio measurement, 2σ uncertainties of the measurements of rock density and porosity, as well as concentrations of U, Th and K in the rock (Airo et al. 2011, Västi 2011), were taken into account in the cumulative error calculation of noble gas residence times (Paper II).

Isotopic analyses of calcites and DIC were conducted at the Department of Geosciences and Geography at the University of Helsinki with a gas-sourced IRMS (Paper IV). In both cases, the component to be analysed was CO_2. Therefore, the calcite samples (150 µg each) were first reacted with concentrated H_3PO_4 for at least 1 h at 70 °C, and DIC samples were extracted in a vacuum line at 50 °C for 2 x 10 minutes. A few DIC samples from 2010 were analysed for their isotopic composition at the University of Jyväskylä with an IRMS without separate CO_2 extraction prior to the analysis (Paper IV). Comparative results for DIC isotopes at 500 m depth, although from different samplings, were gained with both methods. The reproducibility (1σ) of the analyses, based on the measurements of in-house calcite standards, was 0.07‰ and 0.12‰ for the $\delta^{13}C$ and $\delta^{18}O$ values of calcite, respectively and ≤0.60‰ for the $\delta^{13}C$ value of DIC. The concentration and speciation of DIC and saturation index (SI) of calcite were calculated using PHREEQC software (USGS 2014), as described in Paper IV.

4 RESULTS

4.1 Fluid retrieval from depths down to 2.5 km (Papers I, II and IV)

The reliable determination of groundwater properties requires representative samples. Fluid retrieval from depths down to 2450 m in the Outokumpu Deep Drill Hole was achieved with a tube sampler divided into 100 m sections, each of which was considered to represent one sample in order to obtain enough water and gas for analysis (Papers I, II and IV). Continuous profiles were gained, which generally had a good correlation of cations, anions and isotopic composition of water between different sampling campaigns (Paper I). However, mixing along the drill hole cannot be completely avoided in this method (Paper I), and the fluid is also prone to spontaneous degassing and thus potential fractionation of gases (Papers II and IV).

To overcome the problems in gas sampling, pressurised methods were utilised, which allow gas separation under controlled conditions in the lab. The main drawback of the pressurised methods used in this study, in addition to the specialised equipment needed, is the low sample volume (≤ 600 cm^3). Another problem that partly arises from the low sample volume is the contamination risk during degassing and storage, as the samples often remained below atmospheric pressure (Paper II).

By far the largest volumes of fluid were possible to obtain by pumping (Table 2). Thus, the possible drilling fluid component could also be effectively removed. Due to narrowing in the drill hole calliper in places, expandable packers could not be used at Outokumpu when pumping took place at depths of more than 1 km. By adjusting the pumping rate to equal the flow rate from the fracture into the drill hole, well-focused sampling can ideally also be achieved without packers (Purkamo et al. 2013). In practice, pumping large volumes of water from the deepest parts of the Outokumpu Deep Drill Hole, where hydraulic conductivities are the lowest (Paper I, Fig. 4), eventually led to slight changes in the geochemical profile. This was most clearly indicated in the magnesium concentration peak below 1200 m depth.

The differences between the different sampling methods were most clearly seen in the gas samples. In particular, the isotopic compositions varied with sampling type such that the most extreme values of δ^2H_{CH4} and $\delta^{13}C_{CH4}$ were found in the pressurised samples, while the tube sampler seemed to give average compositions due to mixing (Paper IV). For the water samples, the slight fluctuations observed in geochemical composition with depth and time can be related to hydrodynamic changes due to previous sampling activities rather than the sampling techniques themselves.

4.2 Characteristics of deep groundwater at Outokumpu (Paper I)

In order to characterize groundwater in the Outokumpu Deep Drill Hole, major and trace elements, pH and alkalinity were determined, together with the isotopic composition of water (δ^2H and $\delta^{18}O$) and dissolved strontium ($^{87}Sr/^{86}Sr$), as well as the gas composition (Paper I, Appendix 1). Throughout the drill hole, the groundwater was clearly distinct from present precipitation and fresh surface and groundwater in the area. The groundwater salinity increased from 5 g L^{-1} at 180 m to 69 g L^{-1} at 2480 m depth, and the water stable isotope composition was above the local and global meteoric water lines (LMWL and GMWL, respectively), with δ^2H_{H2O} from -89.5 to -55.9 ‰ VSMOW and $\delta^{18}O_{H2O}$ from -13.52 to -10.39 ‰ VSMOW (Fig. 6). Based on these features, the deep groundwater in Outokumpu can be classified as typical deep continental bedrock groundwater (Frape et al. 2004). However, it was noted that simple two-component mixing between fresh shallow groundwater and deep saline shield brine (e.g. Fritz & Frape 1982, Frape & Fritz 1987) cannot explain the vertical variation observed.

The observed differences in the geochemical and isotopic characteristics with depth were used to separate five water types along the drill hole: type I at 0–300 m below surface level (bsl), type II at 300–1300 m bsl, type III at 1300–1700 m bsl, type IV at 1700–2300 m bsl and type V below
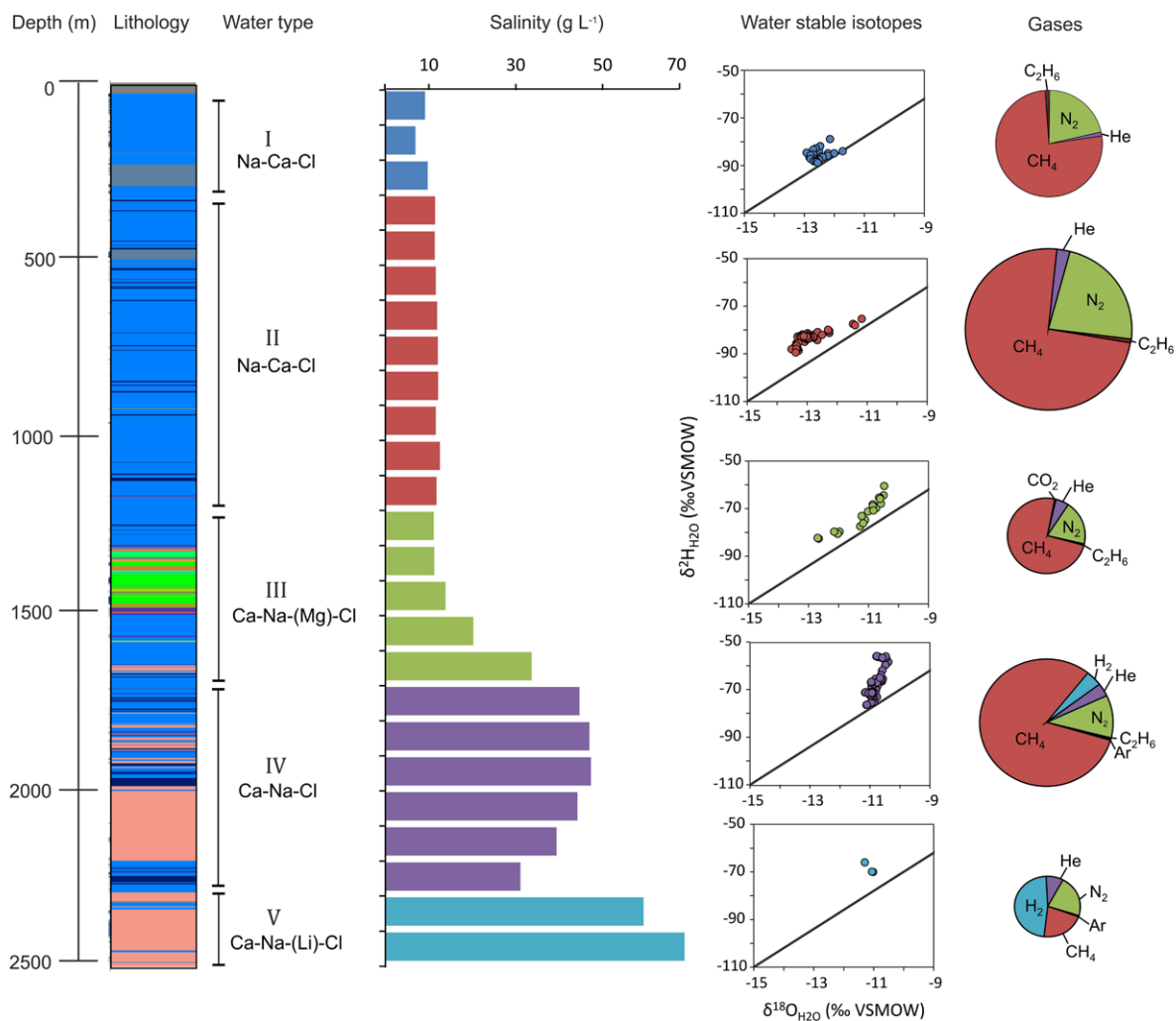
Fig. 6. Characteristic water types (I–V) along the Outokumpu Deep Drill Hole. See Fig. 4 for the explanations of the lithology. Water stable isotopes are plotted against the Global Meteoric Water line (GMWL). Sizes of the gas composition charts are comparative to total gas volumes. Modified after Paper I.

2300 m depth (Fig. 6). Each of the end-member water types discharge in the drill hole from different fracture zones separated from each other by tens to hundreds of metres of impermeable rock. A major divide zone was observed at 1300 m depth, where the salinity suddenly increases, the dominant cation changes from Na to Ca and water becomes enriched in ^{2}H and ^{18}O.

At the time of writing Paper I, the end-member composition of water type I could not be clearly identified in the drill hole because of disturbance caused by the cementation of the drill hole walls and mixing. However, in 2012, the likely source zone of type I at 180 m depth was isolated with packers and pumped for 45 days (Table 2). The results (Appendix 1) confirm that the type I is distinguished from the underlying type II by its δ^2H_{H2O} and $\delta^{18}O_{H2O}$ compositions,

which are closer to the GMWL (Fig. 6). The very high pH (>10) observed in the upper part of the drill hole was rapidly decreased during pumping and eventually levelled down to 8.5, confirming that the highest values were probably caused by the cementation.

In 2010, the pumping of fracture zone water at 500 m between packers revealed a vast homogeneous water body and the most representative samples of water type II. The highest gas/water ratios of up to 1.4 (STP) in pumped fluid and 1.07 in pressurised samples were found in water type II, at 500 and 970 m depths, respectively. The dissolved gas phase was dominated by CH_4 and N_2 (Fig. 6).

Going down in the drill hole, the horizon of water richest in sulphate (up to 17 mg L^{-1}) and magnesium (up to 222 mg L^{-1}) was met around

the ophiolitic rocks of the Outokumpu assemblage, which is the source zone of water type III. Further down, water type IV was found to be enriched in ^{2}H and ^{18}O compared to all other water types in Outokumpu, had a bright yellowish green colour and an unpleasant odour of reduced sulphur compounds. The gas phase was still dominated by CH_4, but a significant increase was observed in the concentration of H_2 in water type IV.

The boundary between water types IV and V at 2300 m was marked by an abrupt increase in salinity, especially in the concentrations of K and Li, an increase in the proportion of radiogenic strontium (^{87}Sr) up to the ^{87}Sr/^{86}Sr value of 0.73668 and a dramatic increase in the concentration of H_2 up to 2.2 mmol L^{-1}. Importantly, the isotopic composition of water was depleted in ^{2}H and ^{18}O compared to water type IV, despite the increase in salinity, which is in contrast to a simple two-component mixing hypothesis. The rock types surrounding the source zones of water type V are pegmatitic tonalite and granodiorite, which have probably shaped the geochemical composition of the adjacent water. Overall, the changes from one water type to other reflect changes in lithology, and point out the stagnancy, at least vertically, and evolution by water–rock interaction of the water types in isolation from the surface and from each other within the Outokumpu bedrock. The changes are also accompanied by changes in the microbial communities (Paper I, Nyyssönen et al. 2014).

4.3 Origin of groundwater (Paper I)

In addition to characterising the geochemical composition of deep fluids in Outokumpu, the main aim of Paper I was to investigate the origin of the groundwater. Potential sources considered were ancient meteoric water, seawater, magmatic and metamorphic fluids, as well as glacial melt water. A Rayleigh distillation (Eq. 5) based model of silicate hydrolysis was applied to assess the changes in the isotopic composition of the water (Fig. 7). Justification for the use of the Rayleigh model comes from the low water/rock ratio in Outokumpu (Airo et al. 2011), which allows an exponential change (enrichment in ^{2}H and depletion in ^{18}O) in the isotopic composition of water to occur (Kloppmann et al. 2002).

A good fit was found in the observed and modelled isotopic evolution pathways by silicate hydrolysis in terms of the deuterium excess and oxygen depletion, especially for water types I and II. The concentrations of Ca, Na and Cl also increase with the increasing deuterium excess. The enhanced O depletion of water types III–IV could be related to the formation of zeolites, which is probably an additional process leading to water stable isotope compositions above the GMWL accompanied by an increase in salinity (Karlsson & Clayton 1990, Stober & Bucher 2004, Bucher & Stober 2010), but may also originate from mixing with ^{2}H- and ^{18}O-depleted water. Fractionation between water and volatile phases was also discussed. Based on the concentrations of compounds that could exchange isotopes with water, only CH_4 was considered to be abundant enough to possibly enable compositional changes in the water stable isotopes.

In compliance with the silicate hydration hypothesis, two starting compositions plotting on the meteoric water line (GMWL) were selected to fit the model with the observed isotopic trends (Fig. 7). The first one (A) corresponds to precipitation and infiltration under 3 °C warmer climatic conditions than today, while the second one (B) is representative of a 10 °C warmer annual temperature. Alternatively, the original water component could contain seawater, in which case more seawater would have contributed to water types IV and V than I and II. However, the key points of evidence that do not support a seawater origin are 1) the different composition of dissolved ions (Ca, Sr, Na, K, B, SO_4, Mg), 2) the low Cl/Br ratio and 3) the continental setting. Previously, Piribauer et al. (2011) studied fluid inclusions from the Outokumpu Deep Drill Core and found no relationship between water stable isotopes or Cl/Br ratios between deep groundwater and the inclusions, which they concluded to be metamorphic palaeofluids. In this thesis research, on the basis of the study by Piribauer et al. (2011) and observations of vast amounts of saline groundwater at Outokumpu (Table 2), metamorphic and magmatic fluids could be excluded as a notable fluid source. Likewise, glacial
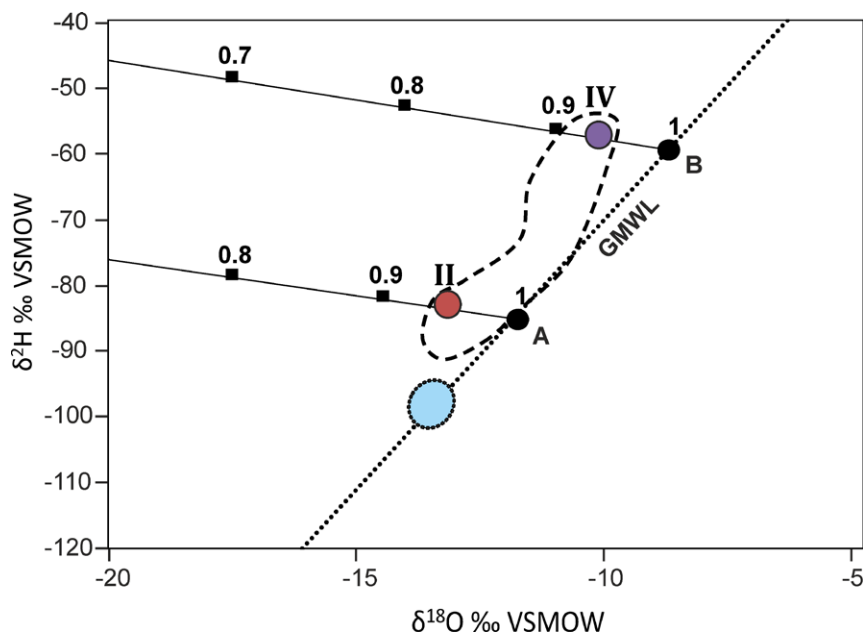
Fig. 7. Isotopic evolution through water-rock interaction (silicate hydration). End-member composition of the two water types (II and IV) with least disturbance by mixing have been depicted as examples and the overall range of isotopic compositions at Outokumpu indicated with the surrounding broken line. Numbers above the black squares show the residual water fractions as the isotopic composition of water evolves according to Rayleigh distillation at 25 °C (Eq. 5). Isotopic separation between the starting compositions A and B is hypothesized to originate from precipitation at 3 to 10 °C warmer than present climatic conditions, respectively. The isotopic range of present precipitation and fresh groundwater along the Global Meteoric Water Line (GMWL) is shown in light blue (from Kortelainen 2007). Simplified from Paper I.

melt waters could be excluded based on the lack of low δ^2H and $\delta^{18}O$ values in the water. Therefore, it could be concluded that the most likely source of deep groundwaters at Outokumpu is meteoric from precipitation under a warmer than present climate.

4.4 Residence time of groundwater (Papers I and II)

Based on the water stable isotope composition of the suggested meteoric water end-member, indirect evidence was gained from the residence time of groundwater (Paper I). The basis for this is the temperature dependence of the isotopic composition of rain water such that under warmer climatic conditions, precipitation is enriched in ^2H and ^{18}O compared to a cooler climate (e.g. Clark & Fritz 1997). Even though the isotopic composition of groundwater at Outokumpu now resides well above the meteoric water line (GMWL), it was possible to model the potential starting compositions on the GMWL using the Rayleigh distillation model for water-rock interaction, as described in the previous section 4.3. By assuming a continental location, the resulting compositions on the GMWL were shown to represent waters precipitated under climatic conditions 3 to 10 °C warmer than at present. In the more unlikely case of a dominantly marine climate, the temperature difference would be even larger (Rozanski et al. 1993). Taking account of the palaeotemperature records and plate tectonic movements, the likely period of groundwater formation at Outokumpu was bracketed to tens of millions of years (Paper I).

To better constrain the groundwater residence times at Outokumpu, the isotopic compositions of dissolved noble gases (He, Ne and Ar) were determined from six samples between 500 and 2480 m depth (Paper II). The method is based on the accumulation of radiogenic noble gases in groundwater at a rate proportional to their production from the decay of U, Th and K in the surrounding bedrock (e.g. Ballentine et al. 2002). After the determination of gas/water ratios and

the relative composition of gas, in addition to the specific measurement of isotope ratios with a noble gas mass spectrometer, the concentrations of radiogenic (^{4}He, ^{40}Ar) and nucleogenic (^{21}Ne) nuclides originating from the crust were defined by separating them from atmospheric sources. An entirely crustal signature of ^{3}He/^{4}He ratios within the range of 1–2 x 10^{-8} precluded the presence of any mantle component. The correction for atmospheric contamination was based on the measured O_2 concentration and, for Ar and Ne, the exclusion of dissolved and excess air components was carried out using known atmospheric ratios for ^{21}Ne/^{20}Ne (Eberhardt et al. 1965) and ^{40}Ar/^{36}Ar (Lee et al. 2006). Before calculating the noble gas residence times, the ^{21}Ne results that were found to be affected by mass fractionation were also excluded. Average U, Th, and K concentrations, effective porosities and rock densities determined from the Outokumpu Deep Drill Core by Airo et al. (2011) and Västi (2011) were used in the calculations, which therefore assume homogeneous properties for the bedrock.

No systematic change was observed in the noble gas concentrations and subsequent residence times with depth. *In situ* model ages indicated by ^{4}He and ^{21}Ne ranged from 17 (±4) to 58 (±14) Ma and 15 (±6) to 45 (±22) Ma, respectively, and were thus in good agreement with each other. However, model ages indicated by ^{40}Ar from 4.1 (±0.9) to 22 (±3) Ma were generally younger. The differences could be related to differences in the release of noble gases into groundwater, the higher sensitivity of Ar to air contamination and mixing with drilling fluid (Paper II).

Crustal flux and diffusion were also considered in order to determine their importance in modifying the concentrations of noble gas nuclides (Paper II). Since the continental crust has more uniform diffusion properties compared to confined aquifers in sedimentary basins, in addition to the substantial production of noble gases within the formation, and because the flux from continental crust has been observed to be consistent with steady-state degassing (Torgersen 2010), the accumulation of noble gases in excess by deep crustal flux was concluded to be very unlikely at Outokumpu. Moreover, a 1D diffusion model was applied to the determined He data, which showed that the diffusive front created by the loss of He into the atmosphere had reached the depth of only a few hundred metres (<500 m) and did not affect the determined *in situ* noble gas residence times.

Although the model ages obtained in this thesis study must be considered first order approximations, they nevertheless prove that the isolated fluids at Outokumpu are ancient and not related to more recent events such as Quaternary glaciations. Importantly, the two independent lines of evidence from water stable isotopes and noble gases are in good agreement, indicating isolation of the Outokumpu Deep Drill Hole groundwaters within the crust since the Eocene-Miocene epochs (56–5.3 Ma).

4.5 Biotic vs. abiotic hydrocarbon generation (Papers III and IV)

The main constituent of the dissolved gas phase above 2300 m depth in the Outokumpu Deep Drill Hole groundwater is CH_4 (Paper I, Fig. 6). As it is also a key component in the interface of geology and biology, CH_4 was targeted in studies presented in Paper III and IV. With the aid of background information compiled in Paper III, the aim of the study reported in Paper IV was to examine the origin of CH_4 and the minor amounts of longer chained hydrocarbons (ethane and propane) associated with it. More than 100 analyses of hydrocarbons were conducted, including the isotopic composition of methane, ethane and, in few cases, propane. To gain a better coverage of phases potentially taking part in the deep carbon cycle, the isotopic composition of H_2, dissolved inorganic carbon (DIC) and fracture calcites was analysed and the results combined with the existing isotope data from water (Paper I) and graphite (Taran et al. 2011).

A wide range of hydrocarbon isotope values were found, which suggests that no single process or source could be responsible for CH_4 formation at Outokumpu (Paper IV). The $\delta^{13}C_{CH_4}$ varied from −39.9 to −13.2‰ VPDB, $\delta^2H_{CH_4}$ from −404 to −136‰ VSMOW, $\delta^{13}C_{C2H6}$ from −49.7 to −22.7‰ VPDB, δ^2H_{C2H6} from −277 to −153‰ VSMOW, and $\delta^{13}C_{C3H8}$ from −39.5 to −35.2‰ VPDB. The $\delta^{13}C_{CH_4}$ values heavier than −20‰ VPDB were more common at depths greater than 1.5 km, and ^{13}C-

depleted CH_4 ($\delta^{13}C$ < -40 ‰ VPDP) was exclusively found in the upper 1 km of the drill hole (Paper IV).

The isotopic composition of DIC varied from -18 to -14‰ VPDB in the upper 1 km of the drill hole, with a general increase in $\delta^{13}C$ with depth, while much ^{12}C-depleted DIC with a $\delta^{13}C$ of -0.8‰ VPDB was found at 2260 m depth (Paper IV). In concert with the microbiological evidence from deep groundwater sites around the world (Paper III), the increase in $\delta^{13}C_{DIC}$ with depth was found to possibly indicate an increase in hydrogenotrophic over aceticlastic methanogenesis at greater depths. However, no correlation was found between Δ_{DIC-CH_4} and the modelled concentrations of DIC, and the values of αC_{DIC-CH_4} and αH_{H2O-CH_4} were most consistent with the aceticlastic pathway (Valentine et al. 2004, Sherwood Lollar et al. 2008) at all studied depths (Paper IV). The reason for these contradictory results may be that, in addition, an abiotic component is involved. This is also supported by the extremely ^{13}C-enriched nature (down to -13.2‰ VPDB) of the deepest sourced CH_4, a feature typically thought to be diagnostic of abiotic CH_4 (Etiope & Sherwood Lollar 2013). In addition, the V-shaped distribution of $\delta^{13}C$ of hydrocarbons from CH_4 to C_3H_8 is similar to gases previously related to the abiotic polymerisation of hydrocarbons (Sherwood Lollar et al. 2008).

As the contents of CO_2/DIC and organic carbon (Appendix 1) in the groundwater are low, and presumably cannot account for the high amounts of CH_4 detected, refractory organic carbon, i.e. graphite, was suggested as a potential primary carbon source for CH_4 in Outokumpu. Isotope fractionation related to this process was concluded to be minimal because 1) the formation takes place on a mineral surface where isotopes are randomly distributed, 2) excess H_2 is available and 3) closed system conditions prevail. Thus, the similar carbon isotope composition of graphite and CH_4 are in line with this hypothesis. Further evidence of the importance of ancient organic compounds was gained by comparing the amount and isotopic composition of CH_4 with lithology across the Fennoscandian Shield: by far the highest concentrations of CH_4 were found in metasedimentary rocks, particularly those containing graphite (Paper IV).

Calcites in the proximity of the hydraulically most active fracture zones at 1000 and 500 m, as well as in the upper 250 m depth, were found to have the most ^{13}C-depleted values below -15‰ VPDB (Paper IV), which may indicate carbon input from the oxidation of CH_4 (methanotrophy). This is in line with microbiological findings from several Fennoscandian Shield study sites, including Outokumpu, where methanotrophs have mainly been found above 1 km depths (Paper III). However, as the ^{13}C depletion of CH_4 was also highest at the shallower depths, microbial oxidation must be significantly outcompeted by CH_4 production, as could also be inferred from the low concentrations of DIC (0.16 mmol L^{-1} on average) compared to CH_4 (up to 32 mmol L^{-1} at 960 m depth; Paper I).

5 DISCUSSION

5.1 Model for the deep groundwater evolution at Outokumpu

The geochemical and isotopic results from deep groundwater at Outokumpu 1) enabled the characterisation of different water types (Paper I), 2) evidenced that long-term water–rock interaction within the time scale of tens of millions of years is responsible for the isotopic evolution and increased salinity of the water (Papers I and II) and 3) showed that both abiotic and biotic processes are actively contributing to the geochemical composition of the deep fluids (Paper IV). Based on these lines of evidence, a model is proposed for the formation and evolution of deep groundwater at Outokumpu (Fig. 8).

In Figure 8, the evolutionary path is divided into four steps. The first step is the groundwater *recharge phase*, which took place following precipitation under climatic conditions 3 to 10°C warmer than at present (Paper I). The exact time in years for step 1 cannot be given, as the residence time is by definition the time that, on average, has passed between the infiltration of

water to the ground and the moment when the sample was taken. In addition, the noble gases probably give a minimum estimate for the residence time. This is due to the assumption that 100% of crustal noble gas nuclides have entered the groundwater, as well as the conservative estimate of bedrock porosity of 0.5%, which does not take wider fractures into account (Paper II). Both the increase in porosity and lower release of noble gases will increase the model ages. The groundwater formation thus probably extends beyond the maximum of 58 (±14) Ma years obtained by the noble gas accumulation method. For example, the Ne isotope ratios gave indications of a fluid component potentially originating from the Precambrian (Paper II). However, the time frame within which the major part of the groundwater recharge took place can be bracketed to tens of millions of years (Paper II), and a major contribution of (Precambrian) metamorphic fluids could also be discarded (Paper I, Piribauer et al. 2011). Furthermore, the warm and humid climate that prevailed during the Eocene–Miocene epochs (e.g. Greenwood et al. 2010, Larsson et al. 2011), combined with the location of the Outokumpu area up to 8° south of its present position (Torsvik et al. 2001), gives support to the average residence time of 30 Ma.

Even though the bedrock was already eroded to its present level during step 1 (Kohonen & Rämö 2005), little evidence exists concerning the sedimentary cover at that time. The study by Gilg et al. (2013) suggests that at least the northern and eastern parts of Finland were on dry land, allowing kaolinites to deposit during the Eocene–Miocene epochs. In any case, it seems that meteoric water penetrated all the way into the fracture networks within the bedrock. As soon as the water was in contact with the rock, chemical water–rock interaction reactions began switching the noble gas clock on, increasing the salinity both by adding ions (mainly Cl, Na and Ca, but depending on the rock type, also Mg and Li) into water and by binding water into minerals and starting the isotopic evolution of hydrogen and oxygen in water molecules above the meteoric water line. The accumulation of hydrocarbons by microbial and abiotic reactions also began in the anaerobic conditions that were reached after the dissolved oxygen was consumed in the upper part of the flow path. As long as the hydraulic conductivity permitted water to flow freely within the fracture network, these changes were minor due to short contact with water and the surrounding rock. However, deeper down, fractures were scarcer and hydraulic conductivity was probably lower, allowing more changes to take place.

At some point, the connection between the surface and the bedrock closed, starting step 2, which is the deep groundwater *isolation phase*. In addition, different fracture networks were separated from each other which, in combination with different rock types, led to the evolution of different water types. The timing of the beginning of isolation must coincide with the mean residence time of groundwater, i.e. to be in the order of tens of millions of years in order to prevent noble gases from escaping and dilution of water by fresh meteoric water. The isolation was probably assisted by the uplift of the Fennoscandian Shield during the Cenozoic (Anell et al. 2009) and precipitation of minerals, mainly calcite and zeolites, on fractures, some of which eventually became filled, thereby losing conductivity (Fig. 8).

Despite the isolation, microorganisms survived without the supply of nutrients and carbon from the surface. The effective recycling of carbon diminished isotopic fractionation and led to ^{13}C-rich CH_4 compared to surface environments. Instead of CH_4 formation from primary organic matter or DIC, carbon sources in the bedrock itself, mainly graphite, were taken into use. In part, the enrichment of CH_4 in ^{13}C, especially below 1500 m depth, was probably due to the high partial pressure of H_2 and high salinity, which may have further diminished isotopic fractionation (Takai et al. 2008) or probably entirely stopped microbial methanogenesis (Thauer 2008). Indeed, based on compositional and isotopic evidence, abiotic CH_4 production, especially at depths below 1.5 km bsl, is likely. Such ^{13}C-enriched and ^{2}H-depleted CH_4, similar to the proposed dominantly abiotic end-member at Outokumpu, has also been found in deeply buried unconventional gas reservoirs in the Appalachian basin, where it was related to late stage processes (i.e. after oil cracking had gone into completion), presumably from graphitic C (Burruss & Laughrey 2010). Compared to methanogenesis, microbial oxidation of CH_4 is a minor process and mainly occurs in the upper 1 km
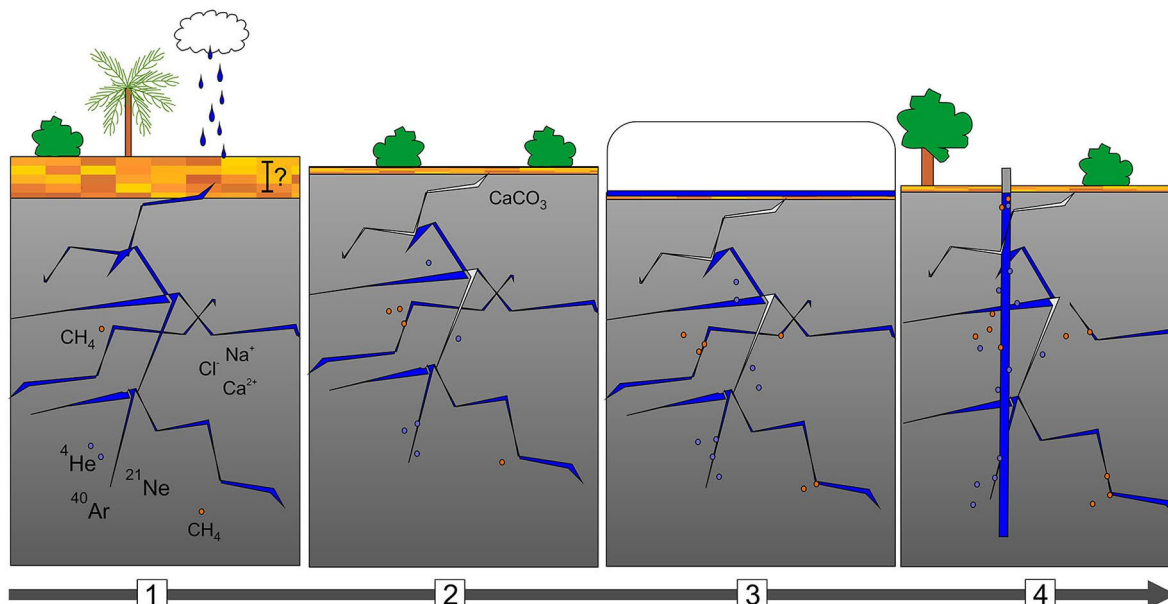
Fig. 8. Schematic of the deep groundwater evolution at Outokumpu. The different steps explained in detail in the text are 1. groundwater recharge phase, 2. isolation phase, 3. glaciations, and 4. drilling and sampling. The reactions producing gases and ions into the water shown in step 1 as well as precipitation of calcite ($CaCO_3$) shown in step 2 continue throughout the groundwater evolution. The figure is not to scale and does not represent the real fracture networks or different rock types of Outokumpu.

depth (Paper III), where ^{13}C-depleted carbon was recorded in some fracture calcites at Outokumpu (Paper IV).

The isolation from the surface was certainly efficient by the time of the Quaternary *glaciations* (step 3 in Fig. 8), as no glacial melt waters have been found from the Outokumpu Deep Drill Hole (Paper I). Instead, the groundwater flow was probably concentrated in the sedimentary layer. However, elsewhere at Outokumpu, characteristically ^{2}H and [18]O depleted glacial waters have been found (Blomqvist 1999), which emphasises the importance of local bedrock conditions in groundwater dynamics. Even though the melt waters did not enter the bedrock in the Outokumpu Deep Drill Hole area, other changes took place during the glacial phase: the bedrock went down due to the heavy load of the ice sheet and the temperature decreased. In fact, disruption of the thermal gradient can still be observed in the upper 1 km of the drill hole (Kukkonen et al. 2011). The present temperature and pressure conditions are above the methane hydrate stability field, but the fluids down to 1 km depth have probably experienced such conditions during the glaciations (Paper I). Nevertheless, it seems that in a closed system without any significant exchange of fluid with the surface or other fracture networks, these changes did not result in permanent changes in the isotopic composition of water or CH_4 (Paper I).

The final step 4 includes the *drilling and sampling* of groundwater. Even though not a natural phase in groundwater evolution, this step is necessary in order to access the groundwater and causes changes by re-opening the connections between different fracture networks and the surface, and possibly mobilising gases due to the pressure release. Fortunately, at Outokumpu, the casing through the sediments was tight enough to prevent modern fresh groundwater from discharging into the drill hole, as evidenced by increased salinity in the drill hole compared to a nearby shallow well at the same depth. Despite the mixing of groundwater with drilling water and along the drill hole, different water types could be discerned (Paper I). However, it is likely that a few hydraulically more conductive fracture zones at around 500, 1000 and 1800 m depths dominate the water column, and even more variability might be found if the drill hole was inspected section by section using packers.

5.2 Deep continental bedrock as a habitat for microbial life

Isolation from the surface for tens of millions of years (Paper II) has probably affected the microbial communities living in the deep continental bedrock environment. Firstly, as there is no constant supply of nutrients and carbon from the surface, the microbes probably utilise geological sources for energy and biosynthesis. The adaptation of microbes to the prevailing conditions at Outokumpu has been demonstrated by molecular biological methods (Nyyssönen et al. 2014), and is supported by the correlation of the microbial community structure with lithology and/or water types (Paper I). In addition to genes related to metabolic functions making use of the available geological sources of energy and nutrients, these methods have revealed protective genes involved in metal resistance and adaptation to high salinity through cation efflux mechanisms, especially at 2300 m, where the salinity is very high (Nyyssönen et al. 2014).

Secondly, under closed system conditions, and where the Gibbs free energy changes of reactions are small, such as in the anoxic deep continental subsurface, thermodynamics become significant compared to kinetic control, and the accumulation of metabolic products begins to affect the energetics of the species producing it (Großkopf & Soyer 2016). Microbes can overcome this waste problem by producing different products from the same substrate, that is, by diversifying (Großkopf & Soyer 2016). Indeed, at Outokumpu, microbial diversity is found to increase despite the decreasing cell density as a function of depth (Itävaara et al. 2011b, Nyyssönen et al. 2014). This gives further evidence for the microbial communities being well adapted to the prevailing hydraulically isolated and nutrient and energy poor conditions.

Another strategy to avoid the accumulation of metabolic products and to utilise the limited resources efficiently is recycling, such that the end product of one species is the substrate for another species. In contrast to the large isotope fractionation commonly related to microbial processes caused by kinetic factors, this recycling can lead to minimal fractionation between the substrate and the product, as observed for microbial CH_4 at Outokumpu (Paper IV) and elsewhere (Paper III). Such syntrophic relationships might be especially well developed in deep continental bedrock fractures, which are among the oldest ecosystems on Earth. The good adaptation of microbial communities to lithological and hydrological conditions in deep continental bedrock also means that variability in microbial community composition and functionality is expected from site to site.

The most productive subsurface environments, at least when carbon cycling is considered, seem to be those containing surface-derived carbon sources. This is demonstrated not only by the higher abundance of microbial cells in the near surface waters, but also by the clear correlation between the most CH_4-rich groundwaters and black (graphitic) schists originating from organic-rich sediments (Paper IV). Furthermore, despite the long isolation from the surface and assumedly slow pace of life, the deep dwelling microorganisms may activate rapidly should a suitable organic carbon source appear (Rajala et al. 2015). Together with the observation that heterotrophic carbon assimilation is common in the Outokumpu Deep Drill Hole biosphere (Purkamo et al. 2015, 2016), this suggests that organic carbon sources are favoured when available, and even refractory organic remains such as graphite may be utilised. Even though no methanogenic archaea are currently known to be capable of using graphite as a carbon source (e.g. Thauer 2008), many of the subsurface microorganisms have not been cultured and their metabolic processes remain unclear. Recently, for example, more diverse metabolic capabilities of the deep subsurface microbes named Hadesarchaea (formerly known as SAG-MEG for South-African Gold Mine Miscellaneous Eryarchaeal Group), which have also been found in Outokumpu (Purkamo et al. 2016), were proposed (Baker et al. 2016). Thus, the view of the deep subsurface as an environment dominated by autotrophs should be reconsidered.

5.3 Global perspective

By comparing the results obtained in this study with previous investigations in Precambrian continental shields in Fennoscandia and globally, common features were observed. These include a water stable isotope composition that has shifted above the GMWL, increased salinity dominated by Ca, Na and Cl, and high amounts of non-atmospheric dissolved gases. Likewise, the residence times obtained in this study from the Outokumpu Deep Drill Hole are in line with other noble gas residence time estimates typically between millions and hundreds of millions of years (Lippmann et al. 2003, Trinchero et al. 2014, Bottomley et al. 1990, Greene et al. 2008) from different sites within the Precambrian continental shields in Fennoscandia, Canada and South Africa (Fig. 9).

Similarities were also observed considering carbon cycling in the deep geobiosphere. Autotrophy plays a role in microbial carbon metabolism, especially in the deeper parts of the Outokumpu deep biosphere, as well as in old saline water within the granitic bedrock of Äspö, Sweden (Wu et al. 2016), while more diverse, heterotrophic pathways are likely to be more important where organic carbon is present, such as in the proximity of graphitic schists and within the more hydraulically dynamic upper crust (Simkus et al. 2016, Paper IV). Hydrocarbons at Outokumpu had a ^{13}C-rich isotope com-

position, but systematically lighter in the order methane, propane and ethane, similar to those previously reported from the Kidd Creek mine and other deep groundwaters in Precambrian continental locations in Canada and South Africa (Sherwood Lollar et al. 2008). By comparing the isotopic compositions and microbiological evidence with depth, it can be concluded that abiotic hydrocarbons apparently become more important at greater depth, as observed, in addition to this study, from South Africa (Simkus et al. 2016). Thus, even though this study was concentrated in one location, the Outokumpu Deep Drill Hole, the results can also shed light on deep groundwater evolution and water–rock–microbe interactions elsewhere in similar continental settings, especially where stagnant saline groundwaters have been found.

However the depth at which saline fluids are found varies from site to site. In contrast to Outokumpu, where increased salinity is observed already at the well head, there is usually a more dynamic upper fresh water layer (e.g. Blomqvist 1999, Gascoyne 2004, Laaksoharju et al. 2008, Trinchero et al. 2014). This can be due to several reasons. Similarly to surface waters, topography also affects advective flow in the bedrock, and greater topography assists in the penetration of fresh water, as observed in the Scandinavian Caledonides (Juhlin et al. 1998). In glaciated ter-
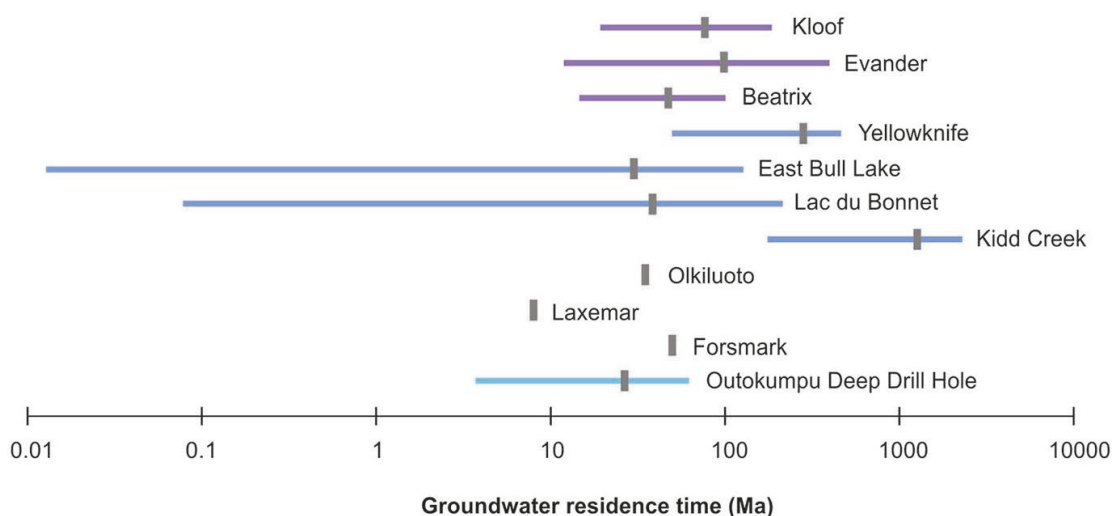
Fig. 9. Noble gas residence times of deep saline groundwaters within continental shields. The average values for each site are indicated with grey bars. Data from Lippmann et al. (2003), Greene et al. (2008), Bottomley et al. (1984, 1990), Holland et al. (2013), Trinchero et al. (2014) and Paper II.

rains, relic glacial melt water is also occasionally encountered, which has probably recharged in the bedrock due to a suitable combination of open fractures and pressure anomalies caused by the glaciation (Blomqvist 1999, Clark et al. 2000, Gascoyne 2004, Provost et al. 2012). In contrast, glacial conditions may also restrict groundwater flow if gas hydrates are formed (Stotler et al. 2010a). In granitic rocks, continuous 3D fracture networks are more likely to form than in strongly lineated rocks, such as schists (Lamminen 1995). As the prevailing rock types also shape the geochemical and even microbiological features of deep groundwaters, as shown in this study, these unique properties must be carefully investigated and taken into account, especially in site assessment studies.

5.4 Practical implications and future outlook

The findings of this study complement previous research demonstrating that deep saline groundwaters may have substantial residence times of up to tens of millions of years (Fig. 9). While this manifests the isolation and immobility of deep groundwaters, the results also highlight the complexity and vulnerability of these hydrosystems as they are being utilised.

Most notably, as similar ancient groundwaters are found in the Olkiluoto nuclear waste repository site, SW Finland, these results have potential implications for the long-term safety of nuclear waste disposal. In addition to the direct (near field or engineered) barrier of copper and bentonite that will be used to seal the waste, the long-term safety of the disposal will be greatly dependent on the properties of the fluid that will fill the fractures and pore spaces within the repository and the surrounding bedrock (far field or geological barrier) (e.g. Tsang et al. 2015). The disposal depth at Olkiluoto, at 400 to 500 m bsl, is now located in the transitional zone between the brackish and saline groundwater types. However, fracture mineral studies have demonstrated that groundwater conditions have fluctuated in the past (Sahlstedt et al. 2010). Thus, although they seem hydrologically stagnant, groundwaters from greater depths provide essential information needed to assess the long-term safety issues. Attention should especially be paid to the dynamic and on-going water–rock–microbe interactions of deep saline groundwaters. For example, CH_4 formation should be taken into account in studies on the mobilisation of potentially hazardous compounds, the accumulation and/or diffusion of gases and microbial activity within the bedrock groundwater.

In this study, the origin and evolution of deep groundwaters from meteoric water to saline gas–rich fluids was mainly demonstrated by using strontium and water stable isotopes, noble gas dating, and the geochemistry and isotopes of hydrocarbons. Additionally, other isotope tracers such as Cl, Br and Li from both groundwater and the rocks could provide a more in-depth view of water–rock interaction mechanisms and especially the origin of salinity. Recently developed isotopic methods based on CH_4 isotopologues (i.e. clumped isotopes) show potential for distinguishing between different CH_4 formation pathways (Stolper et al. 2014, Wang et al. 2015). A closer look at organic geochemistry would also be helpful in constraining the CH_4 production pathways and to test their importance in the deep continental biosphere. Furthermore, the potential for microbial utilisation of graphitic carbon has not been reported and needs further study. In addition to carbon, the source and cycling of other elements critical for life, most notably sulphur and nitrogen, although beyond the scope of this thesis, would be important to investigate for water–rock–microbe interactions in deep groundwaters, even if these studies are often faced with analytical challenges because of high salinity.

6 CONCLUSIONS

Geochemical and isotopic methods applied to water, gas and mineral samples were used to derive a model for deep groundwater evolution in the 2.5 km deep Outokumpu Deep Drill Hole in eastern Finland. The comparison of different sampling methods demonstrated that the tube sampling method provided the most complete profile, but suffered from uncontrolled degassing and mixing. Meanwhile, with the pressurised methods, it was possible to capture small quantities of fluid more precisely and completely. Even though pumping has the advantage of well-focused retrieval of large fluid volumes, it is likely to cause degassing similar to the tube sampler. Based on these results, it is suggested that pressurised sampling techniques should be used in gas sampling.

The evolution of groundwater via water-rock interaction was shown to be a plausible source for the characteristic isotopic composition and increased salinity of deep groundwater. However, simple linear mixing between meteoric water and shield brine could not be established. Instead, local variation in lithology and a substantial residence time have probably created the complex groundwater composition presently observed at Outokumpu.

Based on isotopic evidence, it could be concluded that helium is accumulated through a radiogenic process in the crust *in situ*, since a mantle-derived helium or helium concentration gradient indicative of diffusion from the deeper part of the crust was not observed. Two independent lines of evidence from water stable isotopes and the accumulation of radiogenic and nucleogenic noble gases were in good agreement, indicating isolation of the Outokumpu Deep Drill Hole groundwaters within the crust since the Eocene-Miocene epochs (56–5.3 Ma).

Using geochemical and microbiological evidence, the isotopic composition and concentration of CH_4 was shown to be controlled by the availability of carbon and hydrogen sources, microbial activity and abiotic processes. Abiotic hydrocarbons, typically characterised by the enrichment of ^{13}C, were suggested to prevail deeper in the bedrock, while microbial CH_4 is more common at depths shallower than 1.5 km. Supported by the data from lithologically different sites within the Fennoscandian Shield, it could be concluded that rather than a thermogenic relic, the abundant crustal CH_4 within continental shields is more likely to be the result of long-term, but still on-going, low temperature formation from ancient organic compounds and their inorganic intermediates, most notably graphite.

REFERENCES

Ahonen, L., Kaija, J., Paananen, M., Hakkarainen, V. & Ruskeeniemi, T. 2004. Palmottu natural analogue: A summary of the studies. Geological Survey of Finland, Nuclear Waste Disposal Research Report 121. 39 p.

Ahonen, L., Kietäväinen, R., Kortelainen, N., Kukkonen, I. T., Pullinen, A., Toppi, T., Bomberg, M., Itävaara, M., Nousiainen, A., Nyyssönen, M. & Öster, M. 2011. Hydrogeological characteristics of the Outokumpu Deep Drill Hole. In: Kukkonen, I. T. (ed.) Outokumpu Deep Drilling Project 2003-2010. Geological Survey of Finland, Special Paper 51, 151–168.

Airo, M.-L., Säävuori, H. & Vuoriainen, S. 2011. Petrophysical properties of the Outokumpu deep drill core and the surrounding bedrock. In: Kukkonen, I. T. (ed.) Outokumpu Deep Drilling Project 2003-2010. Geological Survey of Finland, Special Paper 51, 63–82.

Anell, I., Thybo, H. & Artemieva, I. M. 2009. Cenozoic uplift and subsidence in the North Atlantic region: Geological evidence revisited. Tectonophysics 474 (1–2), 78–105.

Anttila, P., Ahokas, H., Front, K., Heikkinen, E., Hinkkanen, H., Johansson, E., Paulamäki, S., Riekkola, R., Saari, J., Saksa, J., Snellman, M., Wikström, L. & Öhberg, A. 1999. Final disposal of spent nuclear fuel in Finnish bedrock - Kivetty site report. Posiva Oy, Posiva Report 99-09. 202 p.

Baker, B. J., Saw, J. H., Lind, A. E., Lazar, C. S., Hinrichs, K.-U., Teske, A. P. & Ettema, T. J. G. 2016. Genomic inference of metabolism of cosmopolitan subsurface Archaea, Hadesarchaea. Nature Microbiology 1, 16002.

Ballentine, C. J., Burgess, R. & Marty, B. 2002. Tracing fluid origin, transport and interaction in the crust. In: Porcelli, D. Ballentine, C. J. & Wieler, R. (eds) Noble Gases in Geochemistry and Cosmochemistry. Reviews in Mineralogy and Geochemistry 47, 539–614.

Bein, A. & Arad, A. 1992. Formation of saline groundwaters in the Baltic region through freezing of seawater during glacial periods. Journal of Hydrology 140 (1–4), 75–87.

Bernard, B. B., Brooks, J. M. & Sackett, W. M 1976. Natural gas seepage in the Gulf of Mexico. Earth and Planetary Science Letters 31 (1), 48–54.

Blomqvist, R. 1999. Hydrogeochemistry of deep groundwaters in the central part of the Fennoscandian Shield.

Geological Survey of Finland, Nuclear Waste Disposal Research Report 101. 41 p. (dissertation)

Blomqvist, R., Lahtinen, R., Lahermo, P., Hakkarainen, V. & Halonen, S. 1986. Kalliopohjavesien geokemia: tutkimustulokset syvistä kairarei'istä vuonna 1986. Geological Survey of Finland, Nuclear Waste Disposal Research Report 53. 87 p., 17 apps. (in Finnish)

Borgonie, G., García-Moyano, A., Litthauer, D., Bert, W., Bester, A., van Heerden, E., Möller, C., Erasmus, M. & Onstott, T. C. 2011. Nematoda from the terrestrial deep subsurface of South Africa. Nature 474 (7349), 79–82.

Bottomley, D. J., Gascoyne, M. & Kamineni, D. C. 1990. The geochemistry, age, and origin of groundwater in a mafic pluton, East Bull Lake, Ontario, Canada. Geochimica et Cosmochimica Acta 54 (4), 933–1008.

Bottomley, D. J., Gregoire, D. C. & Raven, K. G. 1994. Saline groundwaters and brines in the Canadian Shield: Geochemical and isotopic evidence for residual evaporite brine component. Geochimica et Cosmochimica Acta 58 (5), 1483–1498.

Bottomley, D. J., Katz, A., Chan, L. H., Starinsky, A., Douglas, M., Clark, I. D. & Raven, K. G. 1999. The origin and evolution of Canadian shield brines: evaporation or freezing of seawater? New lithium isotope and geochemical evidence from the Slave craton. Chemical Geology 155 (3–4), 295–320.

Bottomley, D. J., Ross, J. D. & Clarke, W. B. 1984. Helium and neon isotope geochemistry of some ground waters from the Canadian Precambrian Shield. Geochimica et Cosmochimica Acta 48 (10), 1973–1985.

Bradley, A. S., Hayes, J. M. & Summons, R. E. 2009. Extraordinary ^{13}C enrichment of diether lipids at the Lost City Hydrothermal Field indicates a carbon-limited ecosystem. Geochimica et Cosmochimica Acta 73 (1), 102–118.

Bucher, K. & Stober, I. 2010. Fluids in the upper continental crust. Geofluids 10 (1–2), 241–253.

Burruss, R. C. & Laughrey, C. D. 2010. Carbon and hydrogen isotopic reversals in deep basin gas: Evidence for limits to the stability of hydrocarbons. Organic Geochemistry 41 (12), 1285–1296.

Canfield, D. E., Thamdrup, B. & Kristensen, E. 2005. Aquatic geomicrobiology. Advances in Marine Biology 48. 640 p.

Chacko, T., Cole, D. R. & Horita, J. 2001. Equilibrium oxygen, hydrogen and carbon isotope fractionation factors applicable to geologic systems. In: Valley, J. W. & Cole, D. R. (eds) Stable Isotope Geochemistry. Reviews in Mineralogy and Geochemistry 43, 1–81.

Chorlton, L. B. 2007. Generalized geology of the world: bedrock domains and major faults in GIS format: a small-scale world geology map with an extended geological attribute database [Electronic resource]. Geological Survey of Canada. Open File 5529.

Clark, I. & Fritz, P. 1997. Environmental isotopes in hydrogeology. Boca Raton: Lewis Publishers. 328 p.

Clark, I. D., Douglas, M., Raven, K. & Bottomley, D. 2000. Recharge and preservation of Laurentide glacial melt water in the Canadian Shield. Ground Water 38 (5), 735–742.

Craig, H. 1961. Isotopic variations in meteoric waters. Science 133 (3465), 1702–1703.

Dansgaard, W. 1964. Stable isotopes in precipitation. Tellus 16 (4), 436–468.

Devirts, A. L., Gagauz, F. G., Grinenko, V. A., Lagutina, Ye. P., Pereverzov, V. V. & Shukolyukov, Yu. A. 1993. Origin of hydrogen in Kempirsay-intrusion ultramafites. Geochemistry International 30 (2), 139–144.

Dzaugis, M. E., Spivack, A. J., Dunlea, A. G., Murray, R. W. & D'Hondt, S. 2016. Radiolytic hydrogen production in the subseafloor basaltic aquifer. Frontiers in Microbiology 7, 76.

Eberhardt, P., Eugster, O. & Marti, K. 1965. A redetermination of the isotopic composition of atmospheric neon. Zeitschrift für Naturforschung A 20 (4), 623–624.

Edmunds, W. M., Kay, R. L. F., Miles, D. L. & Cook, J. M. 1987. The origin of saline groundwaters in the Carnmenellis granite, Cornwall (U.K.): Further evidence from minor and trace elements. In: Fritz, P. & Frape, S. K. (eds) Saline water and gases in crystalline rocks. Geological Association of Canada, Special Paper 33, 127–143.

Etiope, G. & Ionescu, A. 2015. Low-temperature catalytic CO_2 hydrogenation with geological quantities of ruthenium: a possible abiotic CH_4 source in chromitite-rich serpentinized rocks. Geofluids 15 (3), 438–452.

Etiope, G. & Sherwood Lollar, B. 2013. Abiotic methane on Earth. Reviews of Geophysics 51 (2), 276–299.

Frape, S. K. & Fritz, P. 1987. Geochemical trends for groundwaters from the Canadian Shield. In: Fritz, P. & Frape, S. K. (eds) Saline water and gases in crystalline rocks. Geological Association of Canada, Special Paper 33, 19–38.

Frape, S. K., Blyth, A., Blomqvist, R., McNutt, R. H. & Gascoyne, M. 2004. Deep fluids in the continents: II Crystalline rocks. In: Drever, J. I. (ed.) Surface and ground water, weathering, and soils. Treatise in Geochemistry 5, 541–580.

Frape, S. K., Fritz, P. & McNutt, R. H. 1984. Water-rock interaction and chemistry of groundwaters from the Canadian Shield. Geochimica et Cosmochimica Acta 48 (8), 1617–1627.

Fritz, P. & Frape, S. K. 1982. Saline groundwaters in the Canadian Shield – a first overview. Chemical Geology 36 (1–2), 179–190.

Gascoyne, M. 2004. Hydrogeochemistry, groundwater ages and sources of salts in granitic batholith on the Canadian Shield, southeastern Manitoba. Applied Geochemistry 19 (4), 519–560.

Gilg, H. A., Hall, A. M., Ebert, K. & Fallick, A. E. 2013. Cool kaolins in Finland. Palaeogeogaphy, Palaeoclimatology, Palaeoecology 392, 454–462.

Gonfiantini, R. 1986. Environmental isotopes in lake studies. In: Fritz, P. & Fontes, J. Ch. (eds) Handbook of Environmental Isotope Geochemistry, Volume 2, The Terrestrial Environment. Amsterdam: Elsevier, 113–168.

Greene, S., Battye, N., Clark, I., Kotzer, T. & Bottomley, D. 2008. Canadian Shield brine from the Con Mine, Yellowknife, NT, Canada: Noble gas evidence for an evaporated Palaeozoic seawater origin mixed with glacial meltwater and Holocene recharge. Geochimica et Cosmochimica Acta 72 (16), 4008–4019.

Greenwood, D. R., Basinger, J. F. & Smith, R. Y. 2010. How wet was the Arctic Eocene rain forest? Estimates of precipitation from Paleogene Arctic macrofloras. Geology 38 (1), 15–18.

Grimaud, D., Beaucaire, C. & Michard, G. 1990. Modeling of evolution of ground waters in a granite system at low temperature: the Stripa ground waters, Sweden. Applied Geochemistry 5 (4), 515–525.

Großkopf, T. & Soyer, O. S. 2016. Microbiological diversity arising from thermodynamic constraints. The ISME Journal 10 (11), 2725–2733.

Halonen, S., Hakkarainen, V., Blomqvist, R., Lahermo, P. & Lakomaa, T. 1990. Kalliopohjavesien geokemia: Tutkimustulokset syvistä kairarei'istä vuosina 1987–1989. Geological Survey of Finland, Nuclear Waste Disposal Research Report 65. 66 p., 12 apps. (in Finnish)

Haveman, S. A., Pedersen, K. & Ruotsalainen, P. 1999. Distribution and metabolic diversity of microorganisms in deep igneous rock aquifers of Finland. Geomicrobiology Journal 16 (4), 277-294.

Herut, B., Starinsky, A., Katz, A. & Bein, A. 1990. The role of seawater freezing in the formation of subsurface brines. Geochimica et Cosmochimica Acta 54 (1), 13-21.

Hoefs, J. 2004. Stable isotope geochemistry. Berlin: Springer. 244 p.

Hoehler, T. M. & Jørgensen, B. B. 2013. Microbial life under extreme energy limitation. Nature Reviews Microbiology 11 (2), 83-94.

Holland, G., Sherwood Lollar, B., Li, L., Lacrampe-Couloume, G., Slater, G. F. & Ballentine, C. J. 2013. Deep fracture fluids isolated in the crust since the Precambrian era. Nature 497 (7449), 357-360.

Huhma, H. 1986. Sm-Nd, U-Pb and Pb-Pb isotopic evidence for the origin of the early Proterozoic Svecokarelian crust in Finland. Geological Survey of Finland, Bulletin 337. 48 p. (dissertation)

Itävaara, M., Nyyssönen, M., Bomberg, M., Kapanen, A., Nousiainen, A., Ahonen, L., Hultman, J., Paulin, L., Auvinen, P. & Kukkonen, I. T. 2011a. Microbiological sampling and analysis of the Outokumpu Deep Drill Hole biosphere in 2007-2009. In: Kukkonen, I. T. (ed.) Outokumpu Deep Drilling Project 2003-2010. Geological Survey of Finland, Special Paper 51, 199-206.

Itävaara, M., Nyyssönen, M., Kapanen, A., Nousiainen, A., Ahonen, L. & Kukkonen, I. 2011b. Characterization of bacterial diversity to a depth of 1500 m in the Outokumpu deep borehole, Fennoscandian Shield. FEMS Microbiology Ecology 77 (2), 295-309.

Ivanovich, M., Blomqvist, R. & Frape, S. K. 1992. Rock/water interaction study in deep crystalline rocks using isotopic and uranium series radionuclide techniques. Radiochimica Acta 58-59, 401-408.

Juhlin, C., Wallroth, T., Smellie, J., Eliasson, T., Ljunggren, C., Leijon, B. & Beswick, J. 1998. Very Deep Hole Concept: Geoscientific appraisal of conditions at great depth. Swedish Nuclear Fuel and Waste Management Co., Report SKB TR 98-05. 124 p.

Kaija, J., Blomqvist, R., Ahonen, L. & Hakkarainen, V. 1998. The hydrogeochemical database of Palmottu. The Palmottu Natural Analogue Project. Geological Survey of Finland, Technical Report 98-08. 54 p.

Karlsson, H. R. & Clayton, R. N. 1990. Oxygen and hydrogen isotope geochemistry of zeolites. Geochimica et Cosmochimica Acta 54 (5), 1369-1386.

Katz, A., Starinsky, A. & Marion, G. 2011. Saline waters in basement rocks of the Kaapvaal Craton, South Africa. Chemical Geology 289 (1-2), 163-170.

Kloppmann, W., Girard, J.-P. & Négrel, P. 2002. Exotic stable isotope compositions of saline waters and brines from the crystalline basement. Chemical Geology 184 (1-2), 49-70.

Kohonen, J. & Rämö, O. T. 2005. Sedimentary rocks, diabases, and late cratonic evolution. In: Lehtinen, M., Nurmi, P. & Rämö, O. T. (eds) Precambrian Geology of Finland – Key to evolution of the Fennoscandian Shield. Amsterdam: Elsevier, 563-604.

Konhauser, K. 2007. Introduction to geomicrobiology. Oxford: Blackwell Publishing. 425 p.

Kontinen, A. & Sorjonen-Ward, P. 1991. Geochemistry of metagraywackes and metapelites from the Palaeoproterozoic Nuasjärvi Group, Kainuu Schist Belt and the Savo Province, North Karelia: Implications for provenance, lithostratigraphic correlation and depositional setting. In: Autio, S. (ed.) Geological Survey of Finland, Current Research 1989-1990. Geological Survey of Finland, Special Paper 12, 21-22.

Kontinen, A., Peltonen, P. & Huhma, H. 2006. Description and genetic modelling of the Outokumpu-type rock assemblage and associated sulphide deposits. Geological Survey of Finland, archive report M10.4/2006/1. 378 p.

Kortelainen, N. 2007. Isotopic fingerprints in surficial waters: Stable isotope methods applied in hydrogeological studies. Espoo: Geological Survey of Finland. 108 p. (dissertation)

Kremenetsky, A. A. & Ovchinnikov, L. N. 1986. The Precambrian continental crust: Its structure, composition and evolution as revealed by deep drilling in the U.S.S.R.. Precambrian Research 33 (1-3), 11-43.

Kuhn, O. 2004. Ancient Chinese drilling. Canadian Society of Exploration Geophysics, RECORDER 29 (6), 39-43.

Kukkonen, I. 1989. Terrestrial heat flow in Finland, the Central Fennoscandian Shield. Geological Survey of Finland, Nuclear Waste Disposal Research Report 68. 169 p. (dissertation)

Kukkonen, I. T. (ed.) 2011. Outokumpu Deep Drilling Project 2003-2010. Geological Survey of Finland, Special Paper 51. 252 p.

Kukkonen, I. T., Rath, V., Kivekäs, L., Šafanda, J. & ermák, V. 2011. Geothermal studies of the Outokumpu Deep Drill Hole, Finland: Vertical variation in heat flow and palaeoclimatic implications. Physics of the Earth and Planetary Interiors 188 (1-2), 9-25.

Kyle, J. E., Eydal, H. S. C., Ferris, F. G. & Pedersen, K. 2008. Viruses in granitic groundwater from 69 to 450 m depth of the Äspö hard rock laboratory, Sweden. The ISME Journal 2 (5), 571-574.

Laaksoharju, M., Gascoyne, M. & Gurban, I. 2008. Understanding groundwater chemistry using mixing models. Applied Geochemistry 23 (7), 1921-1940.

Lahermo, P. W. & Lampén, P. H. 1987. Brackish and saline groundwaters in Finland. In: Fritz, P. & Frape, S. K. (eds) Saline water and gases in crystalline rocks. Geological Association of Canada, Special Paper 33, 103-109.

Lahtinen, R., Huhma, H., Kontinen, A., Kohonen, J. & Sorjonen-Ward, P. 2010. New constraints for the source characteristics, deposition and age of the 2.1-1.9 Ga metasedimentary cover at the western margin of the Karelian Province. Precambrian Research 176 (1-4), 77-93.

Lamminen, S. 1995. Kiven ja veden välinen vuorovaikutus erilaisissa kivilajiympäristöissä. Geological Survey of Finland, Nuclear Waste Disposal Research Report 91. 60 p., 3 apps. (in Finnish)

Larsson, L. M., Dybkjær, K., Rasmussen, E. S., Piasecki, S., Utescher, T. & Vajda, V. 2011. Miocene climate evolution of northern Europe: A palynological investigation from Denmark. Palaeogeography, Palaeoclimatology, Palaeoecology 309 (3-4), 161-175.

Lee, J.-Y., Marti, K., Severinghaus, J. P., Kawamura, K., Yoo, H.-S., Lee, J. B. & Kim, J. S. 2006. A redetermination of the isotopic abundances of atmospheric Ar. Geochimica et Cosmochimica Acta 70 (17), 4507-4512.

Lin, L.-H., Slater, G. F., Sherwood Lollar, B., Lacrampe-Couloume, G. & Onstott, T. C. 2005. The yield and isotopic composition of radiolytic H_2, a potential energy source for the deep subsurface biosphere. Geochimica et Cosmochimica Acta 69 (4), 893-903.

Lippmann, J., Stute, M., Torgersen, T., Moser, D. P., Hall, J. A., Lin, L., Borcsik, M., Bellamy, R. E. S. & Onstott, T. C. 2003. Dating ultra-deep mine waters with noble gases and ^{36}Cl, Witwatersrand Basin, South Africa. Geochimica et Cosmochimica Acta 67 (23), 4597-4619.

Loukola-Ruskeeniemi, K. 1999. Origin of black shales and the serpentinite-associated Cu-Zn-Co ores at Outokumpu, Finland. Economic Geology 94 (7), 1007-1028.

Louvat, D., Michelot, J. L. & Aranyossy, J. F. 1999. Origin and residence time of salinity in the Äspö groundwater system. Applied Geochemistry 14 (7), 917-925.

Luukkonen, A., Pitkänen, P., Ruotsalainen, P, Leino-Forsman, H. & Snellman, M. 1999. Hydrogeochemical conditions at the Hästholmen site. Posiva Oy, Posiva Report 99-26. 64 p.

Mathurin, F. A., Åström, M. E., Drake, H., Maskenskaya, O. M. & Kalinowski, B. E. 2014. REE and Y in groundwater in the upper 1.2 km of Proterozoic granitoids (Eastern Sweden) – Assessing the role of composition and origin of groundwaters, geochemistry of fractures, and organic/inorganic aqueous complexation. Geochimica et Cosmochimica Acta 144, 342-378.

Matsumoto, T., Honda, M., McDougall, I., Yatsevich, I. & O'Reilly, S. Y. 2004. Isotope fractionation of neon during stepheating extraction? A comment of 'Reinterpretation of the existence of a primitive plume under Australia based on neon isotope fractionation during step heating' by Gautheron and Moreira (2003). Terra Nova 16 (1), 23-26.

Mayhew, L. E., Ellison, E. T., McCollom, T. M., Trainor, T. P. & Templeton, A. S. 2013. Hydrogen generation from low-temperature water-rock reactions. Nature Geoscience 6 (6), 478-484.

McCollom, T. M. & Bach, W. 2009. Thermodynamic constraints on hydrogen generation during serpentinization of ultramafic rocks. Geochimica et Cosmochimica Acta 73 (3), 856-875.

McMahon, S. & Parnell, J. 2014. Weighing the deep continental biosphere. FEMS Microbiology Ecology 87 (1), 113-120.

McNutt, R. H., Frape, S. K., Fritz, P., Jones, M. G. & MacDonald, I. M. 1990. The $^{87}Sr/^{86}Sr$ values of Canadian Shield brines and fracture minerals with applications to groundwater mixing, fracture history and geochronology. Geochimica et Cosmochimica Acta 54 (1), 205-215.

Miettinen, H., Kietäväinen, R., Sohlberg, E., Numminen, M., Ahonen, L. & Itävaara, M. 2015. Microbiome composition and geochemical characteristics of deep subsurface high-pressure environment, Pyhäsalmi mine Finland. Frontiers in Microbiology 6, 1203.

Mitrega, J. & Lahermo, P. 1991. The occurrence of shallow brackish and saline groundwaters in the crystalline bedrock of Finnish coastal areas. Geological Survey of Finland, Report of Investigation 97. 31 p.

Nandi, R. & Sengupta, S. 1998. Microbial production of hydrogen: an overview. Critical Reviews in Microbiology 24 (1), 61-84.

Neal, C. & Stanger, G. 1983. Hydrogen generation from mantle source rocks in Oman. Earth and Planetary Science Letters 66, 315-320.

Négrel, P. & Casanova, J. 2005. Comparison of the Sr isotopic signatures in brines of the Canadian and Fennoscandian shields. Applied Geochemistry 20 (4), 749-766.

Négrel, P., Casanova, J. & Blomqvist, R. 2005. $^{87}Sr/^{86}Sr$ of brines from the Fennoscandian Shield: a synthesis of groundwater isotopic data from the Baltic Sea region. Canadian Journal of Earth Sciences 42 (3), 273-285.

Négrel, P., Casanova, J., Blomqvist, R., Kaija, J. & Frape, S. 2003. Strontium isotopic characterization of the Palmottu hydrosystem (Finland): water-rock interaction and geochemistry of groundwaters. Geofluids 3 (3), 161-175.

Neubeck, A., Thanh Duc, N., Bastviken, D., Crill, P. & Holm, N. G. 2011. Formation of H_2 and CH_4 by weathering of olivine at temperatures between 30 and 70°C. Geochemical Transactions 12:6.

Nordstrom, D. K., Lindblom, S., Donahoe, R. J. & Barton, C. C. 1989. Fluid inclusions in the Stripa granite and their possible influence on the groundwater chemistry. Geochimica et Cosmochimica Acta 53 (8), 1741-1755.

Nurmi, P. A. & Kukkonen, I. T. 1986. A new technique for sampling water and gas from deep drill holes. Canadian Journal of Earth Sciences 23 (9), 1450-1454.

Nurmi, P. A., Kukkonen, I. T. & Lahermo, P. W. 1988. Geochemistry and origin of saline groundwaters in the Fennoscandian Shield. Applied Geochemistry 3 (2), 185-203.

Nyyssönen, M., Hultman, J., Ahonen, L., Kukkonen, I., Paulin, L., Laine, P., Itävaara, M. & Auvinen, P. 2014. Taxonomically and functionally diverse microbial communities in deep crystalline rocks of the Fennoscandian shield. The ISME Journal 8 (1), 126-138.

Onstott, T. C., Lin, L.-H., Davidson, M., Mislowack, B., Borcsik, M., Hall, J., Slater, G., Ward, J., Sherwood Lollar, B., Lippmann-Pipke, J., Boice, E., Pratt, L. M., Pfiffner, S., Moser, D., Gihring, T., Kieft, T. L., Phelps, T. J., Van Heerden, E., Litthaur, D., Deflaun, M., Rothmel, R., Wanger, G. & Southam, G. 2006. The origin and age of biogeochemical trends in deep fracture water of the Witwatersrand Basin, South Africa. Geomicrobiology Journal 23 (6), 369-414.

Pearson, F. J., Jr. 1987. Models of mineral controls on the composition of saline groundwaters of the Canadian Shield. In: Fritz, P. & Frape, S. K. (eds) Saline water and gases in crystalline rocks. Geological Association of Canada, Special Paper 33, 39-51.

Pedersen, K. 1993. The deep subterranean biosphere. Earth-Science Reviews 34 (4), 243-260.

Pedersen, K. 2014. Microbial life in terrestrial hard rock environments. In: Kallmeyer, J. & Wagner, D. (eds) Microbial life of the deep biosphere. Life in Extreme Environments 1, 63-81.

Pedersen, K. & Ekendahl, S. 1990. Distribution and activity of bacteria in deep granitic groundwaters of southeastern Sweden. Microbial Ecology 20 (1), 37-52.

Phreeqc Interactive 2014. Software [Electronic resource]. United States Geological Survey. Available at: http://wwwbrr.cr.usgs.gov/projects/GWC_coupled/phreeqc/ Version 3.3.3.

Pikuta, E. V., Hoover, R. B. & Tang, J. 2007. Microbial extremophiles at the limits of life. Critical Reviews in Microbiology 33 (3), 183-209.

Piribauer, C. J., Sindern, S., Meyer, F. M., Vennemann, T. W. & Prochaska, W. 2011. Fluid inclusions in the Outokumpu Deep Drill Core: Implications for palaeofluid evolution and the composition of modern deep saline fluids. In: Kukkonen, I. T. (ed.) Outokumpu Deep Drilling Project 2003-2010. Geological Survey of Finland, Special Paper 51, 169-180.

Pitkänen, P. & Partamies, S. 2007. Origin and implications of dissolved gases in groundwater at Olkiluoto. Posiva Oy, Posiva Report 2007-04. 54 p.

Pitkänen, P., Luukkonen, A., Ruotsalainen, P., Leino-Forsman, H. & Vuorinen, U. 1998. Geochemical modelling of groundwater evolution and residence time at the Kivetty site. Posiva Oy, Posiva Report 98-07. 139 p.

Pitkänen, P., Snellman, M., Vuorinen, U. & Leino-Forsman, H. 1996. Geochemical modelling study on the age and evolution of the groundwater at the Romuvaara site. Posiva Oy, Posiva Report 96-06. 125 p.

Potter, J., Salvi, S. & Longstaffe, F. J. 2013. Abiogenic hydrocarbon isotopic signatures in granitic rocks: Identifying pathways of formation. Lithos 182-183, 114-124.

Provost, A. M., Voss, C. I. & Neuzil, C. E. 2012. Glaciation and regional groundwater flow in the Fennoscandian shield. Geofluids 12 (1), 79–96.

Purkamo, L. 2015. Microbial ecology and functionality in deep Fennoscandian crystalline bedrock biosphere. VTT Technical Research Centre of Finland Ltd, VTT Science 116. 86 p. (dissertation)

Purkamo, L., Bomberg, M., Kietäväinen, R., Salavirta, H., Nyyssönen, M., Nuppunen-Puputti, M., Ahonen, L., Kukkonen, I. & Itävaara, M. 2016. Microbial co-occurrence patterns in deep Precambrian bedrock fracture fluids. Biogeosciences 13 (10), 3091–3108.

Purkamo, L., Bomberg, M., Nyyssönen, M., Kukkonen, I., Ahonen, L. & Itävaara, M. 2015. Heterotrophic communities supplied by ancient organic carbon predominate in deep Fennoscandian bedrock fluids. Microbial Ecology 69 (2), 319–332.

Purkamo, L., Bomberg, M., Nyyssönen, M., Kukkonen, I., Ahonen, L., Kietäväinen, R. & Itävaara, M. 2013. Dissecting the deep biosphere: retrieving authentic microbial communities from packer-isolated deep crystalline bedrock fracture zones. FEMS Microbiology Ecology 85 (2), 324–337.

Rajala, P., Bomberg, M. Kietäväinen, R., Kukkonen, I., Ahonen, L., Nyyssönen, M. & Itävaara, M. 2015. Rapid reactivation of deep subsurface microbes in the presence of C-1 compounds. Microorganisms 3 (1), 17–33.

Regenspurg, S., Wiersberg, T., Brandt, W., Huenges, E., Saadat, A., Schmidt, K. & Zimmermann, G. 2010. Geochemical properties of saline geothermal fluids from the in-situ geothermal laboratory Groß Schönebeck (Germany). Chemie der Erde 70 (S3), 3–12.

Rozanski, K., Araguás- Araguás, L. & Gonfiantini, R. 1993. Isotopic patterns in modern global precipitation. In: Swart, P. K., Lohmann, K. C., McKenzie, J. & Savin, S. (eds) Climate Change in Continental Isotopic Records. American Geophysical Union, Geophysical Monograph 78. 36 p.

Ruskeeniemi, T., Blomqvist, R., Lindberg, A., Ahonen, L. & Frape, S. 1996. Hydrogeochemistry of deep groundwaters of mafic and ultramafic rocks in Finland. Posiva Oy, Posiva Report 96–21. 123 p.

Sahlstedt, E., Karhu, J. A. & Pitkänen, P. 2010. Indications for past redox environments in deep groundwaters from the isotopic composition of carbon and oxygen in fracture calcite, Olkiluoto, SW Finland. Isotopes in Environmental and Health Studies 46 (3), 370–391.

Säntti, J., Kontinen, A., Sorjonen-Ward, P., Johanson, B. & Pakkanen, L. 2006. Metamorphism and chromite in serpentinized and carbonate-silica-altered peridotites of the Paleoproterozoic Outokumpu-Jormua Ophiolite Belt, eastern Finland. International Geology Review 48 (6), 494–546.

Schoell, M. 1980. The hydrogen and carbon isotopic composition of methane from natural gases of various origins. Geochimica et Cosmochimica Acta 44 (5), 649–661.

Sharma, P., Tsang, C.-F., Kukkonen, I. T. & Niemi, A. 2016. Analysis of 6-year fluid electric conductivity logs to evaluate the hydraulic structure of the deep drill hole at Outokumpu, Finland. International Journal of Earth Sciences 105 (5), 1549–1562.

Sherwood, B., Fritz, P., Frape, S. K., Macko, S. A., Weisi, S. M. & Welhan, J. A. 1988. Methane occurrences in the Canadian Shield. Chemical Geology 71 (1–3), 223–236.

Sherwood Lollar, B., Frape, S. K., Fritz, P., Macko, S. A., Welhan, J. A., Blomqvist, R. & Lahermo, P. W. 1993a. Evidence for bacterially generated hydrocarbon gas in Canadian Shield and Fennoscandian Shield rocks. Geochimica et Cosmochimica Acta 57 (23–24), 5073–5085.

Sherwood Lollar, B., Frape, S. K., Weise, S. M., Fritz, P., Macko, S. A. & Welhan, J. A. 1993b. Abiogenic methanogenesis in crystalline rocks. Geochimica et Cosmochimica Acta 57 (23–24), 5087–5097.

Sherwood Lollar, B., Lacrampe-Couloume, G., Slater, G. F., Ward, J., Moser, D. P., Gihring, T. M., Lin, L.-H. & Onstott, T. C. 2006. Unravelling abiogenic and biogenic sources of methane in the Earth's deep subsurface. Chemical Geology 226 (3–4), 328–339.

Sherwood Lollar, B., Lacrampe-Couloume, G., Voglesonger, K., Onstott, T. C., Pratt, L. M. & Slater, G. F. 2008. Isotopic signatures of CH_4 and higher hydrocarbon gases from Precambrian Shield sites: A model for abiogenic polymerization of hydrocarbons. Geochimica et Cosmochimica Acta 72 (19), 4778–4795.

Sherwood Lollar, B., Onstott, T. C., Lacrampe-Couloume, G. & Ballentine, C. J. 2014. The contribution of the Precambrian continental lithosphere to global H_2 production. Nature 516 (7531), 379–382.

Simkus, D. N., Slater, G. F., Sherwood Lollar, B., Wilkie, K., Kieft, T. L., Magnabosco, C., Lau, M. C. Y., Pullin, M. J., Hendrickson, S. B., Wommack, K. E., Sakowski, E. G., van Heerden, E., Kuloyo, O., Linage, B., Borgonie, G. & Onstott, T. C. 2016. Variations in microbial carbon sources and cycling in the deep continental subsurface. Geochimica et Cosmochimica Acta 173, 264–283.

Smalley, P. C., Blomqvist, R. & Råheim, A. 1988. Sr isotopic evidence for discrete saline components in stratified ground waters from crystalline bedrock, Outokumpu, Finland. Geology 16 (4), 354–357.

Smellie, J. A. T. & Wikberg, B. 1991. Hydrochemical investigations at Finnsjön, Sweden. Journal of Hydrology 126 (1–2), 129–158.

Starinsky, A. & Katz, A. 2003. The formation of natural cryogenic brines. Geochimica et Cosmochimica Acta 67 (8), 1475–1484.

Stober, I. & Bucher, K. 2004. Fluid sinks within the earth's crust. Geofluids 4 (2), 143–151.

Stolper, D. A., Lawson, M., Davis, C. L., Ferreira, A. A., Santos Neto, E. V., Ellis, G. S., Lewan, M. D., Martini, A. M., Tang, Y., Schoell, M., Sessions, A. L. & Eiler, J. M. 2014. Formation temperatures of thermogenic and biogenic methane. Science 344 (6191), 1500–1503.

Stotler, R. L., Frape, S. K., Ahonen, L., Clark, I., Greene, S., Hobbs, M., Johnson, E., Lemieux, J.-M., Peltier, R., Pratt, L., Ruskeeniemi, T., Sudicky, E. & Tarasov, L. 2010a. Origin and stability of a permafrost methane hydrate occurrence in the Canadian Shield. Earth and Planetary Science Letters 296 (3–4), 384–394.

Stotler, R. L., Frape, S. K., Ruskeeniemi, T., Pitkänen, P. & Blowes, D. W. 2012. The interglacial-glacial cycle and geochemical evolution of Canadian and Fennoscandian Shield groundwaters. Geochimica et Cosmochimica Acta 76, 45–67.

Stotler, R. L., Frape, S. K. & Shouakar-Stash, O. 2010b. An isotopic survey of $\delta^{81}Br$ and $\delta^{37}Cl$ of dissolved halides in the Canadian and Fennoscandian Shields. Chemical Geology 274 (1–2), 38–55.

Szewzyk, U., Szewzyk, R. & Stenström, T.-A. 1994. Thermophilic, anaerobic bacteria isolated from a deep borehole in granite in Sweden. Proceedings of the National Academy of Sciences 91 (5), 1810–1813.

Szponar, N., Brazelton, W. J., Schrenk, M. O., Bower, D. M., Steele, A. & Morill, P. L. 2013. Geochemistry of continental site of serpentinization, the Tablelands Ophiolite, Gros Morne National Park: A Mars analogue. Icarus 224 (2), 286–296.

Takai, K., Nakamura, K., Toki, T., Tsunogai, U., Miyazaki, M., Miyazaki, J., Hirayama, H., Nakagawa, S., Nunoura, T. & Horikoshi, K. 2008. Cell proliferation at 122°C and isotopically heavy CH_4 production by a hyperthermophilic methanogen under high-pressure cultivation. Proceedings of the National Academy of Sciences 105 (31), 10949–10954.

Taran, L. N., Onoshko, M. P. & Mikhailov, N. D. 2011. Structure and composition of organic matter and isotope geochemistry of the Palaeoproterozoic graphite and sulphide-rich metasedimentary rocks from the Outokumpu Deep Drill Hole, eastern Finland. In: Kukkonen, I. T. (ed.) Outokumpu Deep Drilling Project 2003–2010. Geological Survey of Finland, Special Paper 51, 219–228.

Tazaz, A. M., Bebout, B. M., Kelley, C. A., Poole, J. & Chanton, J. P. 2013. Redefining the isotopic boundaries of biogenic methane: Methane from endoevaporites. Icarus 224 (2), 268–275.

Thauer, R. K., Kaster, A., Seedorf, H., Buckel, W. & Hedderich, R. 2008. Methanogenic archaea: ecologically relevant differences in energy conservation. Nature Reviews Microbiology 6 (8), 579–591.

Torgersen, T. 1980. Controls on pore-fluid concentration of ^{4}He and ^{222}Rn and the calculation of ^{4}He/^{222}Rn ages. Journal of Geochemical Exploration 13 (1), 57–75.

Torgersen, T. 2010. Continental degassing flux of ^{4}He and its variability. Geochemistry, Geophysics, Geosystems 11 (6), Q06002.

Torsvik, T. H., Van der Voo, R., Meert, J. G., Mosar, J. & Walderhaug, H. J. 2001. Reconstructions of the continents around the North Atlantic at about the 60th parallel. Earth and Planetary Science Letters 187 (1–2), 55–69.

Trinchero, P., Delos, A., Molinero, J., Dentz, M. & Pitkänen, P. 2014. Understanding and modelling dissolved gas transport in the bedrock of three Fennoscandian sites. Journal of Hydrology 512, 506–517.

Tsang, C.-F., Neretnieks, I. & Tsang, Y. 2015. Hydrologic issues associated with nuclear waste repositories. Water Resources Research 51 (9), 6923–6972.

Valentine, D. L., Chidthaisong, A., Rice, A., Reeburgh, W. S. & Tyler, S. C. 2004. Carbon and hydrogen isotope fractionation by moderately thermophilic methanogens. Geochimica et Cosmochimica Acta 68 (7), 1571–1590.

Västi, K. 2011. Petrology of the drill hole R2500 at Outokumpu, eastern Finland – the deepest drill hole ever drilled in Finland. In: Kukkonen, I. T. (ed.) Outokumpu Deep Drilling Project 2003–2010. Geological Survey of Finland, Special Paper 51, 17–46.

Vovk, I. F. 1987. Radiolytic salt enrichment and brines in the crystalline basement of the East European Platform. In: Fritz, P. & Frape, S. K. (eds) Saline water and gases in crystalline rocks. Geological Association of Canada, Special Paper 33, 197–210.

Wallin, B. & Peterman, Z. 2015. Compilation and review of ^{87}Sr/^{86}Sr and stable isotopes from groundwater, calcite fracture fillings, mineral, and whole-rock sampling at Äspö, Sweden. Groundwater 53 (S1), 103–112.

Wang, D. T., Gruen, D. S., Sherwood Lollar, B., Hinrichs, K.-U., Stewart, L. C., Holden, J. F., Hristov, A. N., Pohlman, J. W., Morill, P. L., Könneke, M., Delwiche, K. B., Reeves, E. P., Sutcliffe, C. N., Ritter, D. J., Seewald, J. S., McIntosh, J. C., Hemond, H. F., Kubo, M. D., Cardace, D., Hoehler, T. M. & Ono, S. 2015. Nonequilibrium clumped isotope signals in microbial methane. Science 348 (6233), 428–431.

Ward, J., Slater, G., Moser, D., Lin, L., Lacrampe-Couloume, G., Bonin, A., Davidson, M., Hall, J. A., Mislowack, B., Bellamy, R. E. S., Onstott, T. C. & Sherwood Lollar, B. 2004. Microbial hydrocarbon gases in the Witwatersrand Basin, South Africa: implications for the deep biosphere. Geochimica et Cosmochimica Acta 68 (15), 3239–3250.

Whiticar, M. J. 1999. Carbon and hydrogen isotope systematics of bacterial formation and oxidation of methane. Chemical Geology 161 (1–3), 291–314.

Wu, X., Holmfeldt, K., Hubalek, V., Lundin, D., Åström, M., Bertilsson, S. & Dopson, M. 2016. Microbial metagenomes from three aquifers in the Fennoscandian shield terrestrial deep biosphere reveal metabolic partitioning among populations. The ISME Journal 10 (5), 1192–1203.

Appendix 1. Geochemical data of the Outokumpu Deep Drill Hole groundwater and dissolved gases 2010–2012.

	Water sample code	Gas sample code	Sampling date	Depth m	Ag µg/L + 139M[1]	Al µg/L + 139M	As µg/L + 139M	B µg/L + 139M + 139P
1	OKU2260-4		5/30/2010	2260	0.15	<10	6.49	44.5
2	OKU2260-5		5/31/2010	2260	-	-	-	-
3	OKU2260-6		6/1/2010	2260	-	-	-	-
4	OKU2260-7		6/2/2010	2260	-	-	-	-
5	OKU2260-8		6/3/2010	2260	0.15	<10	5.88	44.4
6	OKU2260-9		6/4/2010	2260	-	-	-	-
7	OKU2260-10		6/5/2010	2260	0.18	<10	5.92	43.9
8	OKU2260-11		6/6/2010	2260	-	-	-	-
9	OKU2260-12		6/8/2010	2260	0.18	<10	6.14	41.6
10	OKU2260-13		6/10/2010	2260	-	-	-	-
11	OKU2260-14		6/11/2010	2260	0.17	<10	6.40	43.3
12	OKU2260-15		6/14/2010	2260	0.16	<10	6.09	42.0
13	OKU2260-16		6/16/2010	2260	0.18	<10	6.16	44.3
14	OKU2260-17		6/18/2010	2260	-	-	-	-
15		OKU2260-G1	6/20/2010	2260	-	-	-	-
16		OKU2260-G2	6/20/2010	2260	-	-	-	-
17		OKU2260-G3	6/20/2010	2260	-	-	-	-
18	OKU2260-18	OKU2260-G4	6/21/2010	2260	0.20	<10	5.80	40.6
19	OKU2260-19		7/2/2010	2260	0.07	9.33	61.1	51.9
20	OKU2260-20		7/15/2010	2260	0.08	9.61	61.6	52.7
21	OKU2260-21		7/27/2010	2260	0.09	9.65	61.5	49.7
22	OKU2260-DIC	OKU2260-G7	7/28/2010	2260	-	-	-	-
23		OKU2260-G9	7/28/2010	2260	-	-	-	-
24		OKU2260-G10	7/28/2010	2260	-	-	-	-
25	OKU2260-22		7/29/2010	2260	0.17	8.77	62.0	48.1
26	OKU2260-23		8/16/2010	2260	0.07	8.48	64.0	46.3
27		OKU2260-G11	9/13/2010	2260	-	-	-	-
28	OKU500-1		9/22/2010	500	0.03	<1	63.4	140
29	OKU500-2	OKU500-G1	9/23/2010	500	0.02	1.35	58.9	140
30		OKU500-G2	9/23/2010	500	-	-	-	-
31	OKU500-3	OKU500-G3	9/30/2010	500	0.03	<1	60.8	140
32		OKU500-G4	9/30/2010	500	-	-	-	-
33		OKU500-G5	9/30/2010	500	-	-	-	-
34		OKU500-G6	10/1/2010	500	-	-	-	-
35	OKU500-4	OKU500-G8	10/1/2010	500	0.02	<1	58.6	140
36	OKU500-5		10/5/2010	500	0.02	<1	59.0	140
37	OKU500-6	OKU500-G9	10/12/2010	500	0.04	<1	61.5	140
38	OKU500-7	OKU500-G11	10/13/2010	500	0.02	2.31	63.3	140
39		OKU500-G12	10/13/2010	500	-	-	-	-
40	OKU500-8		10/19/2010	500	<0.01	<100	1.43	120
41	OKU500-9		10/21/2010	500	<0.01	<100	1.60	120
42	OKU500-10		11/8/2010	500	<0.01	<100	1.25	110
43	OK-1		5/15/2011	25	0.071	23.7	1.81	124
44	OK-2		5/15/2011	100	0.063	16.1	2.07	126
45	OK-3		5/15/2011	200	0.048	12.4	1.95	138
46	OK-4		5/16/2011	300	0.079	14.1	1.5	143
47	OK-5	OK-5	5/16/2011	400	0.057	12.2	1.61	155
48	OK-6	OK-6	5/16/2011	500	0.039	12.3	1.73	163
49	OK-7	OK-7	5/16/2011	600	0.076	37.9	1.77	173
50	OK-8	OK-8	5/16/2011	700	0.063	18.7	1.75	176
51	OK-9	OK-9	5/16/2011	800	0.045	9.94	1.76	185
52	OK-10		5/16/2011	900	0.06	6.95	2.27	213
53	OK-11	OK-11	5/17/2011	1000	0.064	4.81	1.94	183
54	OK-12	OK-12	5/17/2011	1100	0.051	9.23	1.83	176
55	OK-13	OK-13	5/17/2011	1200	0.068	8.26	2.03	168
56	OK-14	OK-14	5/17/2011	1300	0.053	11.9	1.64	149
57	OK-15	OK-15	5/17/2011	1400	0.06	28.3	1.81	115
58	OK-16	OK-16	5/17/2011	1500	0.087	6.48	2.38	63.7
59	OK-17	OK-17	5/17/2011	1600	0.084	14	3.44	51.6
60	OK-18	OK-18	5/18/2011	1700	0.15	13.5	10.1	82.2
61	OK-19	OK-19	5/18/2011	1800	0.184	20	18.1	99.1
62	OK-20	OK-20	5/18/2011	1900	0.252	5.9	23.2	99.3

[1]Analytical methods: +139M = ICP-MS (Labtium Oy), 139P = ICP-OES (Labtium Oy)

Appendix 1. Cont.

	Water sample code	Gas sample code	Sampling date	Depth m	Ag µg/L + 139M[1]	Al µg/L + 139M	As µg/L + 139M	B µg/L + 139M + 139P
63	OK-21	OK-21	5/18/2011	2000	0.189	10	20.6	92.3
64	OK-22	OK-22	5/18/2011	2100	0.249	7.2	18.6	73.3
65	OK-23	OK-23	5/18/2011	2200	0.263	2.15	17.9	69.7
66	OK-24	OK-24	5/18/2011	2300	0.244	2.66	17.9	66.7
67	OK-25	OK-25	5/19/2011	2400	0.369	5.47	45.1	59.9
68	OKU2300-1		6/11/2011	2300	0.13	62.4	11.9	93.6
69	OKU2300-2		6/14/2011	2300	0.11	37.2	11.2	83.8
70	OKU2300-3		6/16/2011	2300	0.11	37.0	12.4	85.3
71		OKU2300-G1	7/19/2011	2300	-	-	-	-
72	OKU2300-5	OKU2300-G2	7/19/2011	2300	0.12	76.0	11.8	83.4
73	OKU2300-6		7/20/2011	2300	0.13	89.5	12.4	82.7
74	OKU2300-7		7/21/2011	2300	-	-	-	-
75	OKU1820-1		8/3/2011	1820	0.13	14.1	19.7	58.0
76	OKU1820-2		8/10/2011	1820	0.10	16.7	28.7	58.3
77	OKU1820-3		8/15/2011	1820	0.10	12.8	29.5	55.8
78		OKU1820-G1	8/17/2011	1820	-	-	-	-
79	OKU1820-5	OKU1820-G2	8/17/2011	1820	0.11	11.0	31.6	51.8
80	OKU1820-6		8/18/2011	1820	-	-	-	-
81	OUTO-500	OUTO-500 (1)	8/25/2011	500	0.12	84.5	14.7	231
82	OUTO-970	OUTO-970 (2)	8/25/2011	970	0.06	28.3	13.4	199
83	OUTO-1470	OUTO-1470 (3)	8/26/2011	1470	0.05	41.9	17.0	66.0
84	OUTO-1820	OUTO-1820 (4)	8/27/2011	1820	0.18	59.1	87.1	144
85	OUTO-2480	OUTO-2480 (5)	8/27/2011	2480	0.22	166	187	129
86	OUTO-500-2	OUTO-500 (6)	8/28/2011	500	0.04	32.9	13.4	199
87	OUTO-1470-2	OUTO-1470 (8)	8/29/2011	1470	0.10	66.3	16.8	62.5
88	OUTO-2350	OUTO-2350 (7)	8/29/2011	2350	0.21	77.6	129	126
89	OKU970-1		9/7/2011	970	0.02	10.0	1.19	128
90	OKU970-2		9/8/2011	970	0.02	9.74	1.08	126
91	OKU970-3		9/9/2011	970	0.02	8.33	1.03	121
92	OKU970-4		9/16/2011	970	0.02	8.92	1.09	126
93	OKU970-5		9/23/2011	970	0.02	8.10	1.09	123
94		OKU970-1G	10/4/2011	970	-	-	-	-
95	OKU970-6	OKU970-G2	10/5/2011	970	0.02	8.65	1.05	120
96	OKU970-7		10/6/2011	970	-	-	-	-
97	OU-1		10/11/2011	25	0.02	14.9	1.11	78.2
98	OU-2		10/11/2011	100	0.02	11.5	0.92	72.0
99	OU-3	OU-3	10/12/2011	200	0.02	13.6	0.76	68.0
100	OU-4	OU-4	10/12/2011	300	0.01	7.90	0.92	80.6
101	OU-5	OU-5	10/12/2011	400	0.02	14.2	1.10	90.2
102	OU-6	OU-6	10/12/2011	500	0.02	9.81	1.13	96.8
103	OU-7	OU-7	10/12/2011	600	0.02	4.26	1.15	97.9
104	OU-8	OU-8	10/13/2011	700	0.04	4.89	1.10	100
105	OU-9	OU-9	10/13/2011	800	0.02	4.17	1.16	99.6
106	OU-10	OU-10	10/13/2011	900	0.02	5.96	1.17	101
107	OU-11	OU-11	10/13/2011	1000	0.02	11.7	1.36	105
108	OKU180-1	OKU180-G1	5/5/2012	180	<0.2	<50	<2	120
109	OKU180-2	OKU180-G2	5/8/2012	180	<0.2	<50	<2	80
110	OKU180-3	OKU180-G3	5/14/2012	180	<0.2	<50	<2	160
111	OKU180-4		5/21/2012	180	<0.2	<50	<2	60
112	OKU180-5	OKU180-G4	5/22/2012	180	<0.2	<50	<2	90
113	OKU180-6	OKU180-G5	5/28/2012	180	<0.2	<50	<2	50
114	OKU180-7		5/29/2012	180	<0.2	<50	<2	320
115	OKU180-8	OKU180-G6	6/5/2012	180	<0.2	<50	<2	80
116	OKU180-9		6/6/2012	180	<0.2	<50	<2	90
117	OKU180-10	OKU180-G7	6/13/2012	180	<0.2	<50	<2	80
118	OKU180-11		6/18/2012	180	-	-	-	-
119		OKU180/iso I	6/18/2012	180	-	-	-	-
120		OKU180/iso II	6/18/2012	180	-	-	-	-
121		OKU180/pieni	6/18/2012	180	-	-	-	-

[1]Analytical methods: +139M = ICP-MS (Labtium Oy), 139P = ICP-OES (Labtium Oy)

Appendix 1. Cont.

	Be µg/L + 139M[1]	Bi µg/L + 139M	Cd µg/L + 139M	Co µg/L + 139M	Cr µg/L + 139M	Cu µg/L + 139M	Li µg/L + 139M + 139P	Mn µg/L + 139M	Mo µg/L + 139M
1	<1	<0.2	1.70	0.73	<2	<1	1510	176	76.4
2	-	-	-	-	-	-	-	-	-
3	-	-	-	-	-	-	-	-	-
4	-	-	-	-	-	-	-	-	-
5	<1	<0.2	1.86	0.65	<2	1.09	1450	178	75.5
6	-	-	-	-	-	-	-	-	-
7	<1	<0.2	1.91	0.69	<2	<1	1440	180	75.4
8	-	-	-	-	-	-	-	-	-
9	<1	0.49	2.31	0.61	<2	2.33	1360	176	74.8
10	-	-	-	-	-	-	-	-	-
11	<1	<0.2	2.17	0.65	<2	<1	1430	181	76.8
12	<1	<0.2	2.26	0.75	<2	1.2	1370	173	72.9
13	<1	<0.2	2.22	0.68	<2	<1	1450	182	76.6
14	-	-	-	-	-	-	-	-	-
15	-	-	-	-	-	-	-	-	-
16	-	-	-	-	-	-	-	-	-
17	-	-	-	-	-	-	-	-	-
18	<1	<0.2	2.12	0.62	<2	<1	1320	171	72.9
19	<0.1	0.16	0.12	0.88	2.15	2.07	2020	204	73.4
20	<0.1	0.17	0.14	0.85	1.92	2.01	2080	199	69.8
21	<0.1	0.15	0.15	0.88	2.3	2.11	2070	192	68.5
22	-	-	-	-	-	-	-	-	-
23	-	-	-	-	-	-	-	-	-
24	-	-	-	-	-	-	-	-	-
25	<0.1	0.13	0.12	0.79	2.00	2.22	2070	193	68.8
26	<0.1	0.12	0.18	1.04	2.70	2.05	2050	190	66.9
27	-	-	-	-	-	-	-	-	-
28	<0.1	<0.02	0.09	0.61	3.10	0.94	81	26.2	17.2
29	<0.1	<0.02	0.08	0.60	2.65	0.93	79	27.8	17.1
30	-	-	-	-	-	-	-	-	-
31	<0.1	<0.02	0.12	0.54	2.92	0.90	80	25.9	17.0
32	-	-	-	-	-	-	-	-	-
33	-	-	-	-	-	-	-	-	-
34	-	-	-	-	-	-	-	-	-
35	<0.1	<0.02	0.09	0.56	2.96	0.84	80	25.4	17.2
36	<0.1	<0.02	0.08	0.52	2.77	0.79	84	24.8	17.3
37	<0.1	<0.02	0.09	0.51	2.89	0.81	83	24.5	17.1
38	<0.1	<0.02	0.08	0.54	3.11	0.83	81	25.1	17.3
39	-	-	-	-	-	-	-	-	-
40	<1	<0.02	0.11	0.32	<2	<1	94	27.4	17.7
41	<1	<0.02	0.08	0.27	<2	<1	93	24.1	16.9
42	<1	<0.02	0.10	0.32	<2	<1	91	26.9	17.4
43	<0.1	<0.02	0.269	14.4	0.259	20.1	228	0.91	52.3
44	<0.1	<0.02	0.142	2.46	<0.2	21.6	135	<0.02	44.3
45	<0.1	<0.02	0.148	13.2	<0.2	11.1	107	<0.02	41.1
46	<0.1	<0.02	0.15	1.73	<0.2	9.89	98.1	<0.02	33.5
47	<0.1	<0.02	0.084	0.668	<0.2	8.28	80.4	2.25	31
48	<0.1	<0.02	<0.02	2.59	0.481	5.34	70.7	4.61	23.8
49	<0.1	<0.02	0.067	0.622	<0.2	5.53	60.4	4.35	17.9
50	<0.1	<0.02	0.125	1.63	<0.2	6.14	46.9	3.39	15.4
51	<0.1	<0.02	0.1	2.09	0.85	6.69	40.5	2.25	14.7
52	<0.1	<0.02	0.026	16.2	<0.2	13.4	35.4	2.33	15.2
53	<0.1	<0.02	0.092	13.6	<0.2	4.38	23.8	<0.02	14.5
54	<0.1	<0.02	0.09	0.892	<0.2	4.64	24.3	<0.02	19.7
55	<0.1	<0.02	0.118	13.1	5.36	5.4	34.1	0.582	30
56	<0.1	<0.02	0.145	13	<0.2	4.13	36.8	8.51	38.1
57	<0.1	<0.02	0.155	2.62	<0.2	4.49	119	52.4	38.9
58	<0.1	<0.02	0.16	5.96	<0.2	2.59	187	224	39
59	<0.1	<0.02	0.178	5.12	4.5	3.44	263	218	47.6
60	<0.1	<0.02	0.203	3.13	0.567	9.68	507	108	63.2
61	<0.1	<0.02	0.103	6.35	10.5	4.4	824	94.9	45.7
62	<0.1	<0.02	0.266	5.1	13.2	8.07	1020	83.9	41.2

[1]Analytical methods: +139M = ICP-MS (Labtium Oy), 139P = ICP-OES (Labtium Oy)

Appendix 1. Cont.

	Be μg/L + 139M[1]	Bi μg/L + 139M	Cd μg/L + 139M	Co μg/L + 139M	Cr μg/L + 139M	Cu μg/L + 139M	Li μg/L + 139M + 139P	Mn μg/L + 139M	Mo μg/L + 139M
63	<0.1	<0.02	0.163	5.31	33.6	4.98	1060	106	47
64	0.138	<0.02	0.148	7.7	24.6	3.6	1310	119	49.1
65	<0.1	<0.02	0.313	6.16	0.249	3.47	1170	132	52.4
66	0.113	<0.02	0.353	19.5	427	13.5	1350	159	120
67	<0.1	<0.02	0.221	6.54	1.16	9.92	14200	42.7	92.9
68	<0.1	0.29	0.33	3.84	2.33	3.64	2800	225	66.6
69	<0.1	0.16	0.27	29.9	0.86	1.88	2710	215	61.3
70	<0.1	0.15	0.26	2.51	1.01	2.28	2710	220	63.2
71	-	-	-	-	-	-	-	-	-
72	<0.1	0.14	0.28	24.6	1.03	1.74	2570	216	61.3
73	<0.1	0.13	0.27	3.60	1.00	3.20	2670	216	61.5
74	-	-	-	-	-	-	-	-	-
75	<0.1	0.06	0.30	6.05	1.12	6.49	2090	209	55.6
76	<0.1	0.04	0.30	6.07	1.33	4.71	1310	140	32.1
77	<0.1	0.03	0.33	4.45	1.24	4.33	1320	141	32.3
78	-	-	-	-	-	-	-	-	-
79	<0.1	<0.02	0.39	5.61	1.27	4.08	1340	139	31.6
80	-	-	-	-	-	-	-	-	-
81	<1	<0.2	0.99	8.29	<2	3.73	80	70.8	23.2
82	<1	<0.2	0.43	11.5	<2	1.26	50	35.4	23.3
83	<1	<0.2	0.21	9.54	<2	<1	340	468	45.4
84	<1	0.93	0.24	38.5	<2	2.75	1480	190	69.8
85	<1	0.26	0.49	56.8	2.55	1.87	50300	260	174
86	<1	<0.2	0.32	7.97	<2	377	60	115	24.9
87	<1	<0.2	0.30	9.50	<2	1.17	350	484	56.4
88	<1	0.41	0.39	44.6	2.25	1.86	22600	115	134
89	<0.1	<0.02	0.12	0.43	0.57	0.62	48	63.1	12.6
90	<0.1	<0.02	0.12	0.40	0.46	0.55	48	59.4	11.9
91	<0.1	<0.02	0.14	0.40	0.40	0.96	46	66.4	12.8
92	<0.1	<0.02	0.14	0.38	0.40	0.57	53	64.9	13.0
93	<0.1	<0.02	0.15	0.33	0.35	0.98	50	36.1	10.4
94	-	-	-	-	-	-	-	-	-
95	<0.1	<0.02	0.15	0.34	0.34	0.44	51	67.4	13.5
96	-	-	-	-	-	-	-	-	-
97	<0.1	<0.02	0.19	0.37	1.09	8.58	99	20.6	38.5
98	<0.0	<0.02	0.16	0.33	1.12	5.75	96	17.9	37.3
99	<0.1	<0.02	0.16	0.26	0.80	4.89	75	13.5	34.7
100	<0.1	<0.02	0.16	0.27	0.99	4.29	65	51.0	29.3
101	<0.1	<0.02	0.17	0.40	1.37	5.35	61	150	19.4
102	<0.1	<0.02	0.15	0.46	1.25	7.63	58	128	17.0
103	<0.1	<0.02	0.17	0.41	1.28	3.59	55	148	15.0
104	<0.1	<0.02	0.15	0.50	1.48	5.25	53	133	14.2
105	<0.1	<0.02	0.15	0.40	1.61	8.74	50	109	14.1
106	<0.1	<0.02	0.13	0.90	1.43	8.58	52	88.4	14.7
107	<0.1	<0.02	0.16	0.43	4.67	1.74	49	43.6	12.6
108	<5	<1	0.33	<0.5	<10	<5	13.3	7.95	37.6
109	<5	<1	<0.3	<0.5	<10	<5	14.8	8.62	37.7
110	<5	<1	0.30	<0.5	<10	<5	9.90	105	19.4
111	<5	<1	0.33	<0.5	<10	<5	10.2	182	17.1
112	<5	<1	0.36	<0.5	<10	<5	8.39	192	16.7
113	<5	<1	<0.3	<0.5	<10	<5	9.38	196	16.0
114	<5	<1	<0.3	<0.5	<10	<5	9.77	213	15.9
115	<5	<1	<0.3	<0.5	<10	<5	6.50	144	12.6
116	<5	<1	<0.3	<0.5	<10	<5	4.78	137	12.4
117	<5	<1	<0.3	<0.5	<10	<5	6.43	133	12.6
118	-	-	-	-	-	-	-	-	-
119	-	-	-	-	-	-	-	-	-
120	-	-	-	-	-	-	-	-	-
121	-	-	-	-	-	-	-	-	-

[1]Analytical methods: +139M = ICP-MS (Labtium Oy), 139P = ICP-OES (Labtium Oy)

Appendix 1. Cont.

	Ni µg/L + 139M[1]	P µg/L + 139M	Pb µg/L + 139M	Rb µg/L + 139M	Sb µg/L + 139M	Se µg/L + 139M	Th µg/L + 139M	Tl µg/L + 139M	U µg/L + 139M
1	2.26	<200	1.48	181	0.20	469	<0.04	0.49	<0.02
2	-	-	-	-	-	-	-	-	-
3	-	-	-	-	-	-	-	-	-
4	-	-	-	-	-	-	-	-	-
5	2.20	<200	1.40	181	<0.2	472	<0.04	0.44	<0.02
6	-	-	-	-	-	-	-	-	-
7	2.41	<200	1.32	184	<0.2	483	<0.04	0.36	<0.02
8	-	-	-	-	-	-	-	-	-
9	2.68	<200	1.36	180	<0.2	474	<0.04	0.33	<0.02
10	-	-	-	-	-	-	-	-	-
11	2.44	<200	1.28	187	0.21	500	<0.04	0.32	<0.02
12	2.36	<200	1.15	178	0.20	485	<0.04	0.27	<0.02
13	2.79	<200	1.12	190	0.21	511	<0.04	0.24	<0.02
14	-	-	-	-	-	-	-	-	-
15	-	-	-	-	-	-	-	-	-
16	-	-	-	-	-	-	-	-	-
17	-	-	-	-	-	-	-	-	-
18	2.19	<200	1.14	179	<0.2	489	<0.04	0.27	<0.02
19	2.99	18.3	0.1	183	0.22	322	0.03	0.01	<0.01
20	3.88	<10	0.08	177	0.20	319	0.02	<0.01	<0.01
21	3.16	<10	0.08	176	0.20	319	0.02	<0.01	<0.01
22	-	-	-	-	-	-	-	-	-
23	-	-	-	-	-	-	-	-	-
24	-	-	-	-	-	-	-	-	-
25	6.77	<10	0.05	177	0.23	323	0.02	0.01	<0.01
26	23.6	<10	<0.05	178	0.19	326	0.02	0.01	<0.01
27	-	-	-	-	-	-	-	-	-
28	3.14	<10	<0.05	43.3	0.20	193	<0.01	<0.01	<0.01
29	3.11	<10	<0.05	42.2	0.18	174	<0.01	<0.01	<0.01
30	-	-	-	-	-	-	-	-	-
31	3.31	<10	<0.05	41.5	0.19	177	<0.01	<0.01	<0.01
32	-	-	-	-	-	-	-	-	-
33	-	-	-	-	-	-	-	-	-
34	-	-	-	-	-	-	-	-	-
35	2.76	<10	<0.05	41.9	0.19	182	<0.01	<0.01	<0.01
36	2.71	<10	<0.05	41.3	0.19	186	<0.01	<0.01	<0.01
37	2.94	<10	<0.05	41.0	0.20	194	<0.01	<0.01	<0.01
38	3.07	<10	<0.05	41.6	0.20	200	<0.01	<0.01	<0.01
39	-	-	-	-	-	-	-	-	-
40	3.14	<50	4.10	39.1	0.22	<10	<0.04	<0.02	<0.02
41	2.50	<50	3.15	38.0	0.20	<10	<0.04	<0.02	<0.02
42	2.54	<50	3.88	37.7	<0.2	<10	<0.04	<0.02	<0.02
43	10.8	142	13.2	82.2	0.53	383	0.01	<0.01	<0.01
44	8.23	104	10.2	55.7	0.298	300	0.01	<0.01	<0.01
45	7.16	121	3.46	50.7	0.3	311	0.01	<0.01	<0.01
46	8.71	82.5	1.92	42.9	0.226	299	0.01	<0.01	<0.01
47	9.52	117	1.99	41.5	0.263	316	<0.01	<0.01	<0.01
48	8.53	6490	1.02	37.8	0.193	324	<0.01	<0.01	<0.01
49	5.72	114	0.136	35.9	0.174	331	<0.01	<0.01	<0.01
50	6.54	130	<0.05	35.1	0.219	339	<0.01	<0.01	<0.01
51	8.42	8050	0.192	35.2	0.207	364	<0.01	<0.01	<0.01
52	7.75	292	0.196	37.9	0.223	388	<0.01	<0.01	<0.01
53	6.88	1230	<0.05	33.9	0.177	335	<0.01	<0.01	<0.01
54	5.49	306	<0.05	35.3	0.215	333	<0.01	<0.01	<0.01
55	9.92	263000	0.098	39.2	0.755	304	<0.01	<0.01	<0.01
56	5.78	1330	0.162	48.4	0.267	288	0.01	<0.01	<0.01
57	5.86	275	0.348	80.8	0.554	293	<0.01	<0.01	<0.01
58	8.46	308	<0.05	158	0.196	354	<0.01	<0.01	<0.01
59	24.7	4350	0.149	186	0.274	456	<0.01	<0.01	<0.01
60	20.9	301	0.322	167	0.353	799	<0.01	<0.01	<0.01
61	36.5	5760	0.203	163	0.353	1090	<0.01	<0.01	<0.01
62	43.4	5240	0.392	185	0.396	1310	<0.01	<0.01	0.037

[1]Analytical methods: +139M = ICP-MS (Labtium Oy)

Appendix 1. Cont.

	Ni µg/L + 139M[1]	P µg/L + 139M	Pb µg/L + 139M	Rb µg/L + 139M	Sb µg/L + 139M	Se µg/L + 139M	Th µg/L + 139M	Tl µg/L + 139M	U µg/L + 139M
63	50.6	9970	0.175	191	0.441	1250	<0.01	<0.01	0.01
64	45.2	7160	0.152	189	0.31	1160	0.01	<0.01	<0.01
65	29.2	246	0.119	196	0.393	1100	<0.01	<0.01	<0.01
66	296	224000	0.224	195	0.966	1110	<0.01	<0.01	<0.01
67	51.4	374	0.196	573	0.369	2060	<0.01	<0.01	0.01
68	12.8	413	<0.05	213	0.36	0.97	0.09	<0.01	0.01
69	9.91	432	<0.05	202	0.28	0.91	0.04	<0.01	<0.01
70	10.3	374	<0.05	209	0.28	0.93	0.03	<0.01	0.01
71	-	-	-	-	-	-	-	-	-
72	9.75	350	<0.05	207	0.29	0.93	0.03	<0.01	<0.01
73	10.4	359	<0.05	211	0.24	0.97	0.02	<0.01	<0.01
74	-	-	-	-	-	-	-	-	-
75	16.5	220	0.16	247	0.21	27.7	<0.01	<0.01	<0.01
76	14.7	189	<0.05	203	0.24	40.8	<0.01	<0.01	<0.01
77	14.5	196	<0.05	207	0.25	42.8	<0.01	<0.01	<0.01
78	-	-	-	-	-	-	-	-	-
79	15.1	40.8	<0.05	205	0.27	44.3	<0.01	<0.01	0.01
80	-	-	-	-	-	-	-	-	-
81	342	<200	4.64	45.7	<0.5	188	<0.1	0.64	<0.05
82	48.1	<200	1.52	37.7	<0.5	179	<0.1	0.39	<0.05
83	117	<200	0.15	220	<0.5	198	<0.1	0.25	<0.05
84	103	<200	<0.1	199	<0.5	620	<0.1	0.17	<0.05
85	72.0	<200	0.16	1010	0.55	1140	<0.1	0.13	<0.05
86	37.2	<200	0.25	41.6	<0.5	184	<0.1	0.24	<0.05
87	105	<200	0.72	216	<0.5	198	<0.1	0.22	<0.05
88	66.0	<200	0.18	656	<0.5	890	<0.1	0.13	<0.05
89	2.03	<10	0.20	30.0	0.13	180	0.02	<0.01	0.01
90	2.02	<10	0.17	29.4	0.11	177	0.01	<0.01	0.01
91	2.44	<10	0.16	29.2	0.12	174	0.01	<0.01	0.01
92	1.85	<10	0.18	30.3	0.11	177	0.01	<0.01	0.01
93	1.66	<10	0.17	28.9	0.08	184	0.01	<0.01	0.01
94	-	-	-	-	-	-	-	-	-
95	1.70	<10	0.17	30.5	0.10	176	0.01	<0.01	0.01
96	-	-	-	-	-	-	-	-	-
97	2.60	55	2.16	46.1	0.22	<0.5	<0.01	<0.01	0.01
98	2.39	<50	0.32	42.5	0.21	<0.5	<0.01	<0.01	0.01
99	1.93	50	0.62	37.8	0.18	<0.5	<0.01	<0.01	<0.01
100	1.88	60	0.37	36.6	0.15	<0.5	<0.01	<0.01	<0.01
101	2.31	<50	<0.05	34.0	0.15	<0.5	<0.01	<0.01	<0.01
102	2.67	<50	<0.05	34.4	0.11	<0.5	<0.01	<0.01	<0.01
103	2.16	<50	<0.05	32.5	0.10	<0.5	<0.01	<0.01	0.01
104	2.20	50	<0.05	32.0	0.13	<0.5	<0.01	<0.01	0.01
105	2.02	<50	0.28	31.4	0.12	<0.5	<0.01	<0.01	<0.01
106	2.22	<50	0.17	31.5	0.13	<0.5	<0.01	<0.01	<0.01
107	4.84	<50	<0.05	30.9	0.11	<0.5	<0.01	<0.01	<0.01
108	20.6	<1000	0.73	39.4	<1	<50	<0.2	0.17	<0.1
109	21.8	<1000	0.86	40.2	<1	53.3	<0.2	<0.1	<0.1
110	28.1	<1000	0.82	34.9	<1	60.5	<0.2	<0.1	<0.1
111	23.6	<1000	1.05	31.1	<1	57.3	<0.2	<0.1	<0.1
112	25.5	<1000	0.82	31.7	<1	54.8	<0.2	<0.1	<0.1
113	24.5	<1000	0.76	31.2	<1	63.6	<0.2	<0.1	<0.1
114	26.5	<1000	1.04	32.6	<1	56.1	<0.2	0.14	<0.1
115	18.7	<1000	1.00	25.2	<1	<50	<0.2	<0.1	<0.1
116	23.0	<1000	0.97	24.9	<1	<50	<0.2	0.10	<0.1
117	23.1	<1000	1.27	27.6	<1	<50	<0.2	0.10	<0.1
118	-	-	-	-	-	-	-	-	-
119	-	-	-	-	-	-	-	-	-
120	-	-	-	-	-	-	-	-	-
121	-	-	-	-	-	-	-	-	-

[1]Analytical methods: +139M = ICP-MS (Labtium Oy)

Appendix 1. Cont.

	V µg/L +139M[1]	Zn µg/L +139M	K mg/L +139M +139P	Ba mg/L +139P +139M	Ca mg/L +139P	Fe_{tot} mg/L +139P +139M	Mg mg/L +139P	Na mg/L +139P	S_{tot} mg/L +139P
1	0.84	14.6	45.4	3.02	6810	<0.03	21.8	2240	11.2
2	-	-	-	-	-	-	-	-	-
3	-	-	-	-	-	-	-	-	-
4	-	-	-	-	-	-	-	-	-
5	1.05	5.69	45.3	3.06	7020	0.10	21.8	2320	5.51
6	-	-	-	-	-	-	-	-	-
7	1.02	10.4	46.1	3.09	6700	0.10	21.8	2210	5.54
8	-	-	-	-	-	-	-	-	-
9	1.03	8.56	44.9	3.09	6660	0.07	21.6	2270	5.34
10	-	-	-	-	-	-	-	-	-
11	1.00	11.4	46.6	3.12	6730	0.06	21.7	2240	5.24
12	1.10	7.87	44.1	3.11	6910	0.07	21.8	2260	4.79
13	1.14	9.72	47.0	3.12	7290	0.06	21.9	2470	4.77
14	-	-	-	-	-	-	-	-	-
15	-	-	-	-	-	-	-	-	-
16	-	-	-	-	-	-	-	-	-
17	-	-	-	-	-	-	-	-	-
18	0.99	13.5	44.1	3.15	7090	0.05	21.7	2310	5.00
19	26.4	6.46	55.8	-	7485	0.04	21.6	2430	3.85
20	26.7	9.83	57.0	-	7500	<0.03	21.6	2400	4.47
21	26.5	6.54	56.0	-	7660	<0.03	21.4	2460	4.81
22	-	-	-	-	-	-	-	-	-
23	-	-	-	-	-	-	-	-	-
24	-	-	-	-	-	-	-	-	-
25	26.6	9.03	56.1	-	7890	<0.03	21.2	2560	4.10
26	26.8	4.50	55.0	-	8130	0.03	21.0	2630	4.80
27	-	-	-	-	-	-	-	-	-
28	15.7	4.65	17.3	1.86	2300	<0.03	12.6	1770	3.00
29	14.7	3.47	17.2	1.73	2130	<0.03	12.5	1640	3.24
30	-	-	-	-	-	-	-	-	-
31	15.4	3.91	16.9	1.73	2180	<0.03	12.4	1660	3.32
32	-	-	-	-	-	-	-	-	-
33	-	-	-	-	-	-	-	-	-
34	-	-	-	-	-	-	-	-	-
35	15.9	3.10	17.1	1.80	2180	<0.03	12.4	1660	3.38
36	15.9	1.70	17.4	1.81	2240	<0.03	12.6	1740	3.48
37	16.5	6.66	17.2	1.84	2300	<0.03	12.2	1760	2.97
38	16.6	7.37	17.2	1.89	2240	<0.03	12.4	1700	3.35
39	-	-	-	-	-	-	-	-	-
40	0.67	15.1	18.6	1.60	2250	<0.03	12.8	1820	3.24
41	0.62	5.75	18.5	1.61	2240	<0.03	12.8	1800	3.48
42	0.69	9.53	18.3	1.61	2250	<0.03	12.9	1810	3.49
43	2.6	56.5	34.9	1.37	2610	0.08	20.7	1700	52.2
44	2.07	39.8	25.9	1.23	2370	0.05	13.7	1680	50.4
45	2.12	26.2	24.2	1.34	2170	<0.03	11.3	1610	49.6
46	1.73	19.4	21.3	1.38	2400	0.04	9.62	1850	51.1
47	1.97	36	20.7	1.50	2300	0.06	8.9	1830	53.5
48	2.08	20.5	19	1.60	2420	0.04	7.92	1970	53.3
49	2.15	22.3	17.7	1.69	2310	0.04	7.09	1900	55
50	2.21	25.7	16.7	1.75	2320	0.06	6.46	1900	57
51	2.33	30	16.8	1.80	2340	0.03	5.74	1930	56.3
52	2.21	26.6	18.3	1.93	2480	0.03	5.16	2060	55.4
53	2.43	21.9	16.4	1.67	2290	0.07	4.53	1890	58.9
54	2.04	14.8	17.5	1.54	2230	<0.03	3.95	1870	59.3
55	1.91	118	19.6	1.33	2210	0.07	6.42	1870	53.9
56	1.97	19.5	23.4	1.19	2040	<0.03	17.8	1720	58.8
57	1.99	16.1	33.4	1.05	2110	0.05	39.4	1550	61.5
58	2.49	21	55.7	0.88	3060	0.03	99	1620	62.3
59	3.1	17.1	62.3	0.95	3930	0.08	194	1810	59.6
60	5.95	60.1	60.5	2.38	8300	0.18	34.6	3330	50.5
61	8.14	12.7	59.5	4.18	11700	0.22	21.9	3900	47.3
62	11.3	13.8	60.3	5.83	14400	0.22	16.3	4250	46.4

[1]Analytical methods: +139M = ICP-MS (Labtium Oy), 139P = ICP-OES (Labtium Oy)

Appendix 1. Cont.

	V µg/L + 139M[1]	Zn µg/L + 139M	K mg/L + 139M + 139P	Ba mg/L + 139P + 139M	Ca mg/L + 139P	Fe$_{tot}$ mg/L + 139P + 139M	Mg mg/L + 139P	Na mg/L + 139P	S$_{tot}$ mg/L + 139P
63	9.64	16.6	60.5	5.97	15600	0.30	16.9	3920	47.2
64	9.49	19.3	56.4	5.65	13300	0.25	17.5	3760	46.2
65	8.28	3.09	55.4	5.43	10000	0.16	18.3	3340	49.2
66	10.3	32.8	57.2	5.07	11900	1.65	18.8	3310	50
67	16.8	<0.2	75.5	0.98	18200	0.26	14	4160	45.5
68	3.02	7.3	64.0	-	9790	<0.03	18.8	3190	6.30
69	3.18	4.72	62.5	-	8680	0.03	18.8	2820	6.09
70	3.10	9.30	62.3	-	9080	0.03	18.9	2990	5.79
71	-	-	-	-	-	-	-	-	-
72	3.26	5.94	60.9	-	9540	0.03	18.7	3150	7.60
73	3.40	8.83	60.9	-	9480	<0.03	18.7	3120	7.42
74	-	-	-	-	-	-	-	-	-
75	3.42	5.26	57.9	3.88	9650	<0.03	18.4	3030	7.37
76	4.26	0.57	49.0	4.31	12200	<0.03	14.9	3930	35.2
77	4.30	0.99	49.3	4.40	11800	<0.03	15.1	3800	42.6
78	-	-	-	-	-	-	-	-	-
79	4.47	0.79	48.5	4.41	11800	0.03	15.1	3820	44.4
80	-	-	-	-	-	-	-	-	-
81	1.16	24.2	18.0	2.43	2320	<0.03	6.92	1900	4.04
82	<1	30.9	15.0	4.49	2420	<0.03	2.04	1900	3.09
83	<1	21.7	71.9	0.75	3210	<0.03	222	1540	7.06
84	3.05	8.19	56.7	4.60	12900	<0.03	14.3	4170	2.92
85	4.15	6.74	97.4	0.82	20600	<0.03	14.2	4700	14.8
86	<1	32.0	16.4	3.54	2330	<0.03	6.81	1890	4.28
87	<1	19.1	71.2	0.71	3180	<0.03	218	1540	6.73
88	3.51	8.14	91.5	3.08	16900	<0.03	13.1	4190	4.69
89	10.1	12.3	12.8	2.12	2470	<0.03	1.89	1950	2.48
90	10.1	10.6	12.5	2.06	2480	<0.03	1.87	1970	4.24
91	9.88	11.6	12.4	1.94	2460	<0.03	2.20	1970	3.10
92	10.3	17.7	12.8	1.98	2430	0.03	2.39	2000	2.34
93	10.6	6.63	12.1	2.05	2510	<0.03	1.63	2000	2.62
94	-	-	-	-	-	-	-	-	-
95	10.4	3.92	13.0	1.92	2340	0.04	2.92	1890	2.93
96	-	-	-	-	-	-	-	-	-
97	0.29	72.7	18.8	1.10	1530	<0.03	7.61	1250	28.5
98	0.25	41.3	18.1	1.03	1490	<0.03	7.34	1220	30.0
99	0.22	30.2	16.6	1.00	1430	<0.03	6.94	1210	34.3
100	0.30	22.1	14.8	1.36	1710	<0.03	7.53	1440	35.4
101	0.36	60.1	13.1	1.78	2170	<0.03	8.04	1770	32.6
102	0.41	70.1	12.4	1.95	2370	<0.03	7.48	1930	35.4
103	0.41	62.0	11.8	1.97	2340	<0.03	6.45	1890	31.7
104	0.44	65.2	11.4	2.05	2370	<0.03	5.47	1910	30.7
105	0.39	54.0	11.2	2.06	2300	<0.03	4.53	1860	31.6
106	0.47	78.7	11.3	1.94	2340	<0.03	3.59	1880	33.6
107	0.48	23.9	10.8	1.98	2450	<0.03	1.91	1930	33.8
108	<2	22.8	21.0	0.88	1260	<0.03	2.84	1120	14.1
109	<2	17.8	21.3	1.01	1330	<0.03	3.19	1170	5.82
110	<2	<10	17.4	1.23	1610	<0.03	14.4	1450	2.76
111	<2	14.7	16.8	0.96	1330	<0.03	16.5	1240	2.20
112	<2	13.3	16.8	0.98	1360	<0.03	17.1	1270	2.03
113	<2	28.8	16.2	0.87	1220	0.12	17.2	1170	1.78
114	<2	29.5	18.3	0.96	1220	0.46	18.0	1190	1.08
115	<2	34.8	13.1	0.72	1120	0.26	16.7	1110	1.16
116	<2	45.1	12.8	0.70	1160	0.26	17.5	1160	1.52
117	<2	46.3	13.7	0.73	1060	0.34	16.7	1070	1.27
118	-	-	-	-	-	-	-	-	-
119	-	-	-	-	-	-	-	-	-
120	-	-	-	-	-	-	-	-	-
121	-	-	-	-	-	-	-	-	-

[1]Analytical methods: +139M = ICP-MS (Labtium Oy), 139P = ICP-OES (Labtium Oy)

Appendix 1. Cont.

	Si mg/L + 139P[1]	Sr mg/L + 139P + 139M	TOC mg/L 142L	DOC mg/L 142L	DIC mmol/L PHREEQC (calculated)	pH	EC mS/m 25°C	Br mg/L + 143R	Cl mg/L + 143R
1	1.50	64.0	-	-	-	9.3	5020	<100	18400
2	-	-	-	-	-	-	-	-	-
3	-	-	-	-	-	-	-	-	-
4	-	-	-	-	-	-	-	-	-
5	1.55	66.6	-	-	-	9.3	4870	<100	16800
6	-	-	-	-	-	-	-	-	-
7	1.52	63.5	-	-	-	9.3	4780	<100	18000
8	-	-	-	-	-	-	-	-	-
9	1.51	65.5	-	-	-	9.3	4720	<100	18700
10	-	-	-	-	-	-	-	-	-
11	1.51	64.1	-	-	-	9.3	4680	<100	17900
12	1.52	64.7	-	-	-	9.3	4660	<100	18500
13	1.56	71.0	-	-	-	9.3	4640	<100	24400
14	-	-	-	-	-	-	-	-	-
15	-	-	-	-	-	-	-	-	-
16	-	-	-	-	-	-	-	-	-
17	-	-	-	-	-	-	-	-	-
18	1.51	66.0	27.2	22.5	0.21	9.3	4630	<100	21700
19	1.60	70.9	-	-		6.7	4570	<1000	16000
20	1.63	70.2	-	-	-	6.8	4690	<1000	16700
21	1.63	72.0	-	-	0.26	6.5	4750	<1000	17000
22	-	-	-	-	-	-	-	-	-
23	-	-	-	-	-	-	-	-	-
24	-	-	-	-	-	-	-	-	-
25	1.63	74.6	-	-	-	6.9	4760	<1000	19000
26	1.64	76.6	-	-	-	8.2	4890	<1000	16400
27	-	-	-	-	-	-	-	-	-
28	1.68	23.6	-	-	-	8.3	1900	<50	6920
29	1.68	21.8	-	-	-	8.3	1880	<50	6990
30	-	-	-	-	-	-	-	-	-
31	1.67	22.2	-	-	0.18	8.4	1880	<50	6750
32	-	-	-	-	-	-	-	-	-
33	-	-	-	-	-	-	-	-	-
34	-	-	-	-	-	-	-	-	-
35	1.67	22.4	-	-	0.08	8.4	1880	<50	6690
36	1.66	23.1	-	-	-	8.4	1900	<50	6830
37	1.64	23.6	-	-	-	8.7	1900	<50	6980
38	1.57	23.2	12.67	12.17	0.09	8.7	1920	<50	6830
39	-	-	-	-	-	-	-	-	-
40	1.54	22.0	-	-	-	7.4	1900	<50	7970
41	1.55	22.1	-	-	-	6.3	1900	<50	7940
42	1.45	22.0	-	-	-	8.3	1900	<50	8180
43	0.92	37.4	220	230	-	9.8	1850	<100	7910
44	0.96	26.6	200	200	-	10.1	1610	<100	6660
45	1.09	26.7	200	200	-	10.1	1530	<100	7670
46	1.27	25.9	210	210	-	9.95	1510	<100	6520
47	1.48	26.1	210	220	0.11	9.6	1490	<100	7910
48	1.92	26.0	220	230	0.12	9.2	1610	<100	7070
49	2.38	27.9	230	220	0.20	8.6	1660	<100	7290
50	2.73	28.4	240	250	0.13	8.5	1680	<100	7640
51	3.09	30.1	240	240	0.12	8.5	1690	<100	7870
52	3.28	28.5	240	240	-	8.9	1700	<100	7500
53	3.49	27.0	250	280	0.15	8.9	1690	<100	7360
54	3.45	29.6	240	280	0.09	8.9	1620	<100	8340
55	3.61	24.5	250	290	0.12	9.1	1520	<100	7300
56	2.43	22.0	250	290	0.12	8.9	1470	<100	7230
57	1.63	30.4	250	290	0.14	8.5	1550	<100	7390
58	0.73	29.7	240	290	0.17	8.5	1860	<100	8230
59	0.71	44.0	240	270	0.09	8.5	2380	<100	14100
60	1.22	92.5	230	260	0.20	8.6	3500	<100	21800
61	1.71	130	220	260	0.16	8.7	4280	145	26200
62	2.09	145	220	260	0.19	8.8	4510	159	27900

[1]Analytical methods: 139P = ICP-OES (Labtium Oy), 142L = TOC and DOC analysis according to the standard method SFS-EN 1484 (Labtium Oy), +148R = ion chromatography (Labtium Oy)

Appendix 1. Cont.

	Si mg/L + 139P[1] + 139M	Sr mg/L + 139P	TOC mg/L 142L	DOC mg/L 142L	DIC mmol/L PHREEQC (calculated)	pH	EC mS/m 25°C	Br mg/L + 143R	Cl mg/L + 143R
63	2.11	133	230	260	0.17	8.6	4360	149	27400
64	2.01	150	230	270	0.11	8.6	4190	145	26700
65	1.92	127	240	280	0.17	8.5	4000	137	25700
66	1.99	122	240	280	0.14	8.4	3900	136	24300
67	2.13	201	200	240	0.19	8.9	5160	241	39300
68	1.76	62.5	-	-	-	8.0	4340	118	24400
69	1.78	62.2	-	-	-	7.7	4390	129	23100
70	1.80	62.6	-	-	-	5.9	4400	121	24200
71	-	-	-	-	-	-	-	-	-
72	1.79	63.4	-	-	-	8.6	4410	130	25100
73	1.78	63.5	-	-	-	8.6	4370	123	24500
74	-	-	34	34	-	-	-	-	-
75	1.84	87.2	-	-	-	8.6	5630	136	23400
76	2.12	110	-	-	-	8.9	6890	166	30000
77	2.08	106	-	-	-	8.9	6910	175	30100
78	-	-	-	-	-	-	-	-	-
79	2.09	107	30	30	-	9.0	6930	159	30300
80	-	-	-	-	-	-	-	-	-
81	2.08	22.8	-	-	-	7.0	2040	<100	7270
82	3.90	24.0	-	-	-	8.6	2060	<100	7190
83	0.50	26.7	-	-	-	6.8	2440	<100	8960
84	2.08	74.6	-	-	-	8.3	6800	153	33300
85	1.99	104	-	-	-	8.5	9560	301	43000
86	1.58	22.9	-	-	-	6.5	2010	<100	7730
87	0.56	26.6	-	-	-	7.7	2410	<100	9280
88	2.20	91.9	-	-	-	8.8	8200	220	35000
89	2.47	24.2	-	-	-	8.4	2110	<100	6920
90	2.48	24.0	-	-	-	8.3	2100	<100	7000
91	2.18	23.6	-	-	-	8.4	2070	<100	7330
92	2.10	23.7	-	-	-	8.4	2060	<100	7030
93	2.84	24.4	-	-	-	8.7	2100	<100	7250
94	-	-	-	-	-	-	-	-	-
95	1.98	23.3	11	11	-	8.7	2020	<100	6880
96	-	-	-	-	-	-	-	-	-
97	0.58	16.0	140	130	-	9.1	1390	< 100	4625
98	0.51	15.6	140	130	-	9.2	1370	< 100	4620
99	0.49	15.1	150	150	-	9.7	1300	< 100	4440
100	0.44	18.1	150	150	-	9.5	1510	< 100	5380
101	0.45	22.8	160	160	-	8.6	1900	< 100	6720
102	0.58	25.0	150	150	-	8.5	1990	< 100	7110
103	0.88	24.6	120	120	-	8.4	2010	< 100	7300
104	1.14	25.0	120	120	-	8.4	2010	< 100	7510
105	1.36	24.2	130	130	-	8.5	2000	< 100	7610
106	1.48	24.6	150	140	-	8.5	2010	< 100	7760
107	2.54	25.8	140	140	-	8.7	2060	< 100	7760
108	0.50	13.3	-	-	-	10	1180	21	3820
109	0.52	14.1	-	-	-	10	1240	28	4090
110	1.28	17.3	-	-	-	7.9	1480	35	4710
111	1.94	14.3	-	-	-	7.4	1280	31	4080
112	2.02	14.6	-	-	-	7.5	1260	28	4070
113	2.30	13.1	-	-	-	7.1	1180	27	3660
114	3.98	13.3	-	-	-	7.3	1160	27	3640
115	2.60	12.3	-	-	-	7.2	1110	26	3380
116	2.65	12.9	12.8	9	-	7.2	1100	24	3720
117	2.72	11.7	-	-	-	7.4	1060	23	3280
118	-	-	-	-	-	-	-	-	-
119	-	-	-	-	-	-	-	-	-
120	-	-	-	-	-	-	-	-	-
121	-	-	-	-	-	-	-	-	-

[1]Analytical methods: 139P = ICP-OES (Labtium Oy), 142L = TOC and DOC analysis according to the standard method SFS-EN 1484 (Labtium Oy), +148R = ion chromatography (Labtium Oy)

Appendix 1. Cont.

	I µg/L +139M[1] (IC)	F mg/L +143R IC	SO$_4$ mg/L +143R IC	NO$_3$ mg/L +143R	Alkalinity mmol/L 143T	Sulphide mg/L SP	TDS g/L	^{87}Sr/^{86}Sr TIMS	δ^{2}H$_{H2O}$ ‰ VSMOW Picarro IRMS
1	215	<100	<100	<200	0.46	-	28	-	-72.9
2	-	-	-	-	-	-	-	-	-72.7
3	-	-	-	-	-	-	-	-	-71.1
4	-	-	-	-	-	-	-	-	-70.6
5	220	<100	<100	<200	0.46	-	26	-	-68.6
6	-	-	-	-	-	-	-	-	-71.2
7	<200	<100	<100	<200	0.47	-	27	-	-70.9
8	-	-	-	-	-	-	-	-	-72.3
9	204	<100	<100	<200	0.46	-	28	-	-71.9
10	-	-	-	-	-	-	-	-	-72.4
11	<200	<100	<100	<200	0.45	-	27	-	-71.7
12	<200	<100	<100	<200	0.50	-	28	-	-71.1
13	<200	<100	<100	<200	0.47	-	34	-	-70.7
14	-	-	-	-	-	-	-	-	-68.7
15	-	-	-	-	-	-	-	-	-68.7
16	-	-	-	-	-	-	-	-	-
17	-	-	-	-	-	-	-	-	-
18	328	<100	<16	<200	0.49	0.042	31	-	-70.7
19	1285	<1000	<1000	<2000	0.25	-	26	-	-71.4
20	1440	<1000	<1000	<2000	0.24	-	27	-	-70.9
21	1410	<1000	<1000	<2000	0.25	-	27	-	-67.1
22	-	-	-	-	-	-	-	-	-
23	-	-	-	-	-	-	-	-	-
24	-	-	-	-	-	-	-	-	-
25	1430	<1000	<1000	<2000	0.24	-	30	-	-71.3
26	1550	<1000	<1000	<2000	0.25	-	27	-	-66.7
27	-	-	-	-	-	-	-	-	-
28	<1000	<50	<50	<100	0.20	-	11	-	-82.8
29	<1000	<50	<50	<100	0.19	-	11	-	-82.8
30	-	-	-	-	-	-	-	-	-
31	<1000	<50	<50	<100	0.20	-	11	-	-82.8
32	-	-	-	-	-	-	-	-	-
33	-	-	-	-	-	-	-	-	-
34	-	-	-	-	-	-	-	-	-
35	1020	<50	<50	<100	0.19	-	11	-	-82.9
36	<1000	<50	<50	<100	0.20	-	11	-	-82.6
37	<1000	<50	<50	<100	0.20	-	11	-	-82.7
38	<1000	<50	<50	<100	0.20	0.016	11	-	-82.7
39	-	-	-	-	-	-	-	-	-
40	<1000	<50	<50	<100	0.19	-	12	-	-82.8
41	1690	<50	<50	<100	0.17	-	12	-	-82.6
42	1100	<50	<50	<100	0.19	-	12	-	-83.0
43	1450	<100	2.1	<200	0.49	-	12	0.725	-78.9
44	1160	<100	1.5	<200	0.63	< 0.02	11	0.725	-81.8
45	1120	<100	1.4	<200	0.49	< 0.015	12	0.725	-82.8
46	1190	<100	1.2	<200	0.46	-	11	0.724	-83.3
47	1230	<100	1.0	<200	0.29	< 0.02	12	0.724	-83.1
48	1250	<100	0.7	<200	0.24	-	12	0.724	-83.0
49	1130	<100	0.6	<200	0.27	0.020	12	0.724	-82.7
50	1310	<100	0.6	<200	0.22	-	12	0.724	-82.6
51	1550	<100	0.6	<200	0.23	-	12	0.724	-82.5
52	1410	<100	0.6	<200	0.25	0.029	12	0.724	-82.6
53	1460	<100	0.7	<200	0.29	-	12	0.724	-82.8
54	1350	<100	1.1	<200	0.24	-	13	0.724	-82.8
55	801	<100	2.0	<200	0.32	-	12	0.724	-82.9
56	578	<100	3.5	<200	0.27	-	11	0.724	-82.3
57	1230	<100	8.9	<200	0.28	0.07	11	0.725	-79.7
58	952	<100	17.0	<200	0.25	-	13	0.725	-73.1
59	1090	<100	13.0	<200	0.21	0.170	20	0.726	-68.9
60	1690	<100	2.6	<200	0.36	-	34	0.727	-60.5
61	1920	<100	< 3	<200	0.35	-	42	0.727	-58.4
62	2060	<100	< 3	<200	0.38	0.15	47	0.728	-56.6

[1]Analytical methods: +139M = ICP-MS (Labtium Oy), +148R = ion chromatography (Labtium Oy),
IC = ion chromatography (TVO nuclear services), 143T = titrimetry (Labtium Oy), SP =spectrophotometry (Ramboll Analytics),
TIMS = thermal ionisation mass spectrometry (GTK)

Appendix 1. Cont.

	I µg/L + 139M[1] 	F mg/L + 143R IC	SO$_4$ mg/L + 143R IC	NO$_3$ mg/L + 143R	Alkalinity mmol/L 143T	Sulphide mg/L SP	TDS g/L	^{87}Sr/^{86}Sr TIMS	δ^{2}H$_{H2O}$ ‰ VSMOW Picarro IRMS
63	1860	<100	< 3	<200	0.37	-	47	0.728	-59.6
64	2310	<100	< 2	<200	0.28	-	44	0.728	-61.9
65	1890	<100	< 2	<200	0.31	0.42	39	0.729	-63.9
66	2280	<100	< 2	<200	0.29	-	40	0.729	-65.3
67	1300	<100	6.4	<200	0.41	0.640	62	0.737	-70.0
68	543	<100	<100	<200	0.32	-	38	-	-66.4
69	515	<100	<100	<200	0.29	-	35	-	-66.0
70	490	<100	<100	<200	0.26	-	37	-	-65.9
71	-	-	-	-	-	-	-	-	-
72	460	<100	<2	<200	0.30	-	38	-	-65.4
73	467	<100	<100	<200	0.29	-	37	-	-65.4
74	-	-	-	-	-	0.086	-	-	-
75	700	<100	<100	<200	0.29	-	36	-	-65.0
76	604	<100	<100	<200	0.34	-	47	-	-56.2
77	584	<100	<2	<200	0.36	-	46	-	-55.9
78	-	-	-	-	-	-	-	-	-
79	636	<100	<100	<200	0.37	-	46	-	-56.0
80	-	-	-	-	-	0.87	-	-	-
81	360	<100	<100	<200	0.18	-	12	-	-82.7
82	399	<100	<100	<200	0.27	-	12	-	-82.8
83	571	<100	<100	<200	0.19	-	14	-	-71.2
84	775	<100	<100	<200	0.34	-	51	-	-56.6
85	1020	<100	<100	<200	0.41	-	69	-	-66.0
86	406	<100	<100	<200	0.23	-	12	-	-82.9
87	425	<100	<100	<200	0.21	-	14	-	-70.8
88	911	<100	<100	<200	0.39	-	57	-	-69.9
89	461	<100	<100	<200	0.18	-	11	-	-83.0
90	452	<100	<100	<200	0.18	-	11	-	-82.9
91	491	<100	<100	<200	0.18	-	12	-	-83.1
92	445	<100	<100	<200	0.18	-	12	-	-83.1
93	440	<100	<100	<200	0.19	-	12	-	-82.8
94	-	-	-	-	-	-	-	-	-
95	433	<100	<100	<200	0.21	-	11	-	-83.1
96	-	-	-	-	-	<0.014	-	-	-
97	408	< 100	< 0.1	< 200	0.35	-	7	-	-84.8
98	305	< 100	< 0.1	< 200	0.31	-	7	-	-85.9
99	289	< 100	< 0.1	< 200	0.37	-	7	-	-86.5
100	378	< 100	< 0.1	< 200	0.26	-	9	-	-85.4
101	532	< 100	< 0.1	< 200	0.20	-	11	-	-83.5
102	555	< 100	< 0.1	< 200	0.20	-	11	-	-82.8
103	581	< 100	< 0.1	< 200	0.21	-	12	-	-82.6
104	547	< 100	< 0.1	< 200	0.21	-	12	-	-83.0
105	1490	< 100	< 0.1	< 200	0.20	-	12	-	-83.1
106	1060	< 100	< 0.1	< 200	0.21	-	12	-	-82.8
107	866	< 100	< 0.1	< 200	0.20	-	12	-	-82.6
108	295	<10	<10	<20	0.70	-	6	-	-87.2
109	314	<10	<10	<20	0.51	-	7	-	-87.0
110	385	<10	<10	<20	0.13	-	8	-	-85.7
111	279	<10	<10	<20	0.18	-	7	-	-87.2
112	283	<10	<10	<20	0.19	-	7	-	-87.5
113	320	<10	<10	<20	0.24	-	6	-	-88.2
114	359	<10	<10	<20	0.26	-	6	-	-88.0
115	302	0.2	0.7	<20	0.25	-	6	-	-88.6
116	318	<10	<10	<20	0.25	0.057	6	-	-88.4
117	300	<10	<10	<20	0.31	-	5	-	-88.4
118	-	-	-	-	-	-	-	-	-88.8
119	-	-	-	-	-	-	-	-	-
120	-	-	-	-	-	-	-	-	-
121	-	-	-	-	-	-	-	-	-

[1]Analytical methods: +139M = ICP-MS (Labtium Oy), +148R = ion chromatography (Labtium Oy), IC = ion chroma-
tography (TVO nuclear services), 143T = titrimetry (Labtium Oy), SP =spectrophotometry (Ramboll Analytics),
TIMS = thermal ionisation mass spectrometry (GTK)

Appendix 1. Cont.

	δ18OH2O ‰ VSMOW Picarro IRMS[1]	δ13CDIC ‰ VPDB IRMS	Ar vol-% GC QMS	O2 vol-% GC QMS	N2 vol-% GC QMS	CO2 vol-% GC QMS	He vol-% GC QMS	CH4 vol-% GC QMS	H2 vol-% GC QMS
1	-10.88	-	-	-	-	-	-	-	-
2	-10.93	-	-	-	-	-	-	-	-
3	-10.96	-	-	-	-	-	-	-	-
4	-10.96	-	-	-	-	-	-	-	-
5	-10.94	-	-	-	-	-	-	-	-
6	-10.96	-	-	-	-	-	-	-	-
7	-10.96	-	-	-	-	-	-	-	-
8	-10.99	-	-	-	-	-	-	-	-
9	-10.97	-	-	-	-	-	-	-	-
10	-10.97	-	-	-	-	-	-	-	-
11	-10.93	-	-	-	-	-	-	-	-
12	-11.16	-	-	-	-	-	-	-	-
13	-10.99	-	-	-	-	-	-	-	-
14	-10.94	-	-	-	-	-	-	-	-
15	-10.94	-	0.28	0.24	15.3	< 0.003	2.7	78.3	0.17
16	-	-	0.55	6.3	34.4	< 0.003	2	53.8	0.12
17	-	-	0.37	0.5	16.4	< 0.003	2.7	77	0.17
18	-10.91	-	0.23	0.55	16.5	< 0.003	2.8	76.8	0.17
19	-11.04	-	-	-	-	-	-	-	-
20	-10.93	-	-	-	-	-	-	-	-
21	-10.95	-	-	-	-	-	-	-	-
22	-	-0.8	-	-	-	-	-	-	-
23	-	-	0.44	0.32	15.5	< 0.003	1.9	78.8	0.068
24	-	-	-	-	-	-	-	-	-
25	-10.94	-	-	-	-	-	-	-	-
26	-10.96	-	-	-	-	-	-	-	-
27	-	-	0.11	0.24	15.9	< 0.003	1.6	79.1	0.02
28	-13.10	-	-	-	-	-	-	-	-
29	-13.15	-	0.098	0.11	15	< 0.003	0.96	80	0.005
30	-	-	0.15	0.31	15	< 0.003	0.75	80	0.005
31	-13.06	-	0.093	0.15	20	< 0.003	1.7	75	0.006
32	-	-	-	-	-	-	-	-	-
33	-	-	0.11	0.19	17	< 0.003	1.2	78	0.006
34	-	-	0.12	0.3	22	< 0.003	2	73	0.007
35	-13.09	-	0.13	0.27	21	< 0.003	2	73	0.007
36	-13.10	-	-	-	-	-	-	-	-
37	-13.07	-	0.21	0.1	20	< 0.003	1.6	75	0.004
38	-13.07	-16.1	0.13	0.27	21	< 0.003	1.8	74	< 0.003
39	-	-	-	-	-	-	-	-	-
40	-13.32	-	-	-	-	-	-	-	-
41	-13.18	-	-	-	-	-	-	-	-
42	-13.17	-	-	-	-	-	-	-	-
43	-12.14	-	-	-	-	-	-	-	-
44	-12.47	-	-	-	-	-	-	-	-
45	-12.62	-	-	-	-	-	-	-	-
46	-12.70	-	-	-	-	-	-	-	-
47	-12.85	-	-	-	-	-	-	-	-
48	-12.89	-	-	-	-	-	-	-	-
49	-12.93	-	0.65	0.53	28	< 0.003	1.80	66	0.007
50	-12.96	-	-	-	-	-	-	-	-
51	-12.97	-	-	-	-	-	-	-	-
52	-12.91	-	-	-	-	-	-	-	-
53	-12.92	-	1.10	0.62	20	< 0.003	0.50	74	< 0.003
54	-12.93	-	0.41	0.32	26	< 0.003	0.88	69	0.005
55	-12.79	-	0.34	0.56	26	< 0.003	1.00	69	< 0.003
56	-12.70	-	0.34	0.36	22	< 0.003	1.00	73	< 0.003
57	-12.15	-	0.38	0.31	21	< 0.003	1.40	74	< 0.003
58	-11.23	-	0.86	0.27	19	< 0.003	1.90	75	< 0.003
59	-10.86	-	0.22	0.41	20	< 0.003	1.00	76	0.005
60	-10.48	-	0.20	0.20	18	< 0.003	1.10	78	0.011
61	-10.39	-	0.21	0.17	17	< 0.003	1.40	78	0.01
62	-10.46	-	0.30	0.19	16	< 0.003	1.70	79	0.015

[1]Analytical methods: IRMS = isotope ratio mass spectrometry, GC = gas cromatography (Ramboll analytics),
QMS = quadrupole mass spectrometry (in the field)

Appendix 1. Cont.

	$\delta^{18}O_{H2O}$ ‰ VSMOW Picarro IRMS	$\delta^{13}C_{DIC}$ ‰ VPDB IRMS	Ar vol-% GC QMS	O_2 vol-% GC QMS	N_2 vol-% GC QMS	CO_2 vol-% GC QMS	He vol-% GC QMS	CH_4 vol-% GC QMS	H_2 vol-% GC QMS
63	-10.48	-	0.18	0.27	16	< 0.003	2.00	79	0.031
64	-10.59	-	0.21	0.39	16	< 0.003	2.20	78	0.027
65	-10.63	-	0.23	0.40	19	< 0.003	4.20	74	0.041
66	-10.81	-	0.25	0.34	21	< 0.003	4.80	71	0.054
67	-11.02	-	-	-	-	-	-	-	-
68	-10.59	-	-	-	-	-	-	-	-
69	-10.62	-	-	-	-	-	-	-	-
70	-10.70	-	-	-	-	-	-	-	-
71	-	-	-	-	-	-	-	-	-
72	-10.56	-	0.19	0.27	13	0.03	3.6	79	0.47
73	-10.62	-	-	-	-	-	-	-	-
74	-	-	-	-	-	-	-	-	-
75	-10.67	-	-	-	-	-	-	-	-
76	-10.71	-	-	-	-	-	-	-	-
77	-10.78	-	-	-	-	-	-	-	-
78	-	-	-	-	-	-	-	-	-
79	-10.47	-	0.13	0.30	13	< 0.003	2.6	81	0.073
80	-	-	-	-	-	-	-	-	-
81	-13.00	-	0.278	4.03	32.5	0.042	1.81	61.27	0.06
82	-12.94	-	0.31	5.2	36	0.05	1.9	54	0.018
83	-11.02	-	0.361	4.29	29.8	0.026	5.21	60.3	0.042
84	-10.59	-	0.11	0.12	11	<0.003	3.3	79	3.7
85	-11.30	-	0.59	5.8	37	0.2	6	15	33
86	-13.11	-	0.16	0.071	21	< 0.003	2.5	73	0.027
87	-10.84	-	0.2	0.07	19	0.42	5.4	72	0.004
88	-11.06	-	0.57	0.65	33	0.61	7.7	17	38
89	-13.18	-	-	-	-	-	-	-	-
90	-12.99	-	-	-	-	-	-	-	-
91	-12.97	-	-	-	-	-	-	-	-
92	-12.88	-	-	-	-	-	-	-	-
93	-13.07	-	-	-	-	-	-	-	-
94	-	-	0.14	0.87	20	<0.003	1.2	74	0.004
95	-13.01	-	0.13	0.30	19	<0.003	1.5	76	0.009
96	-	-	-	-	-	-	-	-	-
97	-12.00	-14.0	-	-	-	-	-	-	-
98	-12.22	-	-	-	-	-	-	-	-
99	-12.38	-17.5	0.28	1.8	26	< 0.003	1.6	67	0.045
100	-12.69	-17.9	0.27	0.95	26	< 0.003	1.9	68	0.057
101	-12.95	-17.9	0.12	0.54	26	< 0.003	1.8	69	0.043
102	-13.05	-16.7	0.15	0.46	24	< 0.003	1.6	71	0.034
103	-12.98	-18.1	0.16	0.38	23	< 0.003	1.5	72	0.026
104	-13.11	-16.2	0.18	0.41	16	< 0.003	0.22	80	0.008
105	-13.06	-16.2	0.12	0.19	25	< 0.003	1.10	70	< 0.003
106	-13.01	-15.7	0.12	0.23	28	< 0.003	0.93	68	0.024
107	-13.11	-14.7	0.13	0.20	25	< 0.003	0.78	71	0.016
108	-12.54	-	0.35	0.31	19	<0.003	1.5	76	<0.003
109	-12.68	-	0.32	0.29	21	<0.003	2.3	73	<0.003
110	-12.79	-	0.19	0.35	22	<0.003	2.2	72	0.012
111	-12.79	-	-	-	-	-	-	-	-
112	-12.50	-	0.15	0.29	19	<0.003	1.4	76	0.008
113	-12.68	-	0.14	0.25	19	<0.003	1.3	76	0.007
114	-12.60	-	-	-	-	-	-	-	-
115	-12.57	-	0.23	0.32	20	<0.003	1.5	74	0.006
116	-12.61	-	-	-	-	-	-	-	-
117	-12.60	-	0.27	0.37	21	<0.003	1.5	74	<0.003
118	-12.55	-	-	-	-	-	-	-	-
119	-	-	0.27	0.020	20.7	0.039	1.2	74	0.36
120	-	-	0.23	0.04	19.9	0.053	1.1	75.2	0.15
121	-	-	0.24	0.14	21.9	0.047	1.2	72.8	0.32

[1]Analytical methods: IRMS = isotope ratio mass spectrometry, GC = gas cromatography (Ramboll analytics),
QMS = quadrupole mass spectrometry (in the field)

Appendix 1. Cont.

	C$_2$H$_6$ vol-% GC[1]	C$_2$H$_4$ vol-% GC	C$_2$H$_2$ vol-% GC	C$_3$H$_8$ vol-% GC	C$_3$H$_4$ vol-% GC	δ^{2}H$_{H2}$ ‰ VSMOW IRMS	δ^{13}C$_{CH4}$ ‰ VPDB IRMS	δ^{2}H$_{CH4}$ ‰ VSMOW IRMS	δ^{13}C$_{C2H6}$ ‰ VPDB IRMS
1	-	-	-	-	-	-	-	-	-
2	-	-	-	-	-	-	-	-	-
3	-	-	-	-	-	-	-	-	-
4	-	-	-	-	-	-	-	-	-
5	-	-	-	-	-	-	-	-	-
6	-	-	-	-	-	-	-	-	-
7	-	-	-	-	-	-	-	-	-
8	-	-	-	-	-	-	-	-	-
9	-	-	-	-	-	-	-	-	-
10	-	-	-	-	-	-	-	-	-
11	-	-	-	-	-	-	-	-	-
12	-	-	-	-	-	-	-	-	-
13	-	-	-	-	-	-	-	-	-
14	-	-	-	-	-	-	-	-	-
15	0.41	< 0.001	< 0.001	0.012	< 0.001	-727	-27.6	-297	-45.3
16	0.27	< 0.001	< 0.001	0.008	< 0.001	-	-	-	-
17	0.39	< 0.001	< 0.001	0.012	< 0.001	-771	-28.7	-297	-45.1
18	0.39	< 0.001	< 0.001	0.012	< 0.001	-	-	-	-
19	-	-	-	-	-	-	-	-	-
20	-	-	-	-	-	-	-	-	-
21	-	-	-	-	-	-	-	-	-
22	-	-	-	-	-	-	-25.6	-295	-49.6
23	0.46	< 0.001	< 0.001	0.015	< 0.001	-	-	-	-
24	-	-	-	-	-	-	-25.3	-297	-48.6
25	-	-	-	-	-	-	-	-	-
26	-	-	-	-	-	-	-	-	-
27	0.48	< 0.001	< 0.001	0.016	< 0.001	-	-	-	-
28	-	-	-	-	-	-	-	-	-
29	1.1	< 0.001	< 0.001	0.032	< 0.001	-	-	-	-
30	1.1	< 0.001	< 0.001	0.032	< 0.001	-	-	-	-
31	0.87	< 0.001	< 0.001	0.028	< 0.001	<	-34.0	-292	-43.4
32	-	-	-	-	-	-	-32.8	-291	-49.2
33	1	< 0.001	< 0.001	0.032	< 0.001	-	-	-	-
34	0.85	< 0.001	< 0.001	0.027	< 0.001	-	-	-	-
35	0.86	< 0.001	< 0.001	0.027	< 0.001	-798	-34.6	-294	-43.8
36	-	-	-	-	-	-	-	-	-
37	0.89	< 0.001	< 0.001	0.028	< 0.001	-	-	-	-
38	0.7	< 0.001	< 0.001	0.022	< 0.001	-	-	-	-
39	-	-	-	-	-	-	-33.5	-294	-49.7
40	-	-	-	-	-	-	-	-	-
41	-	-	-	-	-	-	-	-	-
42	-	-	-	-	-	-	-	-	-
43	-	-	-	-	-	-	-	-	-
44	-	-	-	-	-	-	-	-	-
45	-	-	-	-	-	-	-	-	-
46	-	-	-	-	-	-	-	-	-
47	-	-	-	-	-	-	-31.0	-273	-31.2
48	-	-	-	-	-	-	-34.1	-279	-27.9
49	0.40	< 0.001	< 0.001	0.006	< 0.001	-	-34.8	-280	-27.7
50	-	-	-	-	-	-	-30.6	-282	-27.1
51	-	-	-	-	-	-	-32.9	-287	-28.1
52	-	-	-	-	-	-	-	-	-
53	0.45	< 0.001	< 0.001	0.007	< 0.001	-	-33.6	-283	-29.5
54	0.39	< 0.001	< 0.001	0.007	< 0.001	-	-32.0	-290	-28.3
55	0.40	< 0.001	< 0.001	0.007	< 0.001	-	-33.4	-286	-29.3
56	0.44	< 0.001	< 0.001	0.009	< 0.001	-	-32.3	-282	-28.7
57	0.48	< 0.001	< 0.001	0.010	< 0.001	-	-33.7	-280	-28.2
58	0.40	< 0.001	< 0.001	0.009	< 0.001	-	-30.9	-279	-25.7
59	0.34	< 0.001	< 0.001	0.008	< 0.001	-	-28.3	-278	-23.2
60	0.30	< 0.001	< 0.001	0.006	< 0.001	-	-26.6	-282	<
61	0.27	< 0.001	< 0.001	0.006	< 0.001	-	-26.5	-291	<
62	0.29	< 0.001	< 0.001	0.006	< 0.001	-	-25.7	-289	<

[1]Analytical methods: IRMS = isotope ratio mass spectrometry, GC = gas cromatography (Ramboll analytics)

Appendix 1. Cont.

	C_2H_6 vol-% GC[1]	C_2H_4 vol-% GC	C_2H_2 vol-% GC	C_3H_8 vol-% GC	C_3H_4 vol-% GC	δ^2H_{H2} ‰ VSMOW IRMS	$\delta^{13}C_{CH4}$ ‰ VPDB IRMS	δ^2H_{CH4} ‰ VSMOW IRMS	$\delta^{13}C_{C2H6}$ ‰ VPDB IRMS
63	0.29	< 0.001	< 0.001	0.006	< 0.001	-	-25.5	-293	<
64	0.28	< 0.001	< 0.001	0.006	< 0.001	-	-30.2	-292	<
65	0.22	< 0.001	< 0.001	0.005	< 0.001	-	-29.7	-288	<
66	0.23	< 0.001	< 0.001	0.006	< 0.001	-	-30.7	-283	<
67	-	-	-	-	-	-	-28.5	-289	<
68	-	-	-	-	-	-	-	-	-
69	-	-	-	-	-	-	-	-	-
70	-	-	-	-	-	-	-	-	-
71	-	-	-	-	-	-	-19.2	-293	-35.4
72	0.47	<0.001	<0.001	0.018	<0.001	-	-	-	-
73	-	-	-	-	-	-	-	-	-
74	-	-	-	-	-	-	-	-	-
75	-	-	-	-	-	-	-	-	-
76	-	-	-	-	-	-	-	-	-
77	-	-	-	-	-	-	-	-	-
78	-	-	-	-	-	-	-18.7	-286	-33
79	0.43	< 0.001	<0.001	0.018	<0.001	-	-	-	-
80	-	-	-	-	-	-	-	-	-
81	-	-	-	-	-	-	-	-	-
82	0.61	<0.001	<0.001	0.021	<0.001	-	-38.1	-230	-42
83	-	-	-	-	-	-	-	-	-
84	0.37	<0.001	<0.001	0.017	<0.001	-	-34.1	-269	-38
85	0.045	<0.001	<0.001	<0.001	<0.001	-	-13.2	-369	-23
86	0.8	<0.001	<0.001	0.025	<0.001	-	-25.1	-237	-41
87	0.51	<0.001	<0.001	0.022	<0.001	-	-36.4	-136	-46
88	0.078	<0.001	<0.001	0.004	<0.001	-	-15.9	-404	-42
89	-	-	-	-	-	-	-	-	-
90	-	-	-	-	-	-	-	-	-
91	-	-	-	-	-	-	-	-	-
92	-	-	-	-	-	-	-	-	-
93	-	-	-	-	-	-	-	-	-
94	0.88	<0.001	<0.001	0.028	<0.001	-	-	-	-
95	0.87	<0.001	<0.001	0.027	<0.001	-	-	-	-
96	-	-	-	-	-	-	-	-	-
97	-	-	-	-	-	-	-	-	-
98	-	-	-	-	-	-	-	-	-
99	0.51	< 0.001	< 0.001	0.011	< 0.001	-	-31.8	-269	-43.4
100	0.48	< 0.001	< 0.001	0.009	< 0.001	-	-29.5	-281	-43.4
101	0.49	< 0.001	< 0.001	0.009	< 0.001	-	-29.2	-237	-44.5
102	0.52	< 0.001	< 0.001	0.010	< 0.001	-	-31.7	-291	-45.8
103	0.61	< 0.001	< 0.001	0.013	< 0.001	-	-33.1	-242	-31.6
104	0.80	< 0.001	< 0.001	0.017	< 0.001	-	-36.9	-266	-43.6
105	0.58	< 0.001	< 0.001	0.014	< 0.001	-	-27.9	-289	-44.9
106	0.53	< 0.001	< 0.001	0.014	< 0.001	-	-29.4	-277	-46.0
107	0.60	< 0.001	< 0.001	0.016	< 0.001	-	-34.0	-247	-45.4
108	0.22	<0.001	<0.001	0.028	<0.001	-	-37.3	-276	-45.8
109	0.80	<0.001	<0.001	0.026	<0.001	-	-36.1	-280	-45.4
110	0.80	<0.001	<0.001	0.025	<0.001	-	-36.5	-284	-45.1
111	-	-	-	-	-	-	-	-	-
112	0.90	<0.001	<0.001	0.027	<0.001	-	-	-	-
113	0.90	<0.001	<0.001	0.026	<0.001	-	-	-	-
114	-	-	-	-	-	-	-	-	-
115	0.86	<0.001	<0.001	0.025	<0.001	-	-36.5	-263	-45.1
116	-	-	-	-	-	-	-	-	-
117	0.86	<0.001	<0.001	0.025	<0.001	-	-39.9	-281	-45.5
118	-	-	-	-	-	-	-	-	-
119	0.90	<0.001	<0.001	0.025	<0.001	-	-27.5	-263	-43.1
120	0.92	<0.001	<0.001	0.026	<0.001	-	-38.2	-246	-45.0
121	0.87	<0.001	<0.001	0.024	<0.001	-	-	-	-

[1]Analytical methods: IRMS = isotope ratio mass spectrometry, GC = gas cromatography (Ramboll analytics)

Appendix 1. Cont.

	δ^2H_{C2H6} ‰ VSMOW IRMS[1]	$\delta^{13}C_{C3H8}$ ‰ VPDB IRMS	δ^2H_{C3H8} ‰ VSMOW IRMS	Gas/water[2] L/L		δ^2H_{C2H6} ‰ VSMOW IRMS[1]	$\delta^{13}C_{C3H8}$ ‰ VPDB IRMS	δ^2H_{C3H8} ‰ VSMOW IRMS	Gas/water[2] L/L
1	-	-	-	-	63	-276	-	-	-
2	-	-	-	-	64	-226	-	-	-
3	-	-	-	-	65	-223	-	-	-
4	-	-	-	-	66	-225	-	-	-
5	-	-	-	-	67	-251	-	-	-
6	-	-	-	-	68	-	-	-	-
7	-	-	-	-	69	-	-	-	-
8	-	-	-	-	70	-	-	-	-
9	-	-	-	-	71	-265	-	-	-
10	-	-	-	-	72	-	-	-	-
11	-	-	-	-	73	-	-	-	-
12	-	-	-	-	74	-	-	-	-
13	-	-	-	-	75	-	-	-	-
14	-	-	-	-	76	-	-	-	-
15	<	-36.2	<	-	77	-	-	-	-
16	-	-	-	-	78	-254	-	-	-
17	<	-39.5	<	-	79	-	-	-	-
18	-	-	-	-	80	-	-	-	-
19	-	-	-	-	81	-	-	-	0.62
20	-	-	-	-	82	-277	-	-	1.07
21	-	-	-	-	83	-	-	-	0.27
22	-239	-	-	-	84	-268	-	-	0.57
23	-	-	-	-	85	<	-	-	0.16
24	-235	-	-	-	86	-265	-	-	0.7
25	-	-	-	-	87	-215	-	-	0.24
26	-	-	-	-	88	<	-	-	0.09
27	-	-	-	-	89	-	-	-	-
28	-	-	-	-	90	-	-	-	-
29	-	-	-	1.0	91	-	-	-	-
30	-	-	-	1.0	92	-	-	-	-
31	<	-35.2	<	-	93	-	-	-	-
32	-249	-	-	-	94	-	-	-	-
33	-	-	-	-	95	-	-	-	-
34	-	-	-	1.0	96	-	-	-	-
35	<	-35.8	<	1.0	97	-	-	-	-
36	-	-	-	-	98	-	-	-	-
37	-	-	-	1.4	99	-242	-	-	-
38	-	-	-	-	100	-234	-	-	-
39	-247	-	-	-	101	-249	-	-	-
40	-	-	-	-	102	-218	-	-	-
41	-	-	-	-	103	-221	-	-	-
42	-	-	-	-	104	-223	-	-	-
43	-	-	-	-	105	-238	-	-	-
44	-	-	-	-	106	-230	-	-	-
45	-	-	-	-	107	-234	-	-	-
46	-	-	-	-	108	-182	-	-	-
47	-227	-	-	-	109	**-163**	-	-	*0.5*
48	**-235**	-	-	-	110	**-194**	-	-	*0.5*
49	-228	-	-	-	111	-	-	-	-
50	**-232**	-	-	-	112	**112**	-	-	*0.4*
51	**-244**	-	-	-	113	-	-	-	*0.3*
52	-	-	-	-	114	-	-	-	-
53	**-238**	-	-	-	115	**-161**	-	-	*0.5*
54	-246	-	-	-	116	-	-	-	-
55	-263	-	-	-	117	-170	-	-	-
56	-270	-	-	-	118	-	-	-	-
57	-256	-	-	-	119	-157	-	-	0.433
58	-203	-	-	-	120	-153	-	-	0.425
59	-243	-	-	-	121	-	-	-	0.44
60	-225	-	-	-					
61	-239	-	-	-					
62	-233	-	-	-					

[1]Analytical methods: IRMS = isotope ratio mass spectrometry

[2]Gas/water ratios in italics are approximate values based on flow measurements

All GTK's publications online at hakku.gtk.fi

The presence of deep saline groundwaters within bedrock fractures and pore spaces of continental shields has been known for more than a century. However, the origin of the salinity and abundant dissolved gases, in addition to their unique isotope composition, is still debated. In addition to geochemical processes, deep-dwelling microorganisms are important, yet poorly understood, change agents in these environments. Access to deep groundwaters only through deep mines and drill holes means that technical challenges are also frequently faced.

This PhD thesis is comprised of a synopsis and four original papers that examine groundwater, dissolved gases and fracture minerals in the 2.5 km deep Outokumpu Deep Drill Hole, eastern Finland, as a case study, in order to understand how bedrock groundwater evolves via geochemical and microbiological processes through time and space. A model is proposed that includes precipitation and infiltration of meteoric water under warmer than present climatic conditions, a change in the isotopic composition and increase in salinity of water through water–rock interaction, and both the abiotic and biotic formation of hydrocarbons. Two independent lines of evidence from water stable isotopes and the accumulation of noble gases place the evolutionary model in the time frame of millions to tens of millions of years.

The results emphasise the complexity of these environments, as they are being increasingly utilised for underground construction and exploitation of deep ores and geothermal energy, and provide background information, for example, for assessment of the long-term safety of nuclear waste disposal.